Plant Functional Types for Land Surface Modelling in South Ecuador – Spatial Delineation, Sensitivity and Parameter Determination

Dietrich Göttlicher

Plant Functional Types for Land Surface Modelling in South Ecuador – Spatial Delineation, Sensitivity and Parameter Determination

Kumulative Dissertation
zur
Erlangung des Doktorgrades
der Naturwissenschaften
(Dr. rer. nat)

dem
Fachbereich Geographie
der Philipps-Universität Marburg
vorgelegt von

Dietrich Göttlicher
aus Marl (Westf.)

Marburg / Lahn 2010

Als Dissertation vom Fachbereich Geographie der Philipps-Universität Marburg am 23. Juni 2010 angenommen.

Erstgutachter: Prof. Dr. Jörg Bendix
Zweitgutachter: Prof. Dr. Thomas Nauss

Tag der Disputation: 14. Juli 2010

Preface

At the end of a challenging time comprising numerous short field trips to the beautiful mountain forests of South Ecuador, I have to thank those persons who accompanied me on the way to finish this work.

First of all I have to thank my supervisor Jörg Bendix. He had open ears at all times and conducted me in many scientific discussions. He overwhelmed me with his enthusiasm on geo-ecological research and provided all that support I needed. I have been proud to be a part of his team.

Special thanks go to my colleagues at the Laboratory for Climatology and Remote Sensing of Philipps-University, Marburg. From little help with everyday problems over in deep scientific discussions to just coffee breaks have been very much appreciated. Particularly, I have to thank Thomas Nauss (now University of Bayreuth) for fruitful discussions and multiple help ranging from solving technical problems to making useful comments on the manuscript. I thank Rütger Rollenbeck for his assistance in logistics around our study site in Ecuador and in Marburg as well as his introduction to the Ecuadorian way of life. The diploma theses of André Reifschneider (now Obregón), Thomas Böth (now Lotz) and Janina Albert (University of Köln) were of great use for this work, as were the help of my additional student assistants Miriam Hachelaf, Meike Kühnlein, Vera Petrikat, Johannes Schwer and Nora Schmid.

I am very thankful to many colleagues within the DFG research unit FOR 816 and its predecessor FOR 402 for collecting so many useful data. Especially I like to thank Kristin Roos (University of Bayreuth) for the help during the field studies with the spectrometer in action, Jürgen Homeier (University of Göttingen) and Florian Werner (University of Oldenburg) for their help with the determination of plant material.

My general work within the research unit was funded by the Deutsche Forschungsgemeinschaft (DFG) under multiple subprograms (Be 1780/15-1, Na 783/1-1) and is gratefully acknowledged.

Furthermore this work could not have been conducted without the contributions of the open source software community. Not only the used Community Land Model but also a lot of other free software was used throughout the study and their existence and non-restrictive availability are very much appreciated.

Finally, I thank my parents and my brother for their multiple support and encouragement those recent years of scientific work. Moreover, I have to deeply thank my wife Veronika and our children Adelheid, Gregor and Bruno for their patience whenever I was not at home and their constant reminder that the real priorities in life can be pursued without a computer.

Dietrich Göttlicher
Marburg, June 2010

Contents

List of Figures

List of Tables

List of Abbreviations

ALMIP	AMMA Land surface Model Intercomparison Project
AMMA	African Monsoon Multidisciplinary Analysis
BATS	Biosphere-Atmosphere-Transfer-Scheme
BET	Broadleaf Evergreen Tree
BVOC	Biogenic Volatile Organic Compound
C^4MIP	Coupled Carbon Cycle Climate Model Intercomparison Project
CCM	Community Climate Model
CCSM	Community Climate System Model
CLM	Community Land Model
CSU	Colorado State University
DFG	Deutsche Forschungsgemeinschaft (German research council)
DGVM	Dynamic Global Vegetation Model
ECSF	Estación Scientífica San Francisco
EROS	Earth Resources Observation and Science
ETM+	Enhanced Thematik Mapper
FOR 816	Research unit *Biodiversity and Sustainable Management of a Megadiverse Mountain Ecosystem in South Ecuador*
GCM	Global Circulation Model
GENESIS	Global Environmental and Ecological Simulation of Interactive Systems
GLCF	Global Land Cover Facility
GOES	Geostationary Operational Environmental Satellites
HadCM3	Hadley Center Climate Model
IAP94	Institute of Atmospheric Physics, Chinese Academy of Sciences land model
IBIS	Integrated Biosphere Simulator
IPCC	Intergovernmental Panel on Climate Change
LAI	Leaf Area Index
LSM	Land Surface Model
MLC	Maximum-Likelihood Classification

NCAR	National Center for Atmospheric Research
NCEP	National Center for Environmental Prediction
NCI	Nature and Culture International
NIR	Near Infrared
NOAA	National Oceanic and Atmosphere Administration
PAR	Photosynthetic Active Radiation
PBL	Planetary Boundary Layer
PFT	Plant Functional Type
PILPS	Project for Intercomparison of Land-Surface Parameterization Schemes
RBSF	Reserva Biológica San Francisco
RTM	River Transport Model
SiB	Simple Biosphere Model
$SRES^2$	Special report on Emissions Scenarios
SRTM	Shuttle Radar Topography Mission
SVAT	Soil-Vegetation-Atmosphere-Transfer
TM	Thematic Mapper
UTM	Universal Transverse Mercator
VIS	Visible
WGS84	World Geodetic System 1984
WP	Work package
WRF	Weather Research and Forecasting Model

1 Introduction

1.1 Motivation

The change of landcover has severe influence on the ecological configuration and the climatic interaction between the land surface and the atmosphere (Feddema et al., 2005; Foley et al., 2005; Zhao et al., 2001). Global change of the climate as well as the change of spatial distribution and biotic occurrence of terrestrial ecosystems pose a challenge to our generation (Thuiller, 2007). Biological diversity is one of the most threatened features in global considerations (Colwell et al., 2008; Brooks et al., 2006). A major task for mankind will be the preservation of the sustainability of natural resources and biological diversity under these changing conditions (Naidoo et al., 2008; Sala et al., 2000). To bear this challenge not only global action is required but also regional steps to gather more understanding of the underlying processes and developing practical solutions.

The research unit 'Biodiversity and Sustainable Management of a Megadiverse Mountain Ecosystem in South Ecuador' (FOR 816) funded by the German research council (Deutsche Forschungsgemeinschaft, DFG) works in one of the hottest hotspots of biodiversity of the world (Barthlott et al., 2007; Brummitt & Lughadha, 2003; Liede-Schumann & Breckle, 2008). For the last 10 years this research unit and its predecessors have been investigating the biotic, abiotic and human interactions to solve the problem of loss of sustainability due to landcover change forced by the pressure of the local inhabitants on the environment (Beck et al., 2008a).

Fundamental knowledge about the geo-ecological processes in this tropical mountain ecosystem is missing or is incomplete (Brehm et al., 2008a,b). Various field experiments and research studies are carried out within the research unit FOR 816 to close this gap in knowledge. Particularly, new land use strategies are developed and investigated to provide the bases for a sustainable management and the conservation the biodiversity (Pohle & Gerique, 2008; Makeschin et al., 2008; Weber et al., 2008).

The use of models to investigate the interactions between the atmosphere and the land surface are a sensible addition to other geo-ecological field studies and experiments. Results of these models do not only provide spatial continuous abiotic data to the ecologists for the investigation of interrelations but primarily help to analyze the whole processes within the ecologic system in regards to energy, water and matter fluxes. Numeric models open up the possibility to investigate the potential

changes in land cover without neither any interference on the actual landscape nor testing new strategies for a sustainable management in a longer period of time.

1.2 Aims

Numerical models are capable to investigate the changes of the mentioned future land cover changes and its response to climatic and hydrologic variability (see section 1.1). The chance to test numerously land use scenarios without interfering into the real environment offers the possibility to investigate and evaluate the proposed management strategies. In recent years global aspects of land cover change and climate change were in focus of the scientific community (e.g. FEDDEMA et al., 2005; BONAN, 2008; GIBBARD et al., 2005). To verify these global considerations with field data on one hand some sort of downscaling has to be applied (e.g. SHIN et al., 2006; MISRA et al., 2003; DRUYAN et al., 2002). On the other hand it is possible to adapt the models to a regional scale with a finer resolution and less generalized input parametrization.

The embedding of this work within the research unit FOR 816 opens up the possibility to access a lot of sophisticated field data gathered by the numerous subprograms. This gives the unique chance to develop and test a regional adaption of a state-of-the-art land model. One of the major hypotheses of the multidisciplinary research unit is stated as follows:

> Sustainable management of the pastures and a regional repastorization of rangeland areas are possible which boost livelihood of the local population, reduce the pressure on clearing natural forests and improve ecosystem services at the landscape scale.

Water- and climate regulation are examples of ecosystem services (DE GROOT et al., 2002) which are dependent on the specification of the environment. These ecosystem services which are reflective of the energy and water fluxes, will be altered under changing land use conditions and can be analyzed using soil-vegetation-atmosphere-transfer (SVAT) schemes (FOLEY et al., 2005). The energy and water fluxes should be calculated with the inclusion of a decided vegetation cover. The used model setup has to be checked of its regional integrity. Underlying these general considerations the central hypotheses of this study can be postulated as follows:

H 1: A continuous spatial delineation of land use classes based on ecological-functional field studies can be mapped in a subpixel accuracy from medium space-resolved satellite data.

H 2: Gradual changes in the composition of vegetation, its morphological, optical and physiological behavior do not have influence on the energy and water fluxes estimated in a SVAT model.

H 3: Clusters of species with similar plant optical properties reflect ecologically derived vegetation types.

Following work packages (WP) are applied on the bases of the preliminary considerations and to finally test the hypotheses as follows:

WP 1: Classification of Landsat Enhanced Thematic Mapper (ETM+) data with a linear spectral unmixing approach (soft classification) to allow subpixel accuracy. Spatial delineation of different vegetation classes to be used as input parameter for the used SVAT model.

WP 2: Conduction of a sensitivity study of the PFT parameters of the used SVAT scheme.

WP 3: Quantification of optical properties of species from all PFTs with a field spectrometer. Comparison of clusters with similar optical characteristics with ecological derived PFTs.

The single WPs assemble the supply of a regional model setup to investigate the interactions between the soil, the vegetation and the atmosphere under changing land cover conditions. The significant innovations in this context can be stated as follows:

- soft classification of land cover using Landsat ETM+ data in rugged terrain,
- first found sensitivity study of the PFT parameter of the used SVAT model,
- regional parametrization of the used SVAT model including the first found regionalization of PFTs,
- operation of a field spectrometer to determine the reflectance and the transmittance of rarely or even insufficiently investigated species from a tropical mountain forest,
- determination of new values for the optical parameters of the used SVAT model,
- contribution to the scientific discussion on the linkage of PFTs to remote sensing data.

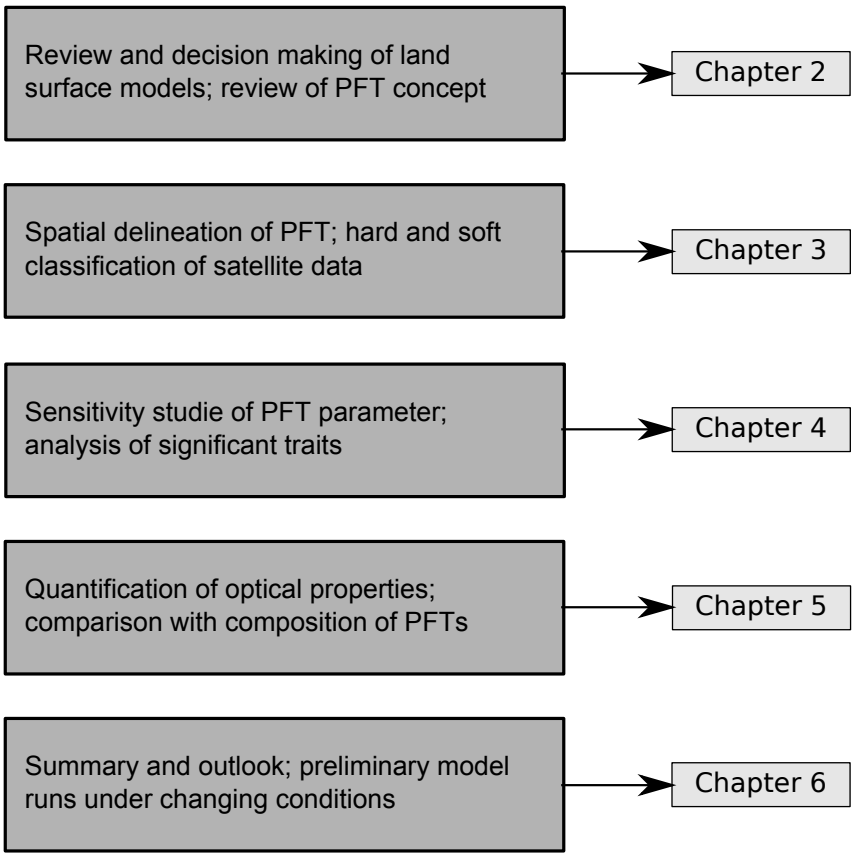

Figure 1.1: Outline of the presented work. Numbers in red refer to the single chapters of this work

1.3 Study outline

The study outline is illustrated in figure 1.1. The introduction in this chapter is completed with a short presentation of the study area (chapter 1.4). Chapter 2 gives an overview of the methodical approach. This comprises the evolution, the principle characteristics and the decision making of SVAT models (chapter 2.1) as well as a review of the concept of PFTs and their implementation in the study area (chapter 2.2). The workflow of the single WPs is presented in chapter 2.3.

Chapter 3 introduces the spatial delineation of the PFTs in the study area from Landsat data with 2 different classification algorithms and a analysis of their different impact on the use within the SVAT model. The sensitivity study of all PFT parameter is presented in chapter 4. The results of the sensitivity study are reflected in the new quantification of optical properties (reflectance and transmittance) and its relevance for the assigned PFTs (chapter 5).

Finally, chapter 6.1 summarizes the work and evaluates the central hypotheses. Additional preliminary case studies and an outlook are given in chapter 6.2.

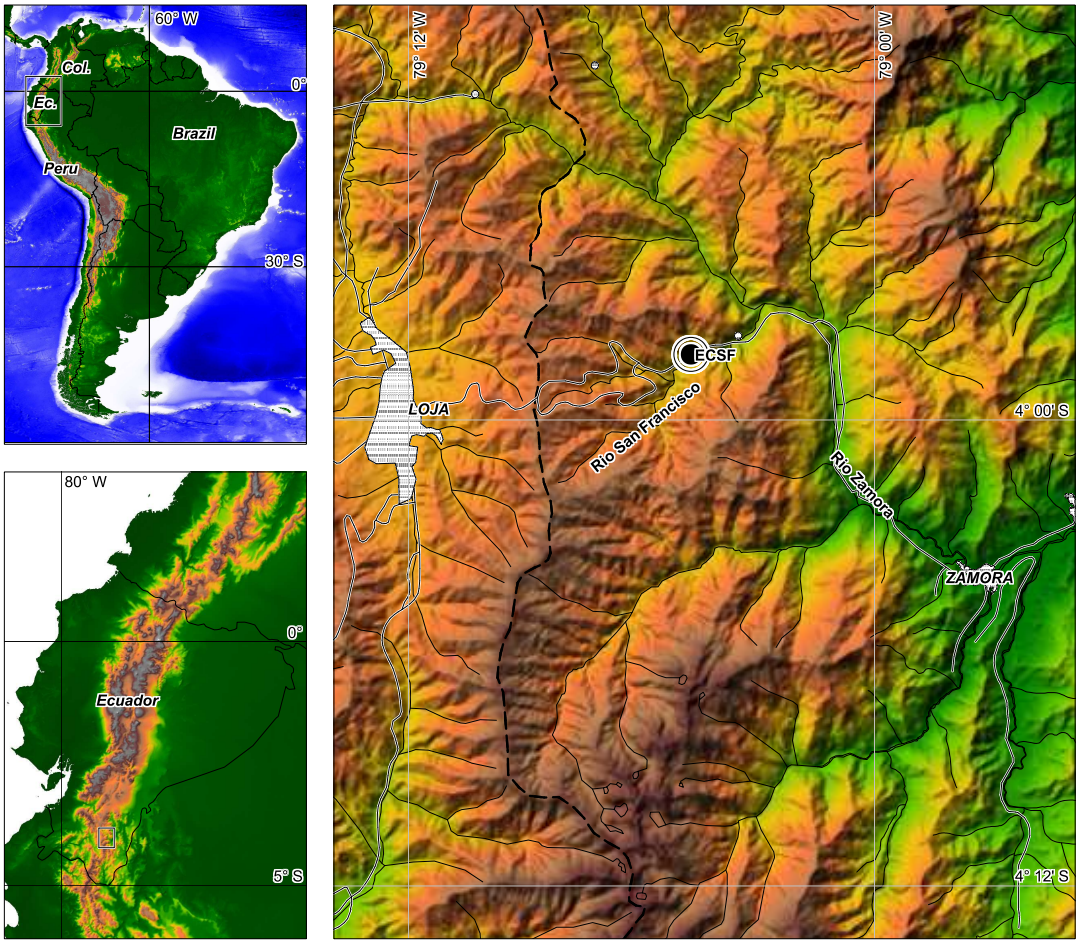

Figure 1.2: The study area in South Ecuador. Altitudinal data from ETOPO5 (National Oceanic and Atmospheric Administration (NOAA), 1988), GTOPO30 (Earth Resources Observation and Science (EROS) Center) and the Shuttle Radar Topography mission (SRTM, Jarvis et al., 2008)

1.4 Study Area

The study area of the research unit FOR 816 is situated in the Andes of southern Ecuador (figure 1.2). Field studies are undertaken within the Reserva Biológica San Francisco (RBSF). This protected area is maintained by the non-governmental organization of Nature & Culture International which also maintains and provides the central research facility Estación Scientífica San Francisco (ECSF). The area is located in the valley of the Rio San Francisco between the two provincial capitals of Loja and Zamora. The altitude starts from 1800 m above sea level (asl) at the valley floor and rises up to 3200 m asl at the Cerro del Consuelo. A comprehensive overview of the whole study area is given by (Beck et al., 2008c).

The perhumid climate of the valley is characterized with a strong altitudinal gradient in all relevant elements (windspeed, winddirection, incoming radiation, humidity, precipitation and temperature). Seasonal variability in cloud cover and precipitation is also found due to the unique position of the research area in the Andes between the Amazonian lowlands and the Pacific coast. The distinct topographic features have severe influence on the local climatic conditions as well (Bendix et al., 2008b,a).

The rugged and steep terrain is dominated on one hand by natural mountain rainforests superseded by Subpáramo and Páramo vegetation in the higher altitudes (Homeier et al., 2008). On the other hand anthropogenic replacement systems mainly in the form of pastures, its successional stages and reforestration areas with exotic trees (pines and eucalyptus) define the landscape (Beck et al., 2008b). The pastures are dominated by *Setaria sphacelata* and are occasionally burnt in some areas. Abandoned pasture areas are completely overgrown by the invasive southern bracken fern *Pteridium arachnoideum* (Hartig & Beck, 2003).

The model domain is set to a bigger area than the RBSF to cover the whole catchment of the Rio San Francisco and adjacent valleys in which new settlement activities are taken place. Human induced and natural landslides are a common factor of disturbance to the ecosystem (Bussmann et al., 2008).

The vegetation in the research area is very heterogeneous. The natural forest can be subdivided into 4 vegetation types by the means of botanical composition and topographic features (hillside situation) (Homeier et al., 2008). Forest type I dominates the valley bottom and major ravines from 1800 m up to 2200 m asl. Forest type II is described as forest along ridges and upper slopes from approximately 1900 m to 2100 m asl. Forest Type III continues on the ridges and upper slopes from 2100 m to 2250 m asl. Forest type IV is monodominated by *Purdiaea nutans* and stretches from 2250 m up to the timberline at around 2700 m asl. The Subpáramo is dominated by shrubs also called evergreen elfin forest and rises from the timberline up to approx. 3150 m asl.

An additional forest type is mentioned in an earlier description of the vegetation units. The type covers the forest in the ravines from 2100 m asl to 2700 m asl but is merged to the corresponding forest types I–IV later (Homeier et al., 2002; Homeier, 2004). Only chapter 3 still refers to the older classification.

References

Barthlott, W., A. Hostert, G. Kier, W. Küper, H. Kreft, J. Mutke, M. Rafiqpoor & J. H. Sommer: (2007): Geographic patterns of vascular plant diversity at continental to global scale, *Erdkunde*, *61*, 305–315.

Beck, E., J. Bendix, I. Kottke, F. Makeschin & R. Mosandl (eds.): (2008a): *Gradients in a Tropical Mountain Ecosystem of Ecuador*, *Ecological Studies*, vol. 198, Springer, Berlin, Heidelberg.

Beck, E., K. Hartig & K. Roos: (2008b): Forest clearing by slash and burn, in Beck, E., J. Bendix, I. Kottke, F. Makeschin & R. Mosandl (eds.) *Gradients in a Tropical Mountain Ecosystem of Ecuador*, *Ecological Studies*, vol. 198, chap. 28, 387–390, Springer, Berlin, Heidelberg.

Beck, E., F. Makeschin, F. Haubrich, M. Richter, J. Bendix & C. Valerezo: (2008c): The ecosystem (reserva biológica san francisco), in Beck, E., J. Bendix, I. Kottke, F. Makeschin & R. Mosandl (eds.) *Gradients in a Tropical Mountain Ecosystem of Ecuador*, *Ecological Studies*, vol. 198, chap. 1, Springer, Berlin, Heidelberg.

Bendix, J., R. Rollenbeck, P. Fabian, P. Emck, M. Richter & E. Beck: (2008a): Climatic variability, in Beck, E., J. Bendix, I. Kottke, F. Makeschin & R. Mosandl (eds.) *Gradients in a Tropical Mountain Ecosystem of Ecuador*, *Ecological Studies*, vol. 198, chap. 20, 281–290, Springer, Berlin, Heidelberg.

Bendix, J., R. Rollenbeck, M. Richter, P. Fabian & P. Emck: (2008b): Climate, in Beck, E., J. Bendix, I. Kottke, F. Makeschin & R. Mosandl (eds.) *Gradients in a Tropical Mountain Ecosystem of Ecuador*, *Ecological Studies*, vol. 198, chap. 8, 63–73, Springer, Berlin, Heidelberg.

Bonan, G. B.: (2008): Forests and climate change: Forcings, feedbacks, and the climate benefits of forests, *Science*, *320*, 1444–1449.

Brehm, G., K. Fiedler, C. Häuser & H. Dalitz: (2008a): Methodological challenges of a megadiverse ecosystem, in Beck, E., J. Bendix, I. Kottke, F. Makeschin & R. Mosandl (eds.) *Gradients in a Tropical Mountain Ecosystem of Ecuador*, *Ecological Studies*, vol. 198, chap. 5, 41–47, Springer, Berlin, Heidelberg.

Brehm, G., J. Homeier, K. Fiedler, I. Kottke, J. Illig, N. M. Nöske, F. Werner & S.-W. Breckle: (2008b): Mountain rain forests in southern ecuador as a hotspot of biodiversity – limited knowledge and diverging patterns,

in Beck, E., J. Bendix, I. Kottke, F. Makeschin & R. Mosandl (eds.) *Gradients in a Tropical Mountain Ecosystem of Ecuador*, *Ecological Studies*, vol. 198, chap. 2, Springer, Berlin, Heidelberg.

Brooks, T. M., R. A. Mittermeier, G. A. B. da Fonseca, J. Gerlach, M. Hoffmann, J. F. Lamoreux, C. G. Mittermeier, J. D. Pilgrim & A. S. L. Rodrigues: (2006): Global biodiversity conservation priorities, *Science*, *313*, 58–61.

Brummitt, N. & E. N. Lughadha: (2003): Biodiversity: Where's hot and where's not, *Conservation Biology*, *17*, 1442–1448.

Bussmann, R., W. Wilcke & M. Richter: (2008): Landslides as important disturbance regimes – causes and regeneration, in Beck, E., J. Bendix, I. Kottke, F. Makeschin & R. Mosandl (eds.) *Gradients in a Tropical Mountain Ecosystem of Ecuador*, *Ecological Studies*, vol. 198, chap. 24, 319–330, Springer, Berlin, Heidelberg.

Colwell, R. K., G. Brehm, C. L. Cardelus, A. C. Gilman & J. T. Longino: (2008): Global warming, elevational range shifts, and lowland biotic attrition in the wet tropics, *Science*, *322*, 258–261.

de Groot, R. S., M. A. Wilson & R. M. J. Boumans: (2002): A typology for the classification, description and valuation of ecosystem functions, goods and services, *Ecological Economics*, *41*, 393–408.

Druyan, L. M., M. Fulakeza & P. Lonergan: (2002): Dynamic downscaling of seasonal climate predictions over brazil, *Journal of Climate*, *15*, 3411–3426.

Feddema, J. J., K. W. Oleson, G. B. Bonan, L. O. Mearns, L. E. Buja, G. A. Meehl & W. M. Washington: (2005): The importance of land-cover change in simulating future climates, *Science*, *310*, 1674–1678.

Foley, J. A., R. DeFries, G. P. Asner, C. Barford, G. Bonan, S. R. Carpenter, F. S. Chapin, M. T. Coe, G. C. Daily, H. K. Gibbs, J. H. Helkowski, T. Holloway, E. A. Howard, C. J. Kucharik, C. Monfreda, J. A. Patz, I. C. Prentice, N. Ramankutty & P. K. Snyder: (2005): Global consequences of land use, *Science*, *309*, 570–574.

Gibbard, S., K. Caldeira, G. Bala, T. J. Phillips & M. Wickett: (2005): Climate effects of global land cover change, *Geophysical Research Letters*, *32*, L23705.

Hartig, K. & E. Beck: (2003): The bracken fern (Pteridium arachnoideum (Kaulf.) Maxon) dilemma in the andes of southern ecuador, *Ecotropica*, *9*, 3–13.

Homeier, J.: (2004): *Baumdiversität, Waldstruktur und Wachstumsdynamik zweier tropischer Bergregenwälder in Ecuador und Costa Rica*, *Dissertationes Botanicae*, vol. 391, Borntraeger, Stuttgart, dissertation Universität Bielefeld.

Homeier, J., H. Dalitz & S.-W. Breckle: (2002): Waldstruktur und baumartendiversität im montanen regenwald der estación científica san francisco in südecuador, *Berichte der Reinhold-Tüxen Gesellschaft*, *14*, 109–118.

Homeier, J., F. Werner, S. Gradstein, S.-W. Breckle & M. Richter: (2008): Potential vegetation and floristic composition of andean forests in south ecuador, with a focus on the rbsf, in Beck, E., J. Bendix, I. Kottke, F. Makeschin & R. Mosandl (eds.) *Gradients in a Tropical Mountain Ecosystem of Ecuador*, *Ecological Studies*, vol. 198, 87–100, Springer, Berlin.

Jarvis, A., H. Reuter, A. Nelson & E.Guevara: (2008): Hole-filled seamless srtm data v4, online, URL `http://srtm.csi.cgiar.org`, International Centre for Tropical Agriculture (CIAT).

Liede-Schumann, S. & S.-W. Breckle (eds.): (2008): *Provisional Checklists of Flora and Fauna of the San Francisco Valley and its Surroundings*, *Ecotropical Monographs*, vol. 4.

Makeschin, F., F. Haubrich, M. Abiy, J. Burneo & T. Klinger: (2008): Pasture management and natural soil regeneration, in Beck, E., J. Bendix, I. Kottke, F. Makeschin & R. Mosandl (eds.) *Gradients in a Tropical Mountain Ecosystem of Ecuador*, *Ecological Studies*, vol. 198, chap. 31, 413–423, Springer, Berlin, Heidelberg.

Misra, V., P. A. Dirmeyer & B. P. Kirtman: (2003): Dynamic downscaling of seasonal simulations over south america, *Journal of Climate*, *16*, 103–117.

Naidoo, R., A. Balmford, R. Costanza, B. Fisher, R. E. Green, B. Lehner, T. R. Malcolm & T. H. Ricketts: (2008): Global mapping of ecosystem services and conservation priorities, *Proceedings of the National Academy of Sciences*, *105*, 9495–9500.

National Oceanic and Atmospheric Administration (NOAA): (1988): Digital relief of the surface of the earth, Data Announcement 88-MGG-02, NOAA, National Geophysical Data Center, Boulder, CO.

Pohle, P. & A. Gerique: (2008): Sustainable and non-sustainable use of natural resources by indigenous and local communities, in Beck, E., J. Bendix, I. Kottke, F. Makeschin & R. Mosandl (eds.) *Gradients in a Tropical Mountain Ecosystem of Ecuador*, *Ecological Studies*, vol. 198, chap. 25, 347–361, Springer, Berlin, Heidelberg.

Sala, O. E., I. Chapin, F. Stuart, J. J. Armesto, E. Berlow, J. Bloomfield, R. Dirzo, E. Huber-Sanwald, L. F. Huenneke, R. B. Jackson, A. Kinzig, R. Leemans, D. M. Lodge, H. A. Mooney, M. Oesterheld, N. L. Poff, M. T. Sykes, B. H. Walker, M. Walker & D. H. Wall: (2000): Global biodiversity scenarios for the year 2100, *Science*, *287*, 1770–1774.

Shin, D. W., J. G. Bellow, T. E. LaRow, S. Cocke & J. J. O'Brien: (2006): The role of an advanced land model in seasonal dynamical downscaling for crop model application, *Journal of Applied Meteorology and Climatology*, *45*, 686–701.

Thuiller, W.: (2007): Biodiversity: Climate change and the ecologist, *Nature*, *448*, 550–552.

Weber, M., S. Günter, N. Aguirre, B. Stimm & R. Mosandl: (2008): Reforestation of abandoned pastures: Silvicultural means to accelerate forest recovery and biodiversity, in Beck, E., J. Bendix, I. Kottke, F. Makeschin & R. Mosandl (eds.) *Gradients in a Tropical Mountain Ecosystem of Ecuador*, *Ecological Studies*, vol. 198, chap. 34, 447–457, Springer, Berlin, Heidelberg.

Zhao, M., A. Pitman & T. Chase: (2001): The impact of land cover change on the atmospheric circulation, *Climate Dynamics*, *17*, 467–477.

2 Conceptual Design

2.1 Land Surface Models

2.1.1 The Role of Land Surface Models

The terms *Land surface models* (LSM) and *soil-vegetation-atmosphere-transfer* (SVAT) schemes are often used synonymously. A clearly separated functionality is not observed but LSM may look beyond the surface coverage concerning anthropogenic classes. The main role of these models is to provide the boundary conditions at the land-atmosphere interface. Several partitions of energy, water and matter fluxes are calculated from the atmosphere into the surface layer and back again closing the important ecological cycles (Bonan, 2008a).

Furthermore these types of models are applied to study ecological processes in the soil column or within the vegetation layer of its own (e.g. Thornton & Zimmermann, 2007; Levis & Bonan, 2004; Barlage & Zeng, 2004; Lawrence & Slater, 2005). In new models all relevant partitions are calculated and can be used without a coupling to a climate or at least an atmospheric model. A dynamical downscaling of climatological features or data assimilation is possible and may be used in appended ecological studies (Shin et al., 2006; Wilby & Wigley, 1997; Rodell et al., 2004; Zhou et al., 2006; Wood et al., 2004).

A real advantage of numeric models in contrast to in-situ measurements or field experiments is the possibility to investigate processes under changing conditions, e.g. land cover changes that cannot not be done in reality (deforestation) or for a longer time period (several hundred years in the future and also in the past) (Gibbard et al., 2005; Otto-Bliesner et al., 2006a,b).

2.1.2 Evolution of Land Surface Models

The evolution of land models started in the 1960s and is still under development. Until now 4 generations of model concepts can be distinguished (Bonan, 2008b; Pitman, 2003; Sellers et al., 1997):

- First generation models: Bucket models for the water cycle, a simple solution of solving the energy balance, no influence of the vegetation, no soil heat storage. Examples are presented in the model of Manabe (1969) and the boundary

condition of the first version of the NCAR Community Climate Model (CCM1, Williamson et al., 1987).

- Second generation models: addition of vegetation and a hydrological cycle. Examples are Biosphere-Atmosphere-Transfer-Scheme (BATS, Dickinson et al., 1986) and Simple Biosphere Model (SiB, Sellers et al., 1986).

- Third generation models: addition of photosynthesis. Examples are the Land Surface Model (LSM, Bonan, 1995, 1996) and the planetary boundary layer (PBL) of the global circulation model (GCM) of Colorado State University (CSU, Denning et al., 1995).

- Fourth generation models: addition of the carbon cycle and dynamic vegetation. Examples are the fully coupled Global Environmental and Ecological Simulation of Interactive Systems - Integrated Biosphere Simulator, a climate-vegetation model (GENESIS–IBIS, Levis et al., 1999, 2000; Foley et al., 1996) and the GCM of the Hadley Center (HadCM3) coupled to a dynamic vegetation model(TRIFFID, Cox et al., 2000).

- further developments: a biogeochemical cycle and human systems in the surface parametrization (urban model). Example is the current version 4.0 of the Community Land Model (CLM, Oleson et al., 2010)

2.1.3 Overview of Land Surface Models

A comprehensive overview and comparison of numerously publicized models is not available. A lot of the studies compare only a limited number of models directly and often focus on a special issue (e.g. Zeng et al., 2002; Chen et al., 1996; Abramowitz et al., 2008). The biggest efforts are made by the *Project for Intercomparison of Land-Surface Parameterization Schemes* (PILPS, Pitman et al., 1999; Qu et al., 1998; Henderson-Sellers et al., 2003), the *Coupled Carbon Cycle Climate Model Intercomparison Project* (C^4MIP, Friedlingstein et al., 2006) and the *AMMA Land surface Model Intercomparison Project* (ALMIP, AMMA=*African Monsoon Multidisciplinary Analysis*, Boone et al., 2009). These international organized studies lead to improvements in the general model parametrization and are not carried out to investigate *good* or *bad* models. Unfortunately, the CLM was only covered by its predecessors through these intercomparisons. However it has shown its scientific eligibility through other studies (Lawrence & Chase, 2010; Dickinson et al., 2006; Bonan et al., 2002b; Bonan & Levis, 2006; Collins et al., 2006; Thornton et al., 2007, 2009).

The selection of one of the published models to use within the research unit is a cascading task satisfying following priority list:

- The source code has to be freely available to modify or to add special features and to fully comprehend the methods and algorithms used.
- The vegetation has to be parametrized in a manner that the regional needs could be implemented, the favourable way would be the use of plant functional types rather than discrete vegetational units like biomes.
- The scaling of the model should be in a dynamic way allowing a fine mesh of vegetation and soil properties in a coarser mesh of atmospheric forcing.
- The model should be still under current development to have the chance to contact the collaborators if necessary.
- All important partitions of the ecological cycles (energy, water, nutrients) should be calculated.
- The model should run alone with a forcing dataset of atmospheric variables and favourable also in a coupled setup in connection with an atmospheric or climatological model.

2.1.4 Characteristics of the CLM

The CLM was first mentioned as *Common Land Model* (Dai et al., 2003) but was renamed in the structure of the NCAR Community Climate System Model (CCSM) family to *Community Land Model* (Zeng, 2003). The parallel developments of the model and a time delay during publication processes lead to an earlier mention of the Community Land Model Bonan et al. (2002b). Generally the CLM is a combination of 3 preexisting land surface parametrization: BATS, LSM and the Institute of Atmospheric Physics, Chinese Academy of Sciences land model (IAP94, Dai & Zeng, 1997). Up to now (June 2010) it has 5 major releases (2.0, 2.1, 3.0, 3.5, 4.0) with several improvements both in parametrization and software engineering aspects. For a comprehensive overview of the model development see NCAR Terrestrial Science Section (2010).

The technical implementation of the CLM is described in Oleson et al. (2004, 2010) with further improvements described by Oleson et al. (2008); Stöckli et al. (2008); Lawrence et al. (2010). Figure 2.1 gives a schematic overview of the single partitions of the model.

Spatial heterogeneity

The CLM is organized in multiple nested subgrids (see fig. 2.2). Atmospheric forcing is applied to a gridcell which can be subdivided in up to 5 landunits (glacier, wetland, lake, urban, vegetated). These landunits imply different calculation of the various processes. All landunits can be split in multiple columns. In the current

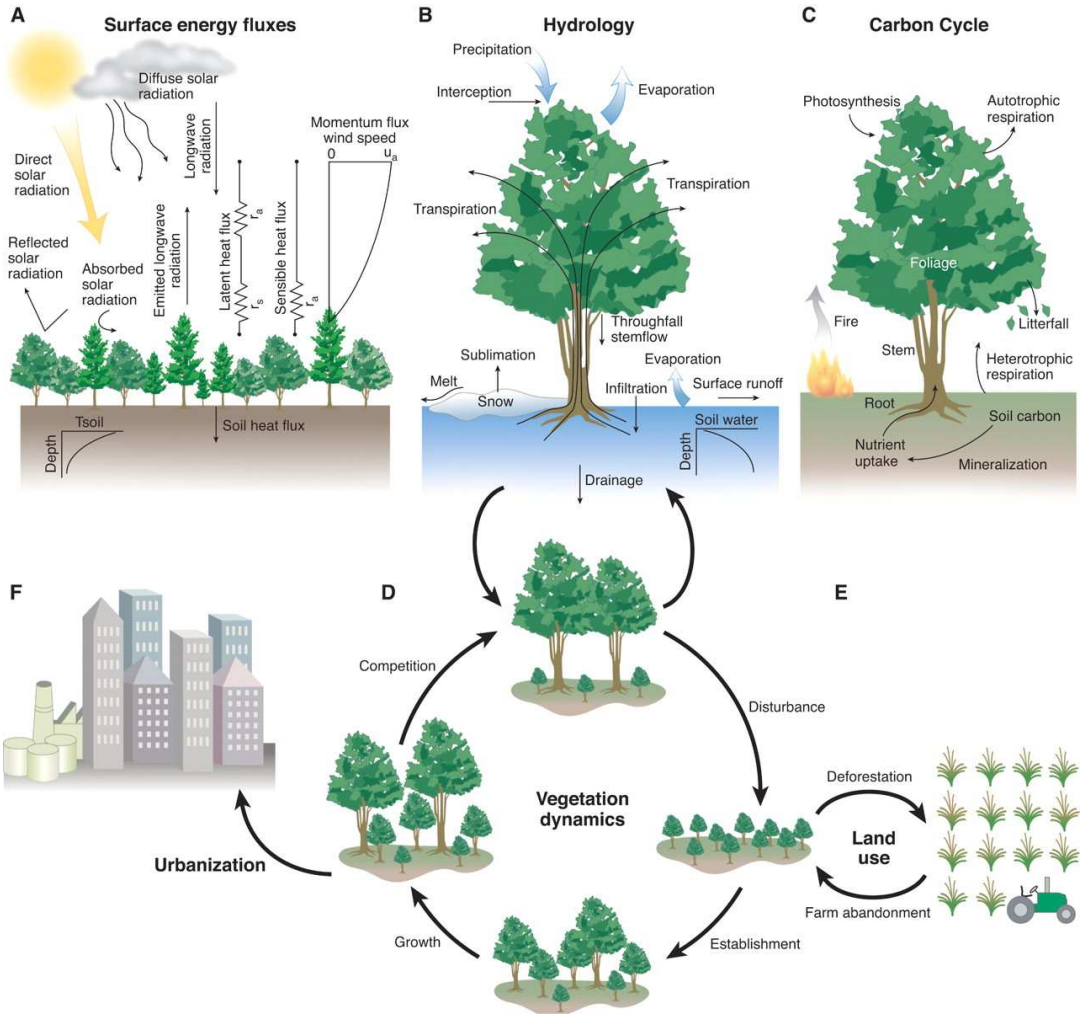

Figure 2.1: Schematic overview of all processed partitions of the CLM (Bonan, 2008b).

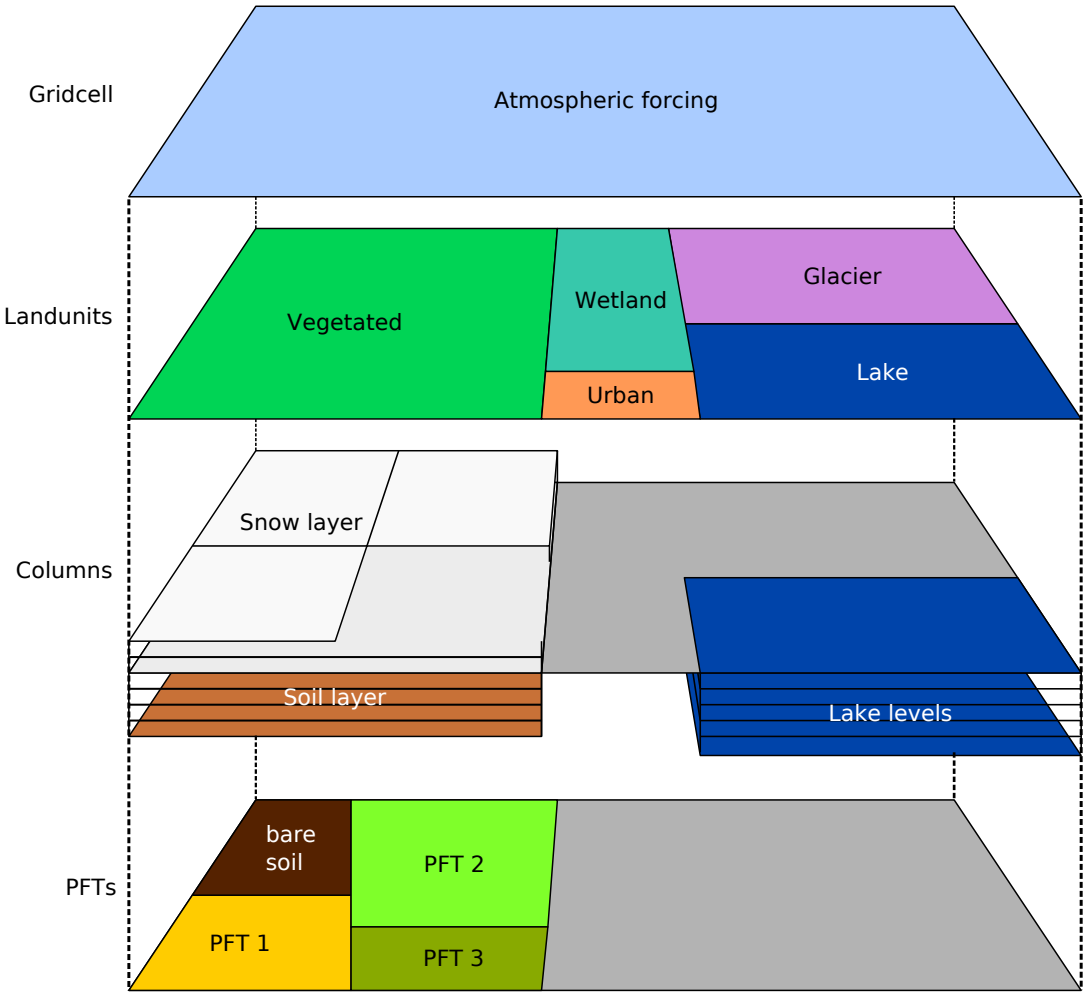

Figure 2.2: Schematic overview of the nested subgrid system of the CLM.

version only the urban landunit is split into 5 columns all others contain just 1. The column of the vegetated landunit represents the information on the soil (15 layers) and snow (up to 5 layers). The column's next subgrid is the PFT level calculating all biogeophysical and biogeochemical processes concerning the plantcover but also the bare soil.

Energy balance

The energy balance is solved for different surfaces from the landunits, the canopy (i.e. the vegetation), the soil and the snow layer. It includes the absorption, reflection and transmittance of incoming solar radiation, the absorption and reflection of longwave radiation, the sensible and latent heat fluxes from the ground and the vegetation as well as the momentum using the Monin-Obukhov similarity theory (Zeng et al.,

1998).

Water balance

The water balance is solved for the surface and separately for the soil and snow layers. The canopy hydrology separates into throughfall, drip and interception. The soil water distribution is calculated using Darcy's Law and Richards equation (Zeng & Decker, 2009). Surface and sub-surface runoff is modelled by simplified TOPMODEL approach (Niu et al., 2005). Routing the surface runoff to the ocean is calculated using a river transport model (RTM, Branstetter, 2001).

Carbon-Nitrogen balance

The photosynthesis and respiration rate is calculated using stomatal resistance in two layers of leaf area (sunlit and shaded), also called two-big-leaf model (Sellers et al., 1996). A fully coupled carbon and nitrogen model (adapted from the Biome-BGC, Thornton et al., 2002; Thornton & Rosenbloom, 2005) consists of 20 single carbon pools and 19 nitrogen pools.

Dynamic vegetation

On one hand the phenology is taken into account supplying a seasonal shift within the leaf area index (LAI) of the single PFTs. On the other hand a transient land cover change can be implemented, changing the spatial distribution of PFTs over time with a forcing dataset of landcover or a dynamic global vegetation model (DGVM) can be added (Levis et al., 2004).

Additional calculations

More partitions in the CLM are calculated with minor priority for this study as follows:

- Dust depositions and fluxes
- Emission of biogenic volatile organic compounds (BVOCs)
- Urban energy balance and fluxes.

The primary intention to develop CLM is to provide a state of the art boundary layer for global climate models but a ongoing task is to examine a fine mesh setup on a regional scale. The work is still in progress and bases on the work of Hahmann & Dickinson (2001).

2.1.5 Decision Making of the Land Surface Model

The CLM covers all aspects of the presented priority list and benefits from a very eager development community reflected in the major updates since its first release in 2002. A lot of the different models are based on the same physical principles and algorithms anyway, so that the availability of the source code and the flexible and dynamic parametrization of the vegetation with plant functional types tipped the scales. Especially the implementation of the nested grid approach makes it very suitable for a regional setup.

2.2 Plant Functional Types

2.2.1 The Concept of PFT

A significant feature within the CLM is the parametrization of the vegetation cover using plant functional types. The development of the concept of PFTs dates back to the exploration of the New World in the 19th century. Ustin & Gamon (2010) gives a comprehensive overview of the history of functional classification of vegetation and is summarized below.

Alexander von Humboldt's classification of species-based, structural classes relating physiognomic forms to the physical environment leads to the first functional classification of Andreas F. W. Schimper at the beginning of the 20th century. Further developments were finalized in the concept of life forms from Raunkiaer. This concept is still present in a lot of fundamental books in vegetation science (e.g. Ellenberg, 1996; Huggett, 1998). An improved understanding of plant physiology in connection with the responses of plants to environmental conditions and plant distribution leads to the formulation of the 'functional convergence hypothesis'(Field, 1991). This theory applied to PFT shows that there is a linkage between the peculiarity of optical, morphological, phenological and physiological traits of plants.

The observing scale (from leaf over stand to landscape or biome) is an important factor to select the traits for functional convergence. Consequently, there is no general procedure to distinguish functional types, rather the functional traits have to be assigned separately for each purpose (Gitay & Noble, 1997). Nevertheless, PFTs have shown there ability to balance between abstraction of the vegetation cover and detail of processes in various scales of ecosystems (Smith et al., 1997).

Classical vegetation classifications are based primarily on climatic and edaphic circumstances and cause generally discrete classes (e.g. Breckle, 2002; Schultz, 2005; Matthews, 1983). The term *functional type* implicate discrete classes as well but the combination of PFTs makes it possible to describe the vegetation as a continuous flow. Particularly, mixed biomes are presented as the combination of two or more PFTs. One example (see fig2.3) is the description of Savannah made from grass and single trees with two PFTs in a variable combination. This allows

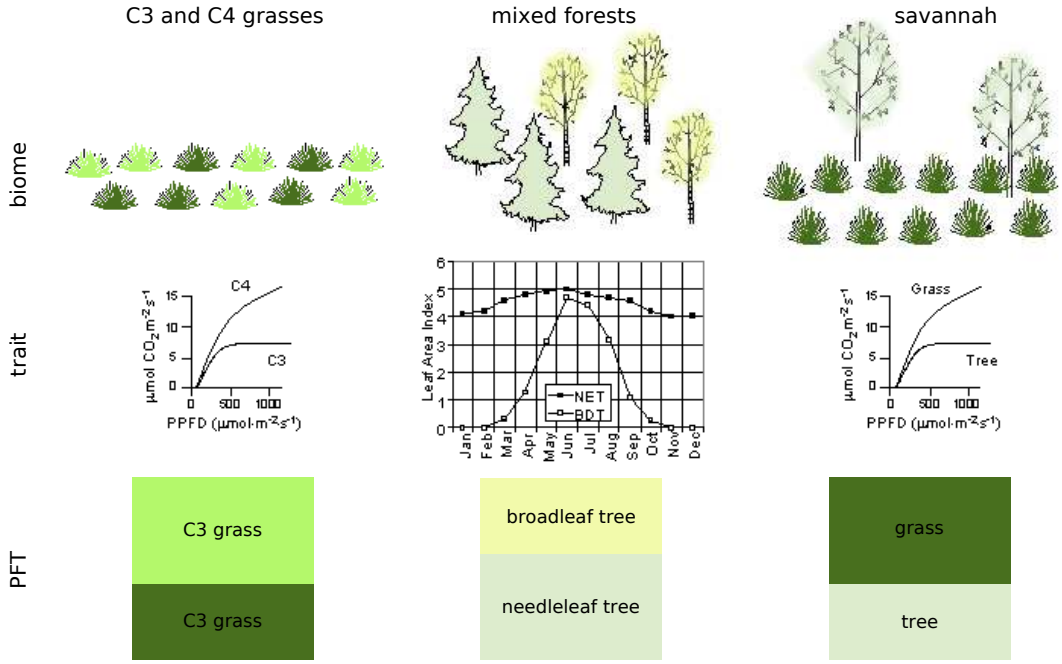

Figure 2.3: Distribution of PFTs and characteristic traits to describe mixed biomes. For further information see text (adapted and modified from NCAR Terrestrial Science Section, 2010).

a smooth changeover from plain grasslands to forests instead of discrete classes of the biomes. Other examples illustrated are the description of a mixed forest with broadleaf and needleleaf trees and grasslands made of C3 and C4 grasses. For all 3 mixed biomes a exemplary functional trait is included to clarify the difference in ecological functioning.

Over the years a lot of scientific papers have been presented on the decision which traits and which plants should be used to distinguish PFTs. Cornelissen et al. (2003) gives a comprehensive overview on methodical approaches to determine all kinds of functional traits. The 16 global defined PFTs of the CLM are presented in the work of Bonan et al. (2002a). PFTs are not limited to the use within models but have found application in a variety of fields of ecological research (Woodward & Cramer, 1996; Lavorel & Cramer, 1999; Duckworth et al., 2000; Pausas et al., 2003). de Bello et al. (2010) review the capabilities of functional types to assess ecosystem services.

There is still criticism on the concept of PFTs (e.g. Lavorel et al., 2007). The main difficulty to determine and to apply PFTs is the lack of a unique method of classification. Especially, this comes true if the geographical area is large and a lot of intermediate traits exist like in megadiverse ecosystems (Lavorel et al., 1997; Westby & Leishman, 1997). Another problem is the large amount of suggested

traits and the deficient foundation of values for PFT parameters (Prentice et al., 2007).

2.2.2 PFTs for the Study Area

Taking the considerations in chapter 2.2.1 into account, the determination of PFTs in the study area is not an easy task. The traits for classification are defined by the PFT parameters of the CLM. The complete determination of the values of these parameters for the species of this megadiverse ecosystem is not practicable. Hence keeping the classes from the ecological survey as described in chapter 1.4 seems to be the appropriate way. A systematic measuring of some functional parameters can be carried out not until a sensitivity study is conducted as presented in chapter 4 to specify the most significant traits regarding the model output.

A priori some PFTs can be very well distinguished (pastures, succession with bracken fern) because of their obvious functional response where other PFTs cannot (different forest types or specific trees within the forest). The crux is to determine the functional types on one hand and delineate the spatial distribution of the PFTs on the other hand.

To start of with the CLM-PFTs for the use within the study area will be defined by the ecologically derived 4 forest types, the pastures (grasslands), the successional stages of bracken fern as well as bushes and the Subpáramo.

2.3 Implementation

All considerations mentioned so far imply a development of a running and tested land surface model system in a landscape scale. The geo-ecological fluxes of water and energy have to be calculated to analyze the the value of ecosystem services under changing environmental conditions. Figure 2.4 is illustrating the concurrence of the single steps presented in the following chapters as explained in the WPs (see section 1.2).

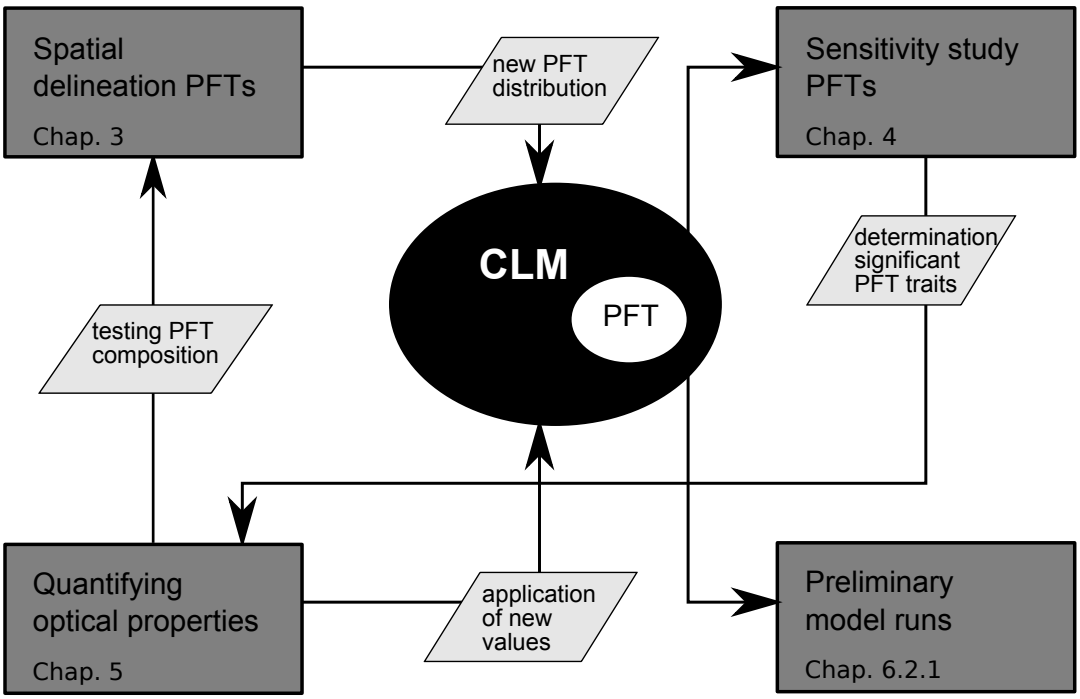

Figure 2.4: Conceptual design of the study.

References

Abramowitz, G., R. Leuning, M. Clark & A. Pitman: (2008): Evaluating the performance of land surface models, *Journal of Climate*, *21*, 5468–5481.

Barlage, M. & X. Zeng: (2004): The effects of observed fractional vegetation cover on the land surface climatology of the community land model, *Journal of Hydrometeorology*, *5*, 823–830.

Bonan, G.: (1996): A land surface model (LSM version 1.0) for ecological, hydrological and atmospheric studies: Technical description and user's guide, Technical Note NCAR/TN-417+STR, National Center for Atmospheric Research (NCAR).

Bonan, G.: (2008a): *Ecological Climatology - Concepts and applications*, 2nd edn., Press Syndicat of the University of Cambridge.

Bonan, G., S. Levis, L. Kergoat & K. Oleson: (2002a): Landscapes as patches of plant functional types: An integrating concept for climate and ecosystem models, *Global Biochemical Cycles*, *16 No.2*, 5–1–5–30.

Bonan, G., K. Oleson, M. Vertenstein, S. Levis, X. Zeng, Y. Dai, R. Dickinson & Z.-L. Yang: (2002b): The land surface climatology of the community land model coupled to the NCAR community climate model, *Journal of Climate*, *15*, 3123–3149.

Bonan, G. B.: (1995): Land-atmosphere co_2 exchange simulated by a land surface process model coupled to an atmospheric general circulation model, *Journal of Geophysical Research*, *100*, 2817–2831.

Bonan, G. B.: (2008b): Forests and climate change: Forcings, feedbacks, and the climate benefits of forests, *Science*, *320*, 1444–1449.

Bonan, G. B. & S. Levis: (2006): Evaluating aspects of the community land and atmosphere models (CLM3 and CAM3) using a dynamic global vegetation model, *Journal of Climate*, *11*, 2290–2301.

Boone, A., B. Decharme, F. Guichard, P. de Rosnay, G. Balsamo, A. Beljaars, F. Chopin, T. Orgeval, J. Polcher, C. Delire, A. Ducharne, S. Gascoin, M. Grippa, L. Jarlan, L. Kergoat, E. Mougin, Y. Gusev, O. Nasonova, P. Harris, C. Taylor, A. Norgaard, I. Sandholt, C. Ottlé, I. Poccard-Leclercq, S. Saux-Picart & Y. Xue: (2009): The amma land surface model intercomparison project (almip), *Bulletin of the American Meteorological Society*, *90*, 1865–1880.

Branstetter, M.: (2001): *2001. Development of a parallel river transport algorithm and applications to climate studies. Ph.D. dissertation,*, Ph.D. thesis, University of Texas at Austin.

Breckle, S.-W.: (2002): *Walter's Vegetation of the Earth*, 4th edn., Ulmer, Stuttgart.

Chen, F., K. Mitchell, J. Schaake, Y. Xue, H.-L. Pan, V. Koren, Q. Y. Duan, M. Ek & A. Betts: (1996): Modeling of land surface evaporation by four schemes and comparison with fife observations, *Journal of Geophysical Research*, *101*, 7251–7268.

Collins, W. D., C. M. Bitz, M. L. Blackmon, G. B. Bonan, C. S. Bretherton, J. A. Carton, P. Chang, S. C. Doney, J. J. Hack, T. B. Henderson, J. T. Kiehl, W. G. Large, D. S. McKenna, B. D. Santer & R. D. Smith: (2006): The community climate system model version 3 (CCSM3), *Journal of Climate*, *11*, 2122–2143.

Cornelissen, J. H. C., S. Lavorel, E. Garnier, S. Díaz, N. Buchmann, D. E. Gurvich, P. B. Reich, H. ter Steege, H. D. Morgan, M. G. A. van der Heijden, J. G. Pausas & H. Poorter: (2003): A handbook of protocols for standardised and easy measurement of plant functional traits worldwide, *Australian Journal of Botany*, *51*, 335–380.

Cox, P. M., R. A. Betts, C. D. Jones, S. A. Spall & I. J. Totterdell: (2000): Acceleration of global warming due to carbon-cycle feedbacks in a coupled climate model, *Nature*, *408*, 184–187.

Dai, Y. & Q. Zeng: (1997): A land surface model (IAP94) for climate studies. part i: Formulation and validation in off-line experiments, *Advances in Atmospheric Science*, *14*, 433–460.

Dai, Y., X. Zeng, R. Dickinson, I. Baker, G. Bonan, M. Bosilovich, A. S. Denning, P. Dirmeyer, P. Houser, G. Niu, K. Oleson, C. Schlosser & Z.-L. Yang: (2003): The common land model, *Bulletin American Meteorological Society*, *84*, 1013–1023.

de Bello, F., S. Lavorel, S. Díaz, R. Harrington, J. Cornelissen, R. Bardgett, M. Berg, P. Cipriotti, C. Feld, D. Hering, P. Martins da Silva, S. Potts, L. Sandin, J. Sousa, J. Storkey, D. Wardle & P. Harrison: (2010): Towards an assessment of multiple ecosystem processes and services via functional traits, *Biodiversity and Conservation, OnlineFirst*.

Denning, A. S., I. Y. Fung & D. Randall: (1995): Latitudinal gradient of atmospheric co_2 due to seasonal exchange with land biota, *Nature*, *376*, 240–243.

Dickinson, R., K. Oleson, G. Bonan, F. Hoffman, P. Thornton, M. Vertenstein, Z. Yang & X. Zeng: (2006): The community land model and its climate statistics as a component of the community climate system model, *Journal of Climate*, *19*, 2302–2324.

Dickinson, R. E., A. Henderson-Sellers, P. J. Kennedy & M. F. Wilson: (1986): Biosphere-atmosphere transfer scheme (BATS) for the NCAR community climate model, Technote, National Center for Atmospheric Research (NCAR).

Duckworth, J. C., M. Kent & P. M. Ramsay: (2000): Plant functional types: an alternative to taxonomic plant community description in biogeography?, *Progress in Physical Geography*, *24*, 515–542.

Ellenberg, H.: (1996): *Vegetation Mitteleuropas mit den Alpen*, 5th edn., Ulmer, Stuttgart, in German.

Field, C. B.: (1991): Ecological scaling of carbon gain to stress and resource availability, in Mooney, H. A., W. E. Winner & E. J. Pell (eds.) *Response of plants to multiple stresses*, 35–65, Academic Press, San Diego, CA.

Foley, J. A., I. C. Prentice, N. Ramankutty, S. Levis, D. Pollard, S. Sitch & A. Haxeltine: (1996): An integrated biosphere model of land surface processes, terrestrial carbon balance, and vegetation dynamics, *Global Biogeochemical Cyclesa*, *10*, 603–628.

Friedlingstein, P., P. M. Cox, R. A. Betts, L. Bopp, W. Von Bloh, V. Brovkin, P. Cadule, S. Doney, M. Eby, I. Fung, G. Bala, J. John, C. D. Jones, F. Joos, T. Kato, M. Kawamiya, W. Knorr, K. Lindsay, H. D. Matthews, T. Raddatz, P. Rayner, C. Reick, E. Roeckner, K.-G. Schnitzler, R. Schnur, K. Strassmann, A. J. Weaver, C. Yoshikawa & N. Zeng: (2006): Climate-carbon cycle feedback analysis: results from the c^4mip model intercomparison, *Journal of Climate*, *19*, 3337–3353.

Gibbard, S., K. Caldeira, G. Bala, T. J. Phillips & M. Wickett: (2005): Climate effects of global land cover change, *Geophysical Research Letters*, *32*, L23705.

Gitay, H. & I. R. Noble: (1997): What are functional types and how should we seek them?, in Smith, T. M., H. H. Shugart & F. I. Woodward (eds.) *Plant functional types – their relevance to ecosystem properties and global change*, *International Geosphere-Biosphere Programme Book Series*, vol. 1, 3–19, Cambridge University Press, New York.

Hahmann, A. N. & R. E. Dickinson: (2001): A fine-mesh land approach for general circulation models and its impact on regional climate, *Journal of Climate*, *14*, 1634–1646.

Henderson-Sellers, A., P. Irannejad, K. McGuffie & A. J. Pitman: (2003): Predicting land-surface climates-better skill or moving targets?, *Geophysical Research Letters*, *30*, 1777–1781.

Huggett, R. J.: (1998): *Fundamentals of Biogeography*, Routledge, London, New York.

Lavorel, S. & W. Cramer (eds.): (1999): *Plant functional types and disturbance dynamics*, *Journal of Vegetation Science Special Feature*, vol. 10.

Lavorel, S., S. Díaz, J. H. C. Cornelissen, E. Garnier, S. P. Harrison, J. G. Pausas, N. Pérez-Harguindeguy, C. Roumet & C. Urcelay: (2007): Plant functional types: Are we getting any closer to the holy grail?, in Canadell, J. G., D. E. Pataki & L. F. Pitelka (eds.) *Terrestrial Ecosystems in a Changing World*, chap. 13, 149–164, Springer, Berlin, Heidelberg.

Lavorel, S., S. McIntyre, J. Landsberg & T. D. A. Forbes: (1997): Plant functional classifications: from general groups to specific groups based on response to disturbance, *Trends in Ecology & Evolution*, *12*, 474–478.

Lawrence, D., K. W. Oleson, M. G. Flanner, P. E. Thornton, S. C. Swenson, P. J. Lawrence, X. Zeng, Z.-L. Yang, S. Levis, K. Sakaguchi, G. B. Bonan & A. G. Slater: (2010): Parameterization improvements and functional and structural advances in version 4 of the community land model, *Journal of Advances in Modeling Earth Systems*, *Submitted*, on Discussion.

Lawrence, D. M. & A. G. Slater: (2005): A projection of severe near-surface permafrost degradation during the 21st century, *Geophysical Research Letters*, *32*, L24401.

Lawrence, P. J. & T. N. Chase: (2010): Investigating the climate impacts of global land cover change in the community climate system model, *International Journal of Climatology*, *Early View*.

Levis, S. & G. Bonan: (2004): Simulating springtime temperature patterns in the community atmosphere model coupled to the community land model using prognostic leaf area, *Journal of Climate*, *17*, 4531–4540.

Levis, S., G. Bonan, M. Vertenstein & K. Oleson: (2004): The community land model's dynamic global vegetation model CLM-DGVM: Technical description and user's guide, NCAR Technical Note NCAR/TN-459+STR, National Center for Atmospheric Research (NCAR), Boulder, CO.

Levis, S., J. A. Foley & D. Pollard: (1999): Co_2, climate, and vegetation feedbacks at the last glacial maximum, *Journal of Geophysical Research*, *104*, 31191–31198.

Levis, S., J. A. Foley & D. Pollard: (2000): Large-scale vegetation feedbacks on a doubled co_2 climate, *Journal of Climate*, *13*, 1313–1325.

Manabe, S.: (1969): Climate and the ocean circulation: I. the atmospheric circulation and the hydrology of the earth's surface, *Monthly Weather Review*, *97*, 739–774.

Matthews, E.: (1983): Global vegetation and land use: New high-resolution data bases for climate studies, *Journal of Climate and Applied Meteorology*, *22*, 474–487.

NCAR Terrestrial Science Section: (2010): Community land model, Online, URL `http://www.cgd.ucar.edu/tss/clm`, 2010-06-05.

Niu, G.-Y., Z.-L. Yang, R. Dickinson & L. Gulden: (2005): A simple TOPMODEL-based runoff parameterization (SIMTOP) for use in global climate, *Journal of Geophysical Research*, *110*, D21106.

Oleson, K., D. Lawrence, G. Bonan, M. Flanner, E. Kluzek, P. Lawrence, S. Levis, S. Swenson, P. Thornton, A. Dai, M. Decker, R. Dickinson, J. Feddema, C. Heald, F. Hoffman, J.-F. Lamarque, N. Mahowald, G.-Y. Niu, T. Qian, J. Randerson, S. Running, K. Sakaguchi, A. Slater, R. Stöckli, A. Wang, Z.-L. Yang, X. Zeng & X. Zeng: (2010): Technical description of version 4.0 of the community land model (CLM), NCAR Technical Note NCAR/TN-478+STR, National Center for Atmospheric Research, Boulder, CO.

Oleson, K. W., Y. Dai, G. Bonan, M. Bosilovich, R. Dickinson, P. Dirmeyer, F. Hoffman, P. Houser, S. Levis, G. Y. Niu, P. Thornton, M. Vertenstein, Z. L. Yang & X. Zeng: (2004): Technical description of the community land model (clm), Tech. Rep. NCAR/TN-461+STR, NCAR Technical Note.

Oleson, K. W., G.-Y. Niu, Z.-L. Yang, D. M. Lawrence, P. E. Thornton, P. J. Lawrence, R. Stöckli, R. E. Dickinson, G. B. Bonan, S. Levis, A. Dai & T. Qian: (2008): Improvements to the community land model and their impact on the hydrological cycle, *Journal of Geophysical Research*, *113*, G01021.

Otto-Bliesner, B. L., E. C. Brady, G. Clauzet, R. Tomas, S. Levis & Z. Kothavala: (2006a): Last glacial maximum and holocene climate in CCSM3, *Journal of Climate*, *11*, 2526–2544.

Otto-Bliesner, B. L., R. Tomas, E. C. Brady, C. Ammann, Z. Kothavala & G. Clauzet: (2006b): Climate sensitivity of moderate- and low-resolution versions of CCSM3 to preindustrial forcings, *Journal of Climate*, *11*, 2567–2583.

Pausas, J., G. Rusch & J. Lepš (eds.): (2003): *Plant Functional Types in relation to disturbance and land use*, *Journal of Vegetaion Science Special Feature*, vol. 14.

Pitman, A. J.: (2003): The evolution of, and revolution in, land surface schemes designed for climate models, *International Journal of Climatology*, *23*, 479–510.

Pitman, A. J., A. Henderson-Sellers, C. E. Desborough, Z.-L. Yang, F. Abramopoulos, A. Boone, R. E. Dickinson, N. Gedney, R. Koster, E. Kowalczyk, D. Lettenmaier, X. Liang, J.-F. Mahfouf, J. Noilhan, J. Polcher, W. Qu, A. Robock, C. Rosenzweig, C. A. Schlosser, A. B. Shmakin, J. Smith, M. Suarez, D. Verseghy, P. Wetzel, E. Wood & Y. Xue: (1999): Key results and implications from phase 1(c) of the project for intercomparison of land-surface parametrization schemes, *Climate Dynamics*, *15*, 673–684.

Prentice, I. C., A. Bondeau, W. Cramer, S. P. Harrison, T. Hickler, W. Lucht, S. Sitch, B. Smith & M. T. Sykes: (2007): Dynamic global vegetation modeling: Quantifying terrestrial ecosystem responses to large-scale environmental changes, in Canadell, J. G., D. E. Pataki & L. F. Pitelka (eds.) *Terrestrial Ecosystems in a Changing World*, chap. 15, 175–192, Springer, Berlin, Heidelberg.

Qu, W., A. Henderson-Sellers, A. Pitman, T. H. Chen, F. Abramopoulos, A. Boone, S. Chang, F. Chen, Y. Dai, R. E. Dickinson, L. Dumenil, M. Ek, N. Gedney, Y. M. Gusev, J. Kim, R. Koster, E. A. Kowalczyk, J. Lean, D. Lettenmaier, X. Liang, J.-F. Mahfouf, H.-T. Mengelkamp, K. Mitchell, O. N. Nasonova, J. Noilhan, A. Robock, C. Rosenzweig, J. Schaake, C. A. Schlosser, J.-P. Schulz, A. B. Shmakin, D. L. Verseghy, P. Wetzel, E. F. Wood, Z.-L. Yang & Q. Zeng: (1998): Sensitivity of latent heat flux from PILPS land-surface schemes to perturbations of surface air temperature, *Journal of Atmospheric Science*, *55*, 1909–1926.

Rodell, M., P. R. Houser, U. Jambor, J. Gottschalck, K. Mitchell, C.-J. Meng, K. Arsenault, B. Cosgrove, J. Radakovich, M. Bosilovich, J. K. Entin, J. P. Walker, D. Lohmann & D. Toll: (2004): The global

land data assimilation system, *Bulletin of the American Meteorological Society*, *85*, 381–394.

Schultz, J.: (2005): *The Ecozones of the World*, 2nd edn., Springer, Berlin.

Sellers, P., D. Randall, G. Collatz, J. Berry, C. Field, D. Dazlich, C. Zhang, G. Collelo & L. Bounoua: (1996): A revised land surface parameterization (sib2) for atmospheric gcms. part i: Model formulation, *Journal of Climate*, *9*, 676–705.

Sellers, P. J., R. E. Dickinson, D. A. Randall, A. K. Betts, F. G. Hall, J. A. Berry, G. J. Collatz, A. S. Denning, H. A. Mooney, C. A. Nobre, N. Sato, C. B. Field & A. Henderson-Sellers: (1997): Modeling the exchanges of energy, water, and carbon between continents and the atmosphere, *Science*, *275*, 502–509.

Sellers, P. J., Y. Mintz, Y. C. Sud & A. Dalcher: (1986): A simple biosphere model (SIB) for use within general circulation models, *Journal of the Atmospheric Sciences*, *43*, 505–531.

Shin, D. W., J. G. Bellow, T. E. LaRow, S. Cocke & J. J. O'Brien: (2006): The role of an advanced land model in seasonal dynamical downscaling for crop model application, *Journal of Applied Meteorology and Climatology*, *45*, 686–701.

Smith, T. M., H. H. Shugart & F. I. Woodward (eds.): (1997): *Plant functional types – their relevance to ecosystem properties and global change*, *International Geosphere-Biosphere Programme Book Series*, vol. 1, Cambridge University Press, New York.

Stöckli, R., D. M. Lawrence, G.-Y. Niu, K. W. Oleson, P. E. Thornton, Z.-L. Yang, G. B. Bonan, A. S. Denning & S. W. Running: (2008): Use of FLUXNET in the community land model development, *Journal of Geophysical Research*, *113*, G01025.

Thornton, P. E., S. C. Doney, K. Lindsay, J. K. Moore, N. Mahowald, J. T. Randerson, I. Fung, J.-F. Lamarque, J. J. Feddema & Y.-H. Lee: (2009): Carbon-nitrogen interactions regulate climate-carbon cycle feedbacks: results from an atmosphere-ocean general circulation model, *Biogeosciences*, *6*, 2099–2120.

Thornton, P. E., J.-F. Lamarque, N. A. Rosenbloom & N. M. Mahowald: (2007): Influence of carbon-nitrogen cycle coupling on land model response to co2 fertilization and climate variability, *Global Biogeochemical Cycles*, *21*, GB4018.

Thornton, P. E., B. E. Law, H. L. Gholz, K. L. Clark, E. Falge, D. S. Ellsworth, A. H. Goldstein, R. K. Monson, D. Hollinger, M. Falk, J. Chen & J. P. Sparks: (2002): Modeling and measuring the effects of disturbance history and climate on carbon and water budgets in evergreen needleleaf forests, *Agricultural and Forest Meteorology*, *113*, 185–222.

Thornton, P. E. & N. A. Rosenbloom: (2005): Ecosystem model spin-up: Estimating steady state conditions in a coupled terrestrial carbon and nitrogen cycle model, *Ecological Modelling*, *189*, 25–48.

Thornton, P. E. & N. Zimmermann: (2007): An improved canopy integration scheme for a land surface model with prognostic canopy structure, *Journal of Climate*, *20*, 3902–3923.

Ustin, S. L. & J. A. Gamon: (2010): Remote sensing of plant functional types, *New Phytologist*, *186*, 795–816.

Westby, M. & M. Leishman: (1997): Categorizing plant species into functional types, in Smith, T. M., H. H. Shugart & F. I. Woodward (eds.) *Plant functional types – their relevance to ecosystem properties and global change*, *International Geosphere-Biosphere Programme Book Series*, vol. 1, 104–121, Cambridge University Press, New York.

Wilby, R. L. & T. M. L. Wigley: (1997): Downscaling general circulation model output: a review of methods and limitations, *Progress in Physical Geography*, *21*, 530–548.

Williamson, D. L., J. T. Kiehl, V. Ramanathan, R. E. Dickinson & J. J. Hack: (1987): Description of the ncar community climate model (ccm1), TechNote NCAR/TN-285+STR, National Center for Atmospheric Research (NCAR).

Wood, A. W., L. R. Leung, V. Sridhar & D. P. Lettenmaier: (2004): Hydrologic implications of dynamical and statistical approaches to downscaling climate model outputs, *Climatic Change*, *62*, 189–216.

Woodward, F. & W. Cramer (eds.): (1996): *Plant functional types and climatic change*, *Special features in Vegetation Science*, vol. 12.

Zeng, X.: (2003): The common land model experience, *Global Change News Letter*, *55*, 19–20.

Zeng, X. & M. Decker: (2009): Improving the numerical solution of soil moisture-based richards equation for land models with a deep or shallow water table, *Journal of Hydrometeorology*, *10*, 308–319.

Zeng, X., M. Shaikh, Y. Dai & R. Dickinson: (2002): Coupling of the common land use model to the NCAR community climate model, *Journal of Climate*, *15*, 1832–1854.

Zeng, X., M. Zhao & R. Dickinson: (1998): Intercomparison of bulk aerodynamic algorithms for the computation of sea surface fluxes using the TOGA COARE and TAO data, *Journal of Climate*, *11*, 2628–2644.

Zhou, Y., D. McLaughlin & D. Entekhabi: (2006): Assessing the performance of the ensemble kalman filter for land surface data assimilation, *Monthly Weather Review*, *134*, 2128–2142.

3 Spatial Delineation

This chapter was printed in *International Journal of Remote Sensing*, Vol. 30, No. 8, 20 April 2009, pp. 1867–1886. The manuscript was submitted 29 January 2007, in final form 22 August 2008.

Land-cover classification in the Andes of southern Ecuador using Landsat ETM+ data as a basis for SVAT modelling

Dietrich Göttlicher*‡, André Obregón‡, Jürgen Homeier§, Rütger Rollenbeck‡, Thomas Nauss‡ and Jörg Bendix‡

‡Department of Geography, Laboratory for Climatology and Remote Sensing, University of Marburg, Deutschhausstr. 10, 35032 Marburg, Germany
§Plant Ecology, Albrecht-von-Haller-Institute for Plant Sciences, University of Göttingen, Untere Karspüle 2, 37073 Göttingen, Germany

A land-cover classification is needed to deduce surface boundary conditions for a soil-vegetation-atmosphere transfer scheme which is operated by a geoecological research unit working in the Andes of southern Ecuador. Landsat ETM+ data is used to classify distinct vegetation types in the tropical mountain forest. Besides a hard classification, a soft classification technique is applied. Dempster-Shafer evidence theory is used to analyse the quality of the spectral training sites and a modified linear spectral unmixing technique is selected to produce abundancies of the spectral end members. The hard classification shows very good results with a Kappa value of 0.86. The Dempster-Shafer ambuigity underlines the good quality of the training sites and the probability guided spectral unmixing is chosen for the determination of plant functional types for the land model. A similar model run done with a spatial distribution of land cover from both the hard and the soft classification clearly points to more realistic model results by using the land surface based on the probability guided spectral unmixing technique.

Keywords: Classification, Land cover, Landsat, CLM, Dempster-Shafer, probability guided spectral unmixing

3.1 Introduction

The changing atmospheric conditions along altitudinal gradients in tropical mountains are one important factor for the biodiversity of various organismic groups. This holds especially true for the research area of a joint ecological research programme in the Andes of southern Ecuador (refer to section 3.2, Beck & Müller-Hohenstein, 2001; Bendix et al., 2004). For instance, air humidity which is related to the latent heat flux plays a major role for the diversity of vascular epiphytes (e. g.

WERNER et al., 2005), while the species turnover among moths along an altitudinal transect is associated with a corresponding change in air temperature (and sensible heat flux) (e. g. BREHM et al., 2003). Moreover, the growth and phenology of the hosting megadiverse mountain forest is clearly related to the course of weather in the area (BENDIX et al., 2006a). Unfortunately, it is not possible to provide meteorological observations for every individual ecological research plot in a project area of 60 km in diameter, considering the rugged terrain of the Andes which, in addition, is characterised by small-scale patterns of meteorological windward and leeward effects. However, numerical weather models can provide a full spatial coverage of the atmospheric conditions in different, question-specific spatial scales. Of particular interest for ecological investigations are models which deal with the interface between soil, vegetation and atmosphere, so-called soil-vegetation-atmosphere transfer (SVAT) schemes. In our joint research effort (Research Unit 816) we use the Community/Common Land Model (CLM) of DAI et al. (2003) to simulate the energy and water fluxes with a spatial resolution of 30 m.

The operation of a SVAT model requires the adaptation of boundary conditions with regard to the study area. The definition of the lower boundary conditions of the CLM must include a detailed description of land cover and functional vegetation units (plant functional types, PFT) for every grid cell. The concept of plant functional types is described in BONAN et al. (2002). Generally, CLM-PFTs are ecological groups of plants with similar morphological and physiological traits. The CLM is designed by a nested grid which permits the application of different PFTs and their percentual coverage to one single gridcell (pixel). It is obvious that the construction of suitable PFTs in a megadiverse mountain forest requires profound botanical knowledge for the local/regional applications of the model. This holds especially true for the composition of appropriate tree groups in the natural forest but also for the main functional species groups in the areas which are currently used as pastures. The latter system is comparatively simple because it is dominated by pasture grasses (*Setaria aphacelata, Melinis minutiflora*) which are completely overgrown by the invasive southern bracken fern *Pteridium arachnoideum* in abandoned areas (HARTIG & BECK, 2003).

Several researchers successfully used satellite data to define the lower boundary conditions of SVAT models on different scales. The basis of those approaches is a multi-sensor land cover classification with special reference to the vegetation cover (e. g. Geostationary Operational Environmental Satellites (GOES) and Landsat Thematic Mapper (TM); ANDERSON et al., 2004).

Land cover classification and mapping in tropical mountain areas are subjected to various difficulties. First of all, the steep topography and limited accessability make terrestrial mapping extremely difficult and cost intensive (SALOVAARA et al., 2005). Thus, remote sensing is principally a useful tool to compensate for this central disadvantage. However, to date, successful classifications by using satellite imagery in the tropics are mostly conducted in rather flat terrain (HELMER et al., 2000), while

image classification in a mountainous region is still a challenging task (Tottrup, 2004). It could be shown for the Andes encompassing southern Ecuador and other high altitude regions that corrections of the satellite signal due to topographic effects such as hill shading or geometric displacements are required to improve classification results and to obtain a similar degree of accuracy as in the lowland tropics (Hill & Foody, 1994; Colby & Keating, 1998; Echavarria, 1998; Shepherd & Dymond, 2003). Moreover, it is not easy to distinguish between different functional types of trees in an area of tropical rain forest (Hill, 1999). Expert knowledge has been proven to improve classification results significantly in previous studies (e. g. Schweitzer et al., 2005).

To obtain the fractional land cover in one single pixel, an unmixing approach is obvious but holds the problem that normal unmixing needs more spectral channels in the satellite data than land cover classes to be distinguished. Especially the commonly used Landsat data needs a modified approach because only six spectral channels are suitable for vegetation classification and are not sufficient in our study with respect to the number of plant functional type and other land cover classes. Other techniques such as the Dempster-Shafer evidence theory can provide information about the quality of the training sites but cannot produce the actual fractional land cover. Generally, spectral mixture analysis based on the ground data acquisition of spectral endmembers by using field spectrometers could help to improve the multi-/hyperspectral classification of vegetation (e. g. Peddle & Smith, 2005), but this is difficult to realise in the complex topography of the Andes, especially if a respective costly field instrument is not available.

Consequently, the current paper follows three main aims:

1. To provide data on land cover and suitable vegetation classes which can be used to define CLM-PFTs. For this purpose, a detailed landuse classification based on 30 m Landsat ETM+ (Enhanced Thematic Mapper) data is performed which considers all relevant vegetation classes such as different forest types. The determination of the land cover map relies on multispectral classification techniques, a high resolution aerial photograph and profound expert knowledge of a big research unit which is necessary for the signature training process (see section 3.3).

2. To apply one hard and two soft classification schemes. The selected soft classifiers are based on the Dempster-Shafer evidence theory and a modified spectral unmixing technique.

3. A comparison of classification results by means of exemplary model runs with both classification types to test the suitability of hard and soft classification approaches for the use in SVAT models.

The current paper is structured as follows: The study area and the data are described in section 3.2. Section 3.3 briefly summarises the applied classification

approaches. The discussion and appraisal of the classification results are presented in section 3.4 and the results of the comparative model runs is the subject of section 3.5.

3.2 Study area and data

The study area is situated in southern Ecuador and comprises parts of the mountain forests of the eastern Andean escarpment. This area is renowned as part of the 'Andean hot spot' of vascular plant diversity (Barthlott et al., 2005; Brummitt & Lughadha, 2003). The study area hosts the model domain in 30 m resolution grid size (see figure 3.1).

The Reserva Biológica San Francisco (RBSF) is the main study area of the ecological research unit 816 (RU 816) of the German Research Council (DFG). It comprises the valley of the Rio San Francisco where the slopes are mainly covered with the natural mountain forest, an environment in which most of the ecological groups are working. It is situated between Loja, a dryer inner-Andean basin in the west and the slopes of the eastern Andean cordillera in the east. A detailed geographic description of the core area is found in Beck & Müller-Hohenstein (2001) and more general information is given in Bendix et al. (2004). The general weather situation is described by Bendix & Lauer (1992); Richter (2003); Bendix et al. (2004, 2006b).

The Landsat ETM+ image used in the current study is a cloud-free scene from 3 November 2001 which was obtained from the Global Land Cover Facility (GLCF, http://glcf.umiacs.umd.edu/index.shtml) as a level 1G product.

Ancillary data are used for signature training and image classification. To determine the exact position of training sites from the vegetation surveys in the core area, a rectified color ortho-aerial photograph was used. The dataset was acquired during several flights in 2001 on behalf of our joint research effort. The ortho-photo was processed using the technique of aero-triangulation (Jordan et al., 2005) and has a spatial resolution of 1 m. A digital elevation model from the national mapping agency IGM (Instituto Geográfico Militar, Quito) with a spatial resolution of 25 m was used during image classification. All resulting land-cover maps are added to the central database of the research unit to provide access for further investigations (Göttlicher & Bendix, 2004).

The natural vegetation of the study area (figure 3.1) can be described as 'bosque siempreverde montano', evergreen montane forest (Balslev & Øllgaard, 2002) or as 'bosque montano nublado', montane cloud forest (Valencia et al., 1999) reaching the treeline at around 2700 m. Above the treeline we find sub-páramos (as part of the evergreen elfin forests of the region).

Some forest areas on the south-facing slopes within the valley of the San Francisco have been converted into pastures. Partly they are now subject to aggressive bracken

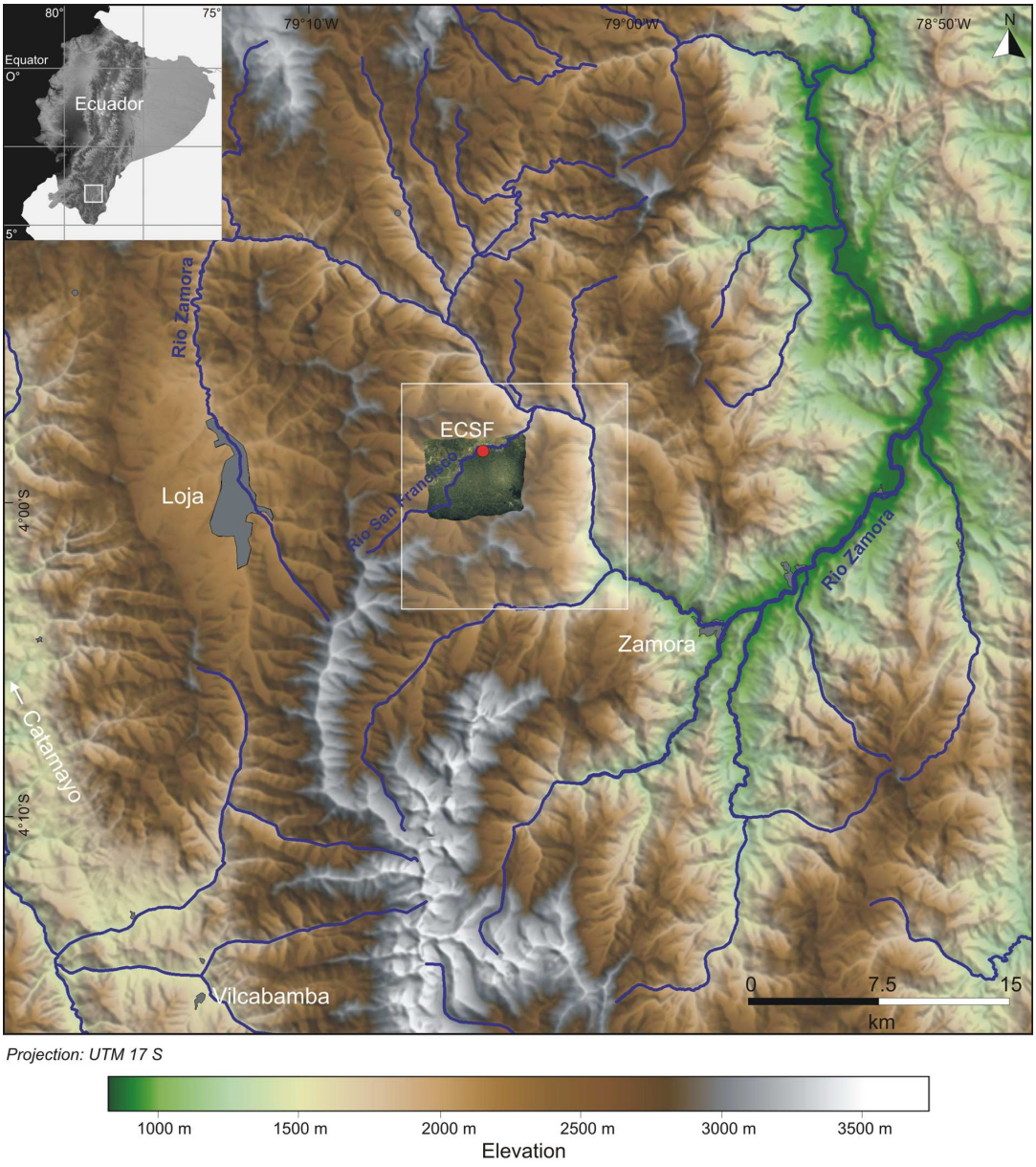

Figure 3.1: The study site is marked with the white rectangle (30 m resolution). The dark green coloured area encompassing the 'Estación Científica San Francisco' (ECSF research station) represents the region covered by the high resolution aerial photograph.

fern succession (Hartig & Beck, 2003).

Combining different approaches of vegetation typification (Homeier et al., 2002; Paulsch, 2002; Homeier, 2004; Parolly & Kürschner, 2004), Homeier et al. (2008) distinguished six main functional types of primary vegetation for the study area based on their detailed description of the natural vegetation. These vegetation types are compiled by combining results of the investigation of forest structure and tree species composition on permanent plots (Homeier et al., 2002; Homeier, 2004), a forest structural analysis on non-permanent plots (Paulsch, 2002) and ecosociological studies of the bryophyte communities (Parolly & Kürschner, 2004).

The tallest and species-richest forest is found on lower slopes and within ravines below 2100 m where the canopy reaches 25 to 30 m with some emergents reaching up to 35 m (type I). Megaphyllous shrubs and large ground herbs are common in the understorey. On nearby upper slopes and ridges, the forest stature and tree species composition is completely different with few trees reaching between 15 and 20 m (type II). Between 2100 and 2250 m on the ridges and upper slopes the trees attain a height of not more than 15 m and the canopy becomes more open with trees covered by dense layers of epiphytes (type III). With increasing elevation the tree height decreases further to 6–8 m, and the forest above 2250 m is dominated by only one tree species, *Purdiaea nutans* Planch. (Cyrillaceae). The herbaceous layer of this forest is well developed and principally composed of terrestrial bromeliads (type IV). The forest in the ravines from 2100 to 2700 m differs also from the upper slopes with greater tree heights and in tree species composition (type V). The sub-páramo (type VI) occurs above the treeline attaining heights of up to 2 m, terrestrial herbs are the most speciose life form of this vegetation type. The characterised vegetation types differ in their composition of life forms and plant species. By their distinctness in structural parameters they are easy to recognise even for non-botanists. Stand basal area (including all trees with a diameter $\geqslant$ 10 cm) decreases with elevation, from maximum values of 40-50 $m^2\,ha^{-1}$ at around 2000 m (type I) to 10–20 $m^2\,ha^{-1}$ above 2300 m (type IV) and average tree stature is shorter compared to trees at lower elevations (Homeier, 2004).

Above ground, forest productivity measured as the annual increment of the tree basal area recedes with elevation. LAI (calculated from hemispherical photos) is highly variable in the stands. Most of the values from below 2250 m are between 5 and 7, within the uppermost forest stands it decreases to values between 2 and 3 (Homeier, 2004). The same structural patterns as in the elevational gradient were found on a smaller scale in the topographic gradient from ravines to ridges especially for forest type I and type II but also in the upper compartments (type III and IV to type V, Homeier, 2004).

3.3 Methodology

The whole processing chain of this study is presented in figure 3.2 and can be subdivided into four working steps: (i) pre-processing of the satellite image, (ii) multispectral image classification based on Landsat ETM+ data including signature training, (iii) appraisal of the classification results and (iv) comparison of CLM-model runs based on hard and soft classification.

3.3.1 Pre-processing

The first pre-processing step was the geometric projection of the Landsat ETM+ scene in order to produce a geo-ortho-rectified image. The ETM+ scene was delivered in the space-oblique-mercator projection which had to be reprojected to the UTM projection zone 17S (WGS84), the standard projection of all spatial data sets of the research unit 816. Even if the level 1G data have undergone a geometric pre-correction, a residual location error of up to 250 m must be taken into account (NASA, 2002). Thus, an additional geo-correction was performed by using 32 ground control points which were obtained from the high-resolution aerial orthophoto, another existing geo-ortho rectified satellite image from 1986 and the digital elevation model. The correction was conducted with the ERDAS Imagine™ (V. 8.6) 'Landsat model' module which uses higher-order polynomic equations including terrain altitude provided by the digital elevation model (DEM). The achieved root-mean-square error was 20 m which means that the final location accuracy is better than one ETM+ pixel.

The second step of pre-processing needed for a proper land-surface classification in high mountain areas is a topographic normalisation of radiances including atmospheric correction. For the ETM+ scene, atmospheric correction was conducted using the COST model of Chavez (1996) which combines a dark object subtraction and a procedure to minimise the effects of absorption and Rayleigh scattering in the atmosphere to calculate absolute reflectance. A dark lake surface in the Paramo of Cajanuma was chosen for the dark object subtraction. To eliminate differences in the reflectance due to topographic slope and aspect, an illumination model is required (Riaño et al., 2003). This is based on the digital elevation model which provides the slope and aspect of every pixel and the calculated sun elevation and azimuth angles. Based on this information, a hill-shade image was derived. The first step of correction is to relate the radiances in the spectral bands (1–5 and 7) of the ETM+ image to illumination by linear regression analysis.

$$L_\lambda = aI + b \tag{3.1}$$

where L_λ is the spectral radiance at wavelength λ (after atmospheric correction), I is the illumination score from the hill-shade image, a and b are the linear regression coefficients.

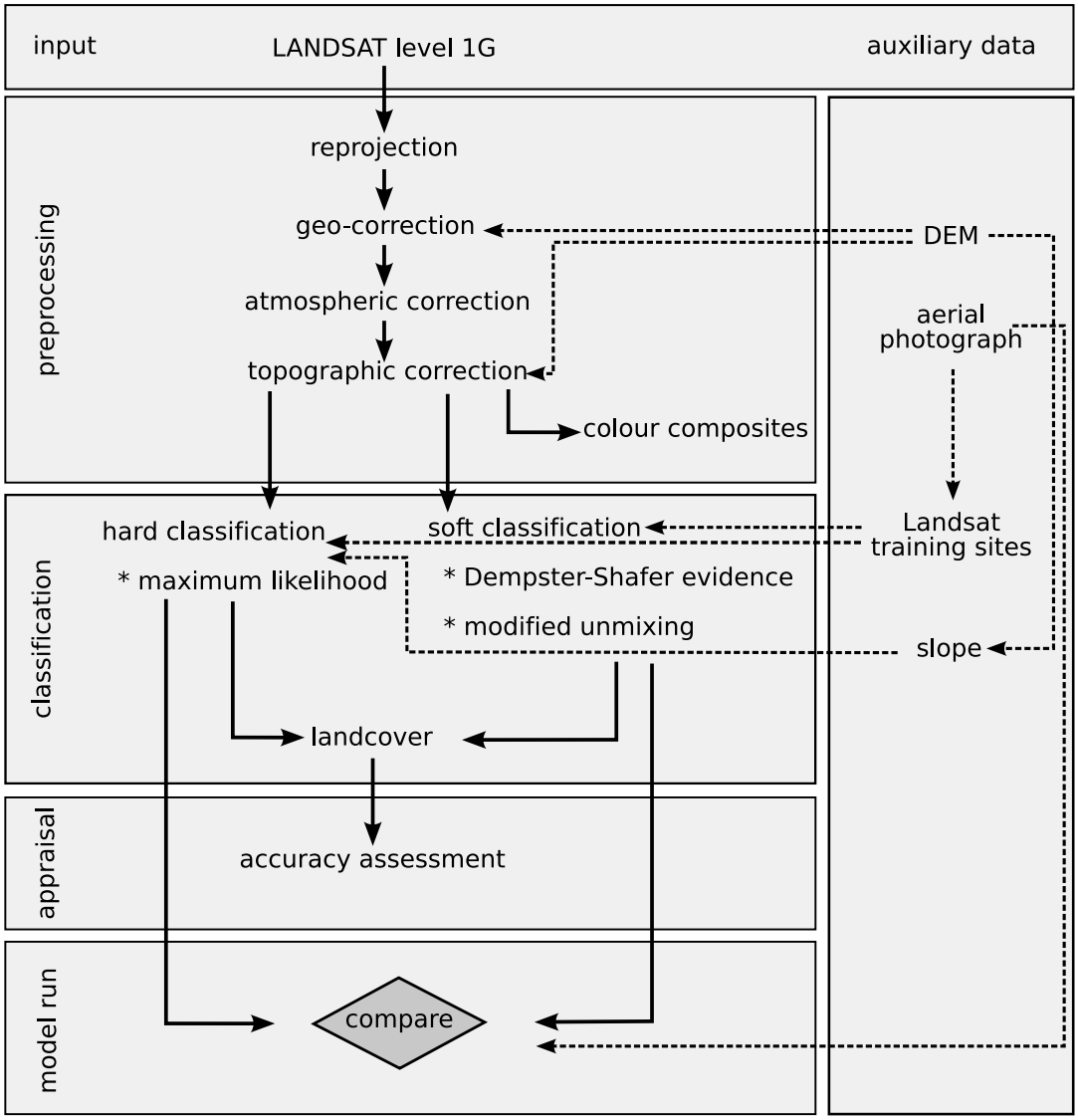

Figure 3.2: Flowchart of the processing steps.

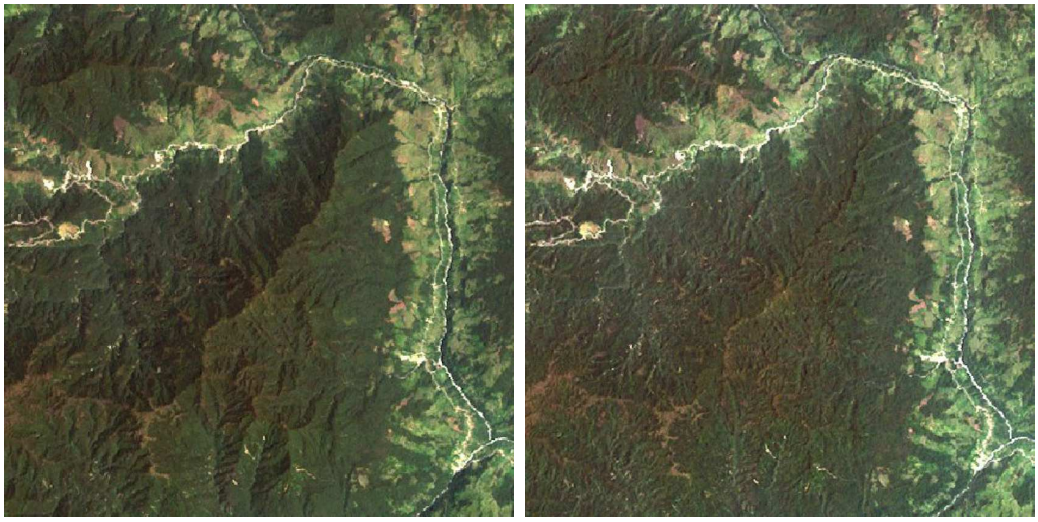

(a) uncorrected (b) corrected

Figure 3.3: Atmospherically and topographically uncorrected (a) and corrected (b) true colour composites (RGB = 3,2,1) of the study site.

The final correction is then achieved by applying the following equation which includes the standard cosine correction due to the angle of incidence:

$$L_\lambda^* = L_\lambda - [\cos\theta(a-b)] + \bar{L}_\lambda \tag{3.2}$$

where L_λ^* is the corrected spectral radiance, $\bar{L}_\lambda$ is the average spectral radiance of the scene with the angle of incidence θ:

$$\cos\theta = \cos\hat{\beta}\cos\beta + \sin\hat{\beta}\sin\beta\cos(\Omega - \hat{\Omega}) \tag{3.3}$$

where β is the sun elevation angle, $\hat{\beta}$ the terrain slope angle, Ω the solar azimuth angle and $\hat{\Omega}$ the terrain azimuth angle.

The results of the atmospheric and topographic correction are depicted in figure 3.3. A visual inspection of the colour-composites reveals the successful removal of terrain shadow effects for the study area of the valley of the Rio San Francisco.

3.3.2 Training Sites and synthetic channel

Regarding the natural vegetation, only areas which could undoubtedly be assigned to pure compositions of the above-described six main units were chosen for signature training. Additionally, pure training sites covered with pasture grasses, bracken fern and successions, but also areas representing bare soil (e. g. current landslides), water surfaces and buildings/streets were digitised using expert knowledge and the aerial photograph (table 3.1, figure 3.4). The selected pure training polygones can

Table 3.1: Selection of land-cover classes and training sites used for the classification in the core area. For the identification of training sites, refer to figure.

ID	Land cover class	Expert Knowledge	Location identification of the training site
1	Pre-Montane forest	Homeier	1
2	Forest type I, ravines 1900–2100 m	Homeier	2
3	Forest type II, crest and upper slopes 1900–2100 m	Homeier	3
4	Forest type III, crest and upper slopes 2100–2250 m	Homeier	4
5	Forest type IV, crest and upper slopes 2250–2700 m	Homeier	5
6	Forest type VI, ravines 2100–2700 m	Homeier	6
7	Subpáramo type VI, >2700 m	Homeier	7
8	Bracken fern	Homeier	8
9	Grassland	Homeier	9
10	Shrubs	Homeier	10
11	unvegetated (roads & landslides)	Homeier, aerial photography, Rollenbeck	11
12	Water	aerial photography, Rollenbeck	12

be treated as spectral endmembers and enable the application of a soft classification based on a modified spectral unmixing technique which is necessary to derive the share of different land surface classes/PFTs on single grid cells. All defined vegetation types show differences in their physiological and morphological characteristics and thus, provide appropriate plant functional types necessary for a proper initialisation of the SVAT model.

Generally, the training sites related to classes of the native mountain forest are intensively surveyed botanical plots (see section 3.2 and Homeier, 2004; Hartig & Beck, 2003; Paulsch, 2002). Additional training sites were determined by using clearly marked areas with a distinct land-cover type (streets, urban, freshly burned forest, landslides) in the aerial photo, in comparison with the colour composite of the satellite image. These training site polygones were also confirmed by expert kowledge. The overall criterion for the selection of the individual training sites was the homogeneity of the surface structure.

A specific classification problem is the distinction of different classes of native

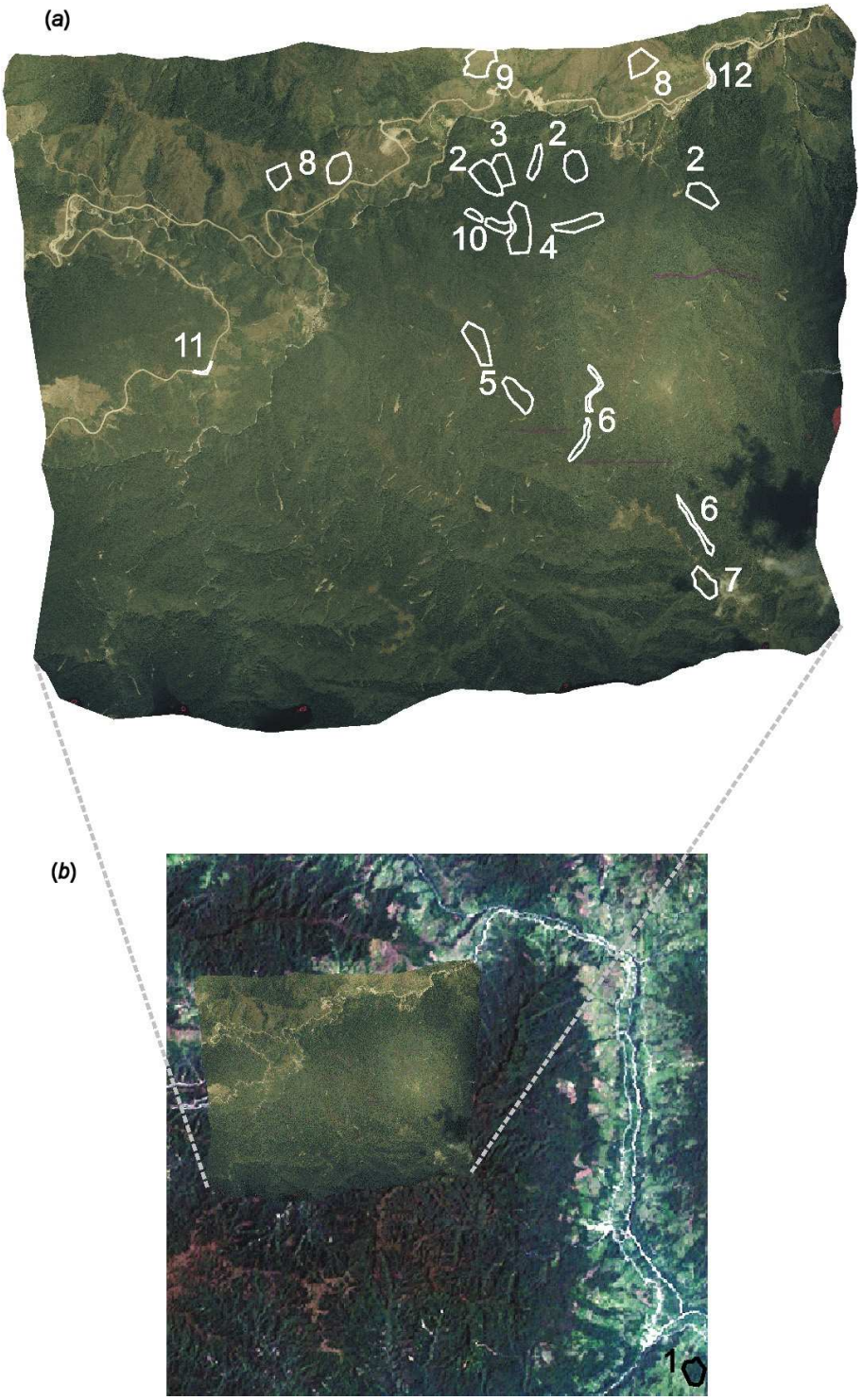

Figure 3.4: Location of the training sites used for the ETM+ classification. Aerial photograph (*a*) with the different vegetation units, superimposed to the Landsat image (*b*) in the study area (for all numbering of the training sites, refer to table 3.1).

forest in the central study area which reveal similar spectral signatures. Hence, the suitability of additional synthetic channels for multispectral classifications e. g. terrain altitude, slope aspect or other topographic parameters (concave/ convex slopes) were examined. After testing all possible variations, only the slope angle caused a clear improvement in the classification result and thus was used in the final classification scheme (refer to section 3.4.1).

3.3.3 Classification

To classify the ETM+ scene, several techniques are applied: (i) A hard classification based on the maximum-likelihood approach, (ii) an evaluation of uncertainty based on Dempster-Shafer evidence theory and (iii) a sub-pixel classification using a modified approach of linear spectral unmixing.

Image segmentation is conducted by means of the image processing software IDRISI™ (Kilimanjaro Version) using the modules 'Maxlike' (Maximum Likelihood classifier), 'Belclass' (Dempster-Shafer belief soft classifier) and 'Unmix' (Linear Spectral Unmixing classifier) (Eastman, 2003).

The maximum-likelihood classification (MLC) belongs to the group of hard classifiers, which make a definite decision about the class membership of any pixel, while soft classification gives explicit information on the degree of class membership (Eastman & Laney, 2002).

In contrast to common soft classifications, Dempster-Shafer does not assume to have full information and explicitly accepts that the existing knowledge i. e. the training site information might be incomplete. Thus, it incorporates the concept of ignorance. Dempster-Shafer as implemented in Idrisi performs a soft classification as it calculates a degree to which evidence provides concrete support for a hypothesis. This degree is known as *belief*, the degree to which a hypothesis cannot be disbelieved is known as *plausibility* (Eastman, 2003). The belief is a lower estimate on the support for a hypothesis, while plausibility represents the confidence band to which a hypothesis cannot be disbelieved. Uncertainty is the difference between belief and plausibility (Comber et al., 2005), also known as belief interval. A full description of the belief calculation method is given by several authors (e. g. Mertikas & Zervakis, 2001; Comber et al., 2004; Malpica et al., 2007). Ambiguity is a further aspect of uncertainty which can be expressed as the difference between the belief interval for a specific class and the overall uncertainty (Eastman, 2003). In this study, the Dempster-Shafer theory was primarily used in order to check the quality of the training sites and to analyse the degree of uncertainty. The role of ambiguity was also investigated.

However, the Dempster-Shafer approach cannot be used for subpixel classification as it outputs belief values per pixel exclusively for only one specific class. Therefore other techniques of soft classification are used in order to derive the proportions of the different vegetation types within a mixed pixel in accordance with the subgrid

PFT concept of the CLM model.

Thus, a second classification done in this study uses a probability guided linear spectral unmixing approach as proposed by Zhu (2005), which is able to provide the fractional cover of functional vegetation units per grid cell. Classical linear unmixing assumes that the image spectra are the results of mixtures of different surface materials, which can be expressed as linear combinations of their respective spectra in the image (Sohn & McCoy, 1997). Although spectral mixture analysis has long been recognized as an effective method for the determination of mixed pixels (Lu & Weng, 2007), it suffers from the limitation that the number of training sites cannot exceed the number of image bands. The approach described by Zhu (2005) offers an effective solution for this shortcoming. In a first step it calculates posterior probabilities for all endmembers in a pixel, according to the classification based on Bayesian probability. Then, the proportions of the identified endmembers are calculated by the linear spectral unmixing model. When mixing endmembers in a backward direction, less endmembers lead to a better correspondence of the data to derive subpixel endmember fractions (Song, 2005). Thus, in our study, three endmembers for each pixel are chosen as candidates for further unmixing to determine their proportions.

All results of the soft classifications are hardened, i. e. the maximum Dempster-Shafer beliefs (Idrisi 'Maxbel') and the maximum mixture fractions ('Maxfrac') are extracted for each pixel to derive a hard classification for comparison reasons.

3.3.4 Accuracy assessment

For the appraisal of the individual classification results, a contingency matrix of the training sites was calculated (Story & Congalton, 1986) in which also independent ground truth sites could be used to calculate the matrix and Kappa values (Congalton, 1991). The appraisal of the classification results is conducted by calculating three indices: (i) the overall, (ii) the producer's and (iii) the user's accuracy. The overall accuracy describes the relation of the pixel number correctly classified to the sum of reference pixel of all training polygones. The producer's accuracy is based on the analysis of the individual object classes and illustrates the likelihood of a correct classification of the training site pixels for individual classes while the user's accuracy explains to what extend the classification result renders reality (for the calculation of the indices refer to Congalton, 1991).

Table 3.2: Contingency matrix for the Landsat classification of the core area. Acc_u = user's accuracy, Acc_p = producer's accuracy. Columns are training sites, rows are land-cover classes, the numbers of the classes are explained in table 3.1. Kappa = 0.86.

	1	2	3	4	5	6	7	8	9	10	11	12	Σ	Acc_u
1	71	0	0	0	0	0	0	0	0	0	2	0	73	0.97
2	0	25	1	0	0	4	0	0	0	0	0	0	30	0.83
3	0	2	37	14	4	0	0	0	0	0	0	0	57	0.65
4	0	0	2	27	9	0	0	0	0	0	0	0	38	0.71
5	0	0	1	4	69	1	0	0	0	0	0	0	75	0.92
6	0	4	1	0	1	49	0	0	0	0	0	0	55	0.89
7	0	0	0	0	0	3	60	0	0	0	0	0	63	0.95
8	0	0	0	0	0	0	0	33	0	0	0	0	33	1.00
9	4	0	0	0	0	0	4	1	85	0	0	0	94	0.90
10	0	0	1	14	0	0	0	0	0	20	0	0	35	0.57
11	0	0	0	0	0	0	0	0	0	0	35	0	35	1.00
12	0	0	0	0	0	0	0	0	0	0	0	20	20	1.00
Σ	75	31	43	59	83	57	64	34	85	20	37	20	608	
Acc_p	0.95	0.81	0.86	0.46	0.83	0.86	0.94	0.97	1.00	1.00	0.95	1.00		0.87

3.4 Results

3.4.1 MLC of the Landsat ETM+ scene

The classification (figure 3.5) of the core area clearly illustrates the well-known altitudinal distribution patterns of the native vegetation (refer to section 3.2), without considering terrain altitude during the classification process. The contingency matrix for all classes is presented in table 3.2.

The overall accuracy of 87.3 % is very high (84.7 %–90 % with a 95 % confidence level); the Kappa value is 0.86. The producer's accuracy of 89 % shows a very good separation of the individual object classes. The user's accuracy of 87 % also points to a good classification result. With regard to the forest classes, the accuracy slightly decreases (producer's accuracy = 80 % and user's accuracy = 83 %) compared to the overall scores. Examining classification runs considering different synthetic bands from topographic parameters showed that the use of the slope angle can clearly improve the classification results, especially in the difficult classes of native forest where the producer's accuracy increases from 69 % to 80 % (see table 3.3).

The spatial statistics of the object classes in different altitudinal belts underlines the human impact especially on the lower parts of the area (figure 3.6). While the native forest is the dominating land-cover type above 2200 m asl, the anthropogenic

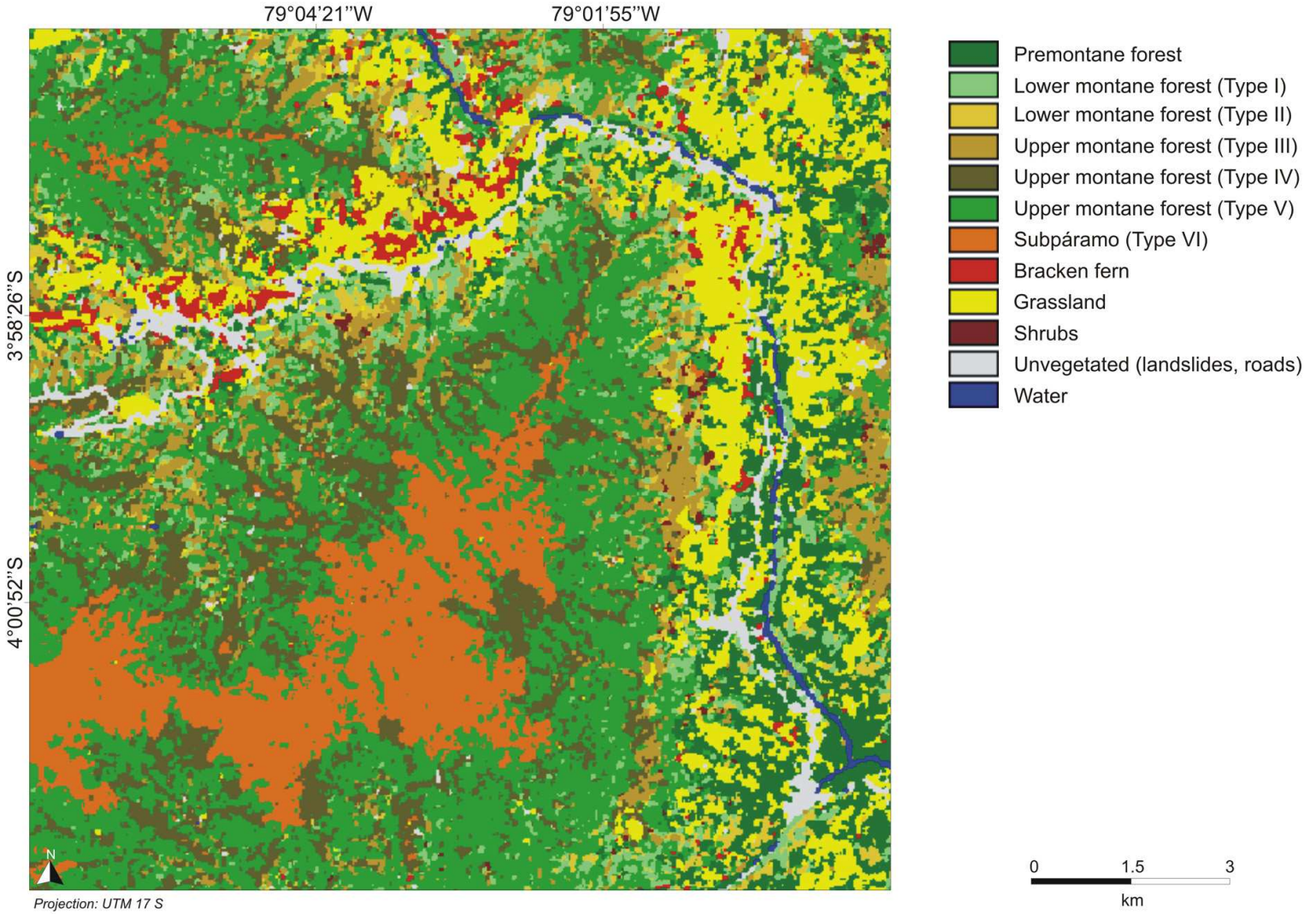

Figure 3.5: Classification result of the ETM+ scene in the study area including a synthetic channel of hill slope derived from the digital elevation model (DEM).

Table 3.3: Comparison of the accuracy indices with and without the use of the synthetic channel (hill slope) in the core area for all vegetation classes and forest classes only. Acc_u = user's accuracy, Acc_p = producer's accuracy.

	Overall accuracy	Acc_p	Acc_u	Kappa	Acc_p(forest)	Acc_u(forest)
Classification with slope	0.87	0.89	0.87	0.86	0.80	0.83
Classification without slope	0.79	0.82	0.78	0.77	0.69	0.67

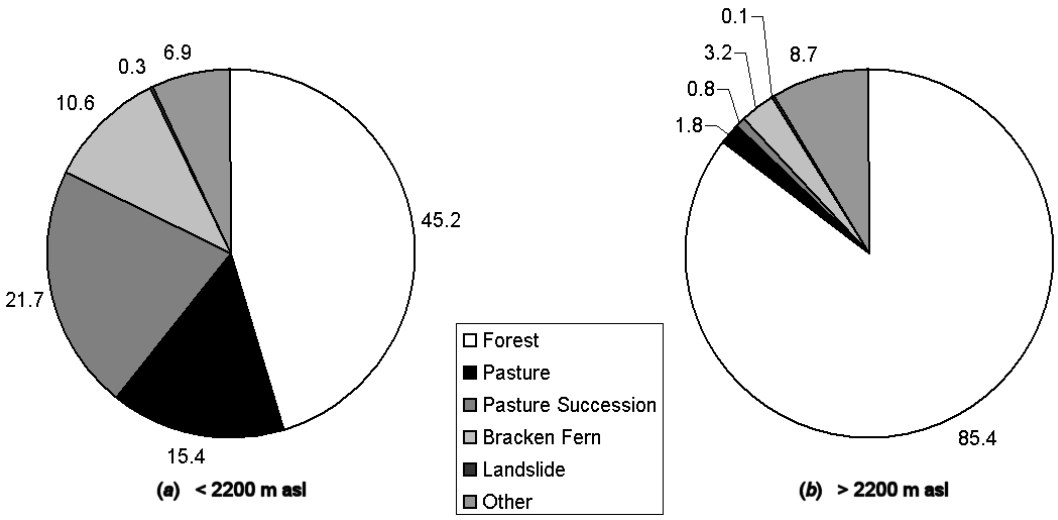

Figure 3.6: Percentages of land-cover classes in (*a*) the lower (<2200 m above sea level) and (*b*) the upper parts (⩾ 2200 m asl) of the study area.

replacement system indicated by a high portion of pastures which originates from the slash-and-burn of the natural forest by the local population covers nearly half the slope area in the lower part of the valley. However, it is obvious that this current land use system is not sustainable because only 15.4 % of this area is still in use. Other former pastures are overgrown by the invasive bracken fern (10.6 %) or other mixed successions (21.7 %). It should be stressed that the abandoned pasture land can neither contribute to the livelihood of the local population nor to the rehabilitation of the lost biodiversity due to the logging of the native forest (for the bracken fern dilemma, refer also to Hartig & Beck, 2003).

The statistics markedly indicate that the threat to the natural ecosystem and thus to the biodiversity clearly radiates from the valley bottom encroaching the native forest aloft.

3.4.2 Soft classification of the Landsat ETM+ scene

The applied techniques of soft classification use the same signatures as the MLC. The belief values of the Dempster-Shafer classification show low values for all land-cover classes. In contrast, plausibilities show very high values, which leads to large belief intervals for all specific classes. Thus, overall uncertainty is also high. Due to the ability of Dempster-Shafer to include the aspect of ignorance, uncertainty in our information becomes apparent. An explanation for the high uncertainty might be that the information of the training sites is not complete and that unknown classes exist. However, the distribution of the belief values for each class matches the land-cover classes determined by the MLC rather well. High belief values occur mainly in the centre of these land-cover classes while pixels in the area of neighbouring land cover classes show very low beliefs and high values of uncertainty. A higher occurrence of mixed pixels in these transition zones might be an explanation for this.

The investigation of ambiguity shows that the transition zones between land cover classes show the highest values, especially for the forest classes. Each forest class shows the highest ambiguity in its neighbouring forest class, e. g. subpáramo shows ambiguity in forest type V, while forest type III shows ambiguous behaviour in forest types II and IV. This fact reflects reality rather well, as the different forest types are not strictly separated. Boundaries between the different forest types are not distinct in the field which is represented in the classification by the occurrence of ambiguity in the areas of transition. All non-forest classes show lower effects of ambiguity, which is also restricted to surrounding areas of the specific land-cover class. Although training site information might be incomplete, the distribution of ambiguity points out the good quality of the training sites in the aspect of permitting a good separation between the different land-cover classes. The problem of mixed pixels and the evidence of unknown land-cover classes finally lead to a high overall uncertainty in the Dempster-Shafer classification.

The result of the hardened Dempster-Shafer belief classification shows a similar distribution of land cover as the MLC. The overall accuracy is also high (80.8 %) with a 95 % confidence interval of 78.6 %–83.1 %. Kappa value is 0.77.

Subpixel classification in order to derive the proportions of land cover in mixed pixels is done by means of probability guided linear spectral unmixing. The outcome of this procedure is a set of separate images for each object class where the digital count indicates the abundance of the individual class in each pixel as required by the SVAT model. Figure 3.7 shows an example for the class 'grassland' done by the probability guided spectral unmixing and Dempster-Shafer belief classification. These images of the probability guided unmixing will be used to define the PFT ensemble for each pixel in the CLM run (see section 3.5).

The overall accuracy of the hardened results of the unmixing shows a low value of only 48.8 % (45.9 %–51.7 % with a 95 % confidence level) in contrast to the MLC

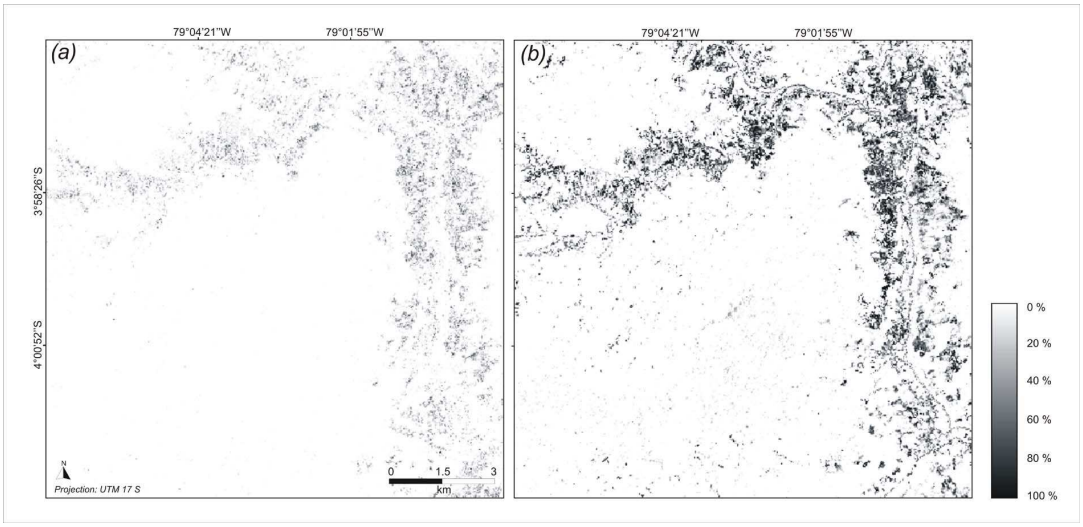

Figure 3.7: Results of the soft classification for the class 'grassland' using (*a*) Dempster-Shafer belief classification (belief value) and (*b*) probability guided spectral unmixing (percentage of fractional cover in each grid cell).

approach. This low value is the result of the representation of the constituent members of each specific pixel.

3.5 Application of classification results in a model run

To test the different classification results in the SVAT-model, two identical runs were performed with the spatial land cover of (i) the MLC and (ii) the modified spectral unmixing technique. The latter gives the chance to determine more than one PFT for the desired grid cell resolution of 30 m.

Atmospheric forcing was included by NCEP/NCAR (National Center for Environmental Prediction/National Center for Atmospheric Research) reanalysis data for a whole year which are provided by the datasets of the model source code. The forcing is homogenous for the whole area. The parameters of the PFT which can be variable through space and time like leaf/stem area index (LAI/SAI) and top/bottom height of the canopy were set static for each PFT and are shown in table 3.4. This is done to eliminate effects of these parameters, so that only the consequences of the variation of the spatial distribution of the PFT, as the result of both classification approaches, are visible.

To save computational time, only a subset of 100 by 100 pixels of the study area is used. Spin-up time in the model run was 1 year, the model time step was set to 3 h. The presented results are from the end of the model run. In figure

Table 3.4: Parameters for the plant functional types (PFTs) used in the model run. All variables are constant over time and space. LAI, leaf area index; SAI, stem area index. Top height is canopy top height above ground. Bottom height is canopy bottom height above ground.

PFT no.	PFT name	LAI	SAI	Top height (m)	Bottom height (m)
0	Bare soil	0.0	0.0	0.00	0.00
1	Forest type I	7.0	1.5	30.00	10.00
2	Forest type II	6.0	1.5	20.00	5.00
3	Forest type III	5.0	1.5	15.00	5.00
4	Forest type IV	4.0	1.5	8.00	3.00
5	Forest type V	6.0	1.5	20.00	5.00
6	Forest type VI, sub-páramo	3.0	1.0	2.00	0.50
7	Bracken fern	1.0	2.0	1.50	0.10
8	Shrubs	0.5	0.5	1.50	0.10
9	Grassland, pastures	1.0	2.0	0.50	0.01

3.8 the transpiration of the canopy is shown exemplarily for the differences caused by the two input datasets for the PFT. In both images, the river valley with the lowest transpiration is clearly marked because of the lack of vegetation. In the nothern part, pastures and various succession stages including bracken fern areas also show low transpiration values compared to the forest areas in the south. Here, higher values in the ravines represent the taller and markedly denser vegetation in contrast to the ridges. It is obvious that the results from the modified spectral unmixing show a much smoother spatial distribution. Especially in the river valley with little vegetation the maximum likelihood parametrisation shows larger areas with no vegetation at all.

Two single grid cells were extracted to have a closer look at how the land-cover is distinguished in the classification schemes. Both pixels contain mixed information of bare ground (a current landslide) and a vegetated part. To determine the respective area of the unvegetated and vegetated sections the aerial photography was digitised in these grid cells using the geographic information system MapInfo™. Figure 3.9 shows the outline of each PFT class in the grid cells. In both pixels the maximum likelihood procedure classifies only bare ground. The modified unmixing comes to a cover of 12 % bare ground and 88 % forest type III in pixel (*a*). In pixel (*b*) the values are 30 % bare ground and 70 % forest type I respectively. The digitising gives rounded results for pixel (*a*) as 14 % bare ground, 84 % vegetated and pixel (*b*) 58 % bare ground and 42 % vegetated.

Canopy transpiration values are zero at all times in the maximum likelihood classification due to the lack of vegetation. In the model run using the modified spectral

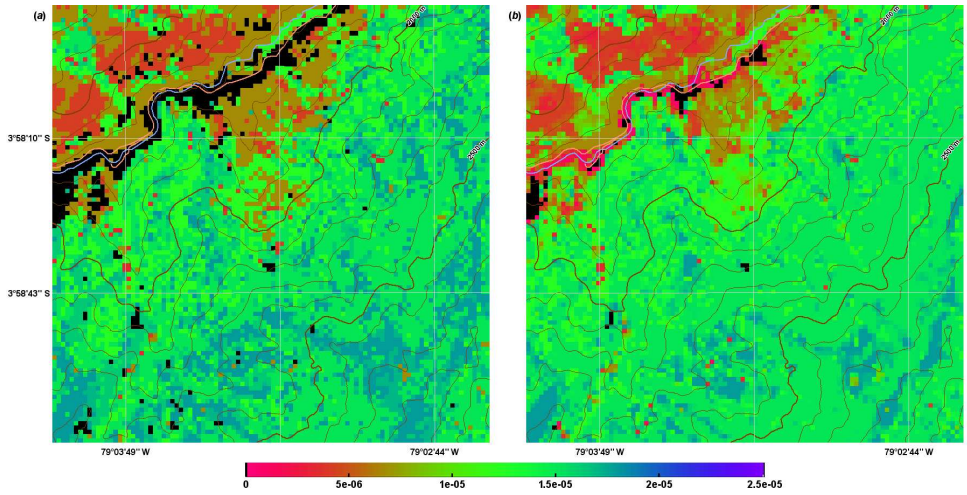

Figure 3.8: Results of a 1-year model run for canopy transpiration rate ($mm\,s^{-1}$) on the basis of PFT coverage with (a) the maximum likelihood hard classification and (b) the modified spectral unmixing technique (soft classifier).

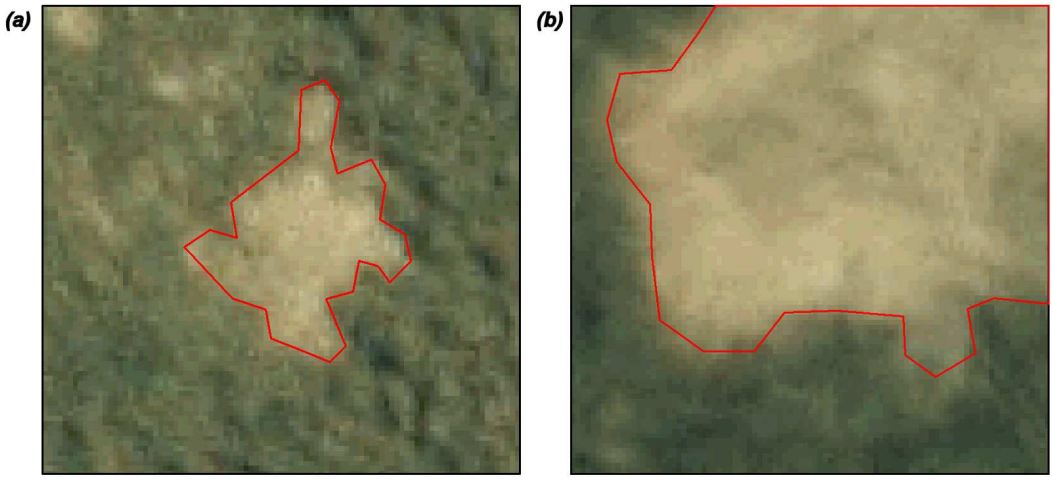

Figure 3.9: Close-up look at two single grid cells with digitised outlines of PFT from the aerial photography for comparison with the classification results. The borders of (a) and (b) indicate the Landsat pixel border, the red line the unvegetated area. Results from the maximum likelihood hard classification are bare ground only for both pixels, the probability guided unmixing results 12 % bare ground, 82 % forest type III pixel (a) and 30 % bare ground, 70 % forest type I pixel (b).

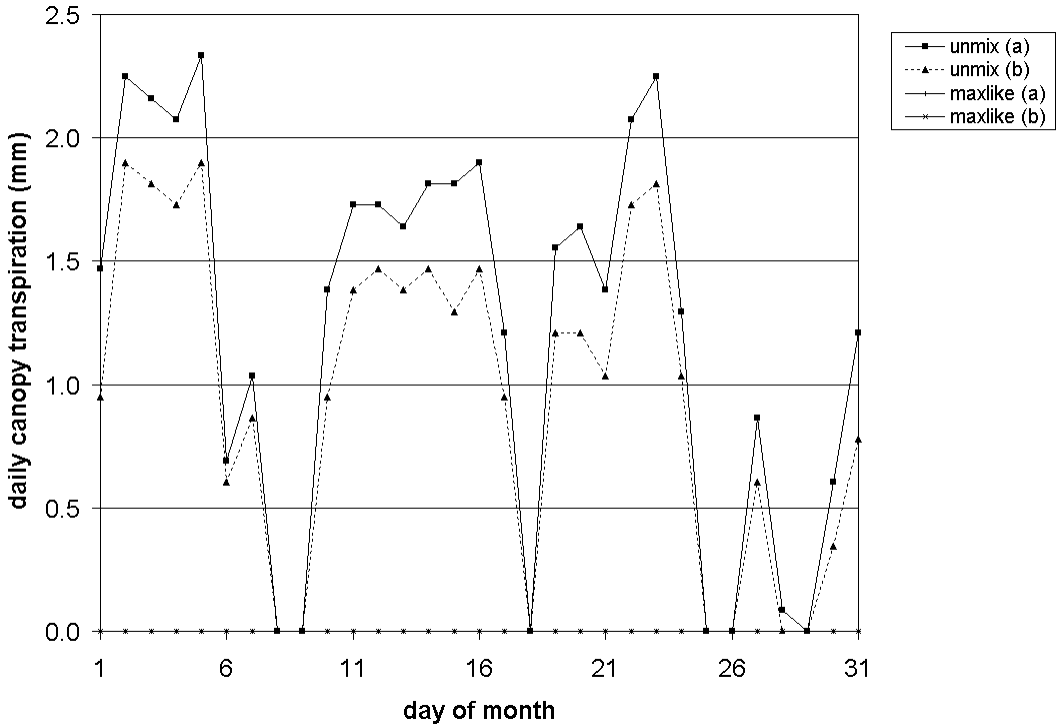

Figure 3.10: Aggregated daily canopy transpiration (mm) from model results of two individual grid cells ((*a*) and (*b*) same as in figure 3.9) for a whole month. PFT coverage for pixel (*a*) is 12 % bare ground and 82 % forest type III, for pixel (*b*) 30 % bare ground and 70 % forest type I using the modified spectral unmixing technique (unmix). Canopy transpiration values in the same pixels (*a*) and (*b*) using the hard maximum likelihood classifier (maxlike) are always 0 mm because of the lack of vegetation (both pixels classified with 100 % bare ground).

unmixing data, maximum transpiration values are 2.3 mm/day for pixel (*a*) and 1.9 mm/day for pixel (*b*). Figure 3.10 shows the canopy transpiration for a whole month in the selected grid cells for the classification results from the end of the model run. This clearly marks the difference between the two classification schemes with no canopy transpiration for unvegetated pixels from the maximum likelihood hard classification and values >0 depending on the vegetation fraction and atmospheric forcing of the corresponding soft classified pixels. This points to a general underestimation of transpiration in unvegetated hard classified pixels. Otherwise, an overestimation of canopy transpiration is expected for pixels which are classified as forest with the maximum likelihood method but show a small amount of bare ground in the soft classification.

3.6 Conclusions

The current study shows that multispectral hard and soft classifications based on Landsat ETM+ images, profound expert knowledge and high resolution orthophotos can also provide suitable land cover classes in the complex terrain of the high Andes of southern Ecuador, assuming a proper correction of atmospheric and topographic effects. Particularly the botanical expert knowledge based on intensive field surveys and the inclusion of a synthetic channel (terrain slope angle) significantly contribute to a successful discrimination of functional types of natural forest for the study area of a joint research effort (RU 816). Thus, the classification is an optimal prerequisite for defining PFTs which are needed for the vegetation parametrisation of the SVAT CLM.

A comparison of the classification results with the aerial photograph reveals that the soft classification, which usually provides more than one PFT/land-cover class in a grid cell (pixel), shows a much more realistic result of spatial land-cover distribution than the maximum likelihood hard classification. Exemplary model results for the canopy transpiration reveal a discrepancy between both classification approaches, especially in mixed pixel environments, with a general underestimation of transpiration in pure bare ground hard-classified pixels. Consequently, the initialisation of SVAT models on the local and regional scale should be supported by a soft land-cover classification based on expert knowledge and/or spectral field measurements of endmembers where the fractional land cover is determined by the modified spectral unmixing technique.

Future studies will focus on the determination of specific plant parameters such as the leaf-area index from the satellite data which are needed for the SVAT model as well. The presented classification will also be the basis for differentiating specific transfer functions between the satellite signal (e. g. vegetation indices) and the plant traits (LAI) for different types of natural vegetation. In addition, further satellite scenes of the same area but different dates will be processed by the method outlined in this paper. Change detection techniques will help to estimate the stability of land-cover classes over time and will allow SVAT modelling for different scenarios of land-use development.

Acknowledgements

The current study was performed within the framework of the DFG Research Unit 816 'Biodiversity and sustainable management of a megadiverse mountain rain forest in south Ecuador' and was generously funded by the German Research Council DFG (Be 1780/15-1, Le 762/10-1, Na783/1-1). We thank Nature and Culture International (NCI, Loja) for logistic support and two anonymous reviewers for constructive comments and suggestions.

References

Anderson, M., J. Norman, J. Mecikalski, R. Torn, W. Kustas & J. B. Basara: (2004): A multiscale remote sensing model for disaggregating regional fluxes to micrometeorological scale, *Journal of Hydrometeorology*, *5*, 343–363.

Balslev, H. & B. Øllgaard: (2002): *Botánica Austroecuatoriana. Estudios sobre los recursos vegetales en las provincias de El Oro, Loja y Zamora-Chinchipe*, chap. Mapa de vegetación del sur de Ecuador, 51–64, Ediciones Abya-Yala, Quito, Ecuador.

Barthlott, W., J. Mutke, M. D. Rafiqpoor, G. Kier & H. Kreft: (2005): Global centres of vascular plant diversity, *Nova Acta Leopoldina*, *NF 92*, 61–83.

Beck, E. & K. Müller-Hohenstein: (2001): Analysis of undisturbed and disturbed tropical mountain forest ecosystems in southern ecuador, *Die Erde*, *132*, 1–8.

Bendix, J., J. Homeier, E. Cueva Ortiz, P. Emck, S.-W. Breckle, M. Richter & E. Beck: (2006a): Seasonality of weather and tree phenology in a tropical evergreen mountain rain forest, *International Journal Biometeorology*, *50*, 370–384.

Bendix, J. & W. Lauer: (1992): Die niederschlagsjahreszeiten in ecuador und ihre klimadynamische interpretation, *Erdkunde*, *46*, 118–134.

Bendix, J., R. Rollenbeck, D. Göttlicher & J. Cermak: (2006b): Cloud occurance and cloud properties in ecuador, *Climate Research*, *30*, 133–147.

Bendix, J., R. Rollenbeck & W. Palacios: (2004): Cloud detection in the tropics: a suitable tool for climate-ecological studies in the high mountains of ecuador, *International Journal of Remote Sensing*, *25*, 4521–4540.

Bonan, G., K. Oleson, M. Vertenstein, S. Levis, X. Zeng, Y. Dai, R. Dickinson & Z.-L. Yang: (2002): The land surface climatology of the community land model coupled to the NCAR community climate model, *Journal of Climate*, *15*, 3123–3149.

Brehm, G., J. Homeier & K. Fiedler: (2003): Beta diversity of geometrid moths (lepidoptera: Geometridae) in an andean montane rainforest, *Diversity and Distributions*, *9*, 351–366.

Brummitt, N. & E. N. Lughadha: (2003): Biodiversity: Where's hot and where's not, *Conservation Biology*, *17*, 1442–1448.

Chavez, P. J.: (1996): Image-based atmospheric corrections - revisited and improved, *Photogrammetric Engineering and Remote Sensing*, *62*, 1025–1036.

Colby, J. & P. L. Keating: (1998): Land cover classification using landsat TM imagery in the tropical highlands: the influence of anisotropic reflectance, *International Journal of Remote Sensing*, *19*, 1476–1500.

Comber, A., P. Fisher & R. Wadsworth: (2004): Integrating land cover data with different ontologies, identifying change from inconsistency, *International Journal of Geographical Information Science*, *18*, 691–708.

Comber, A., P. Fisher & R. Wadsworth: (2005): Comparing the consistency of expert land cover knowledge, *International Journal of Applied Earth Observation and Geoinformation*, *7*, 189–201.

Congalton, R. G.: (1991): A review of assessing the accuracy of classifications of remotely sensed data, *Remote Sensing of Environment*, *37*, 35–46.

Dai, Y., X. Zeng, R. Dickinson, I. Baker, G. Bonan, M. Bosilovich, A. S. Denning, P. Dirmeyer, P. Houser, G. Niu, K. Oleson, C. Schlosser & Z.-L. Yang: (2003): The common land model, *Bulletin American Meteorological Society*, *84*, 1013–1023.

Eastman, J.: (2003): *IDRISI™Kilimanjaro – Guide to GIS and Image Processing*, Clark University, Worcester, MA, USA.

Eastman, J. & R. Laney: (2002): Bayesian soft classification for sub-pixel analysis: A critical evaluation, *Photogrammetric Engineering and Remote Sensing*, *68*, 1149–1154.

Echavarria, F.: (1998): *Nature's Geography: new lessons for conservation in developing countries*, chap. Monitoring Forests in the Andes Using Remote Sensing. An example from Ecuador, 100–120, The University of Wisconsin Press, Madison.

Göttlicher, D. & J. Bendix: (2004): Eine modulare multi-user datenbank für eine ökologische forschergruppe mit heterogenem datenbestand, *Zeitschrift für Agrarinformatik*, *4*, 95–103.

Hartig, K. & E. Beck: (2003): The bracken fern (Pteridium arachnoideum (Kaulf.) Maxon) dilemma in the andes of southern ecuador, *Ecotropica*, *9*, 3–13.

Helmer, E., S. Brown & W. Cohen: (2000): Mapping montane tropical forest successional stage and land use with multi-date landsat imagery, *International Journal of Remote Sensing*, *21*, 2163–2183.

Hill, R.: (1999): Image segmentation for humid tropical forest classification in landsat tm data, *International Journal of Remote Sensing, 20, No. 5*, 1039–1044.

Hill, R. & G. Foody: (1994): Separability of tropical rain-forest types in the tambopata-candamo reserved zone, peru, *International Journal of Remote Sensing, 15*, 2687–2693.

Homeier, J.: (2004): *Baumdiversität, Waldstruktur und Wachstumsdynamik zweier tropischer Bergregenwälder in Ecuador und Costa Rica*, *Dissertationes Botanicae*, vol. 391, Borntraeger, Stuttgart, dissertation Universität Bielefeld.

Homeier, J., H. Dalitz & S.-W. Breckle: (2002): Waldstruktur und baumartendiversität im montanen regenwald der estación científica san francisco in südecuador, *Berichte der Reinhold-Tüxen Gesellschaft, 14*, 109–118.

Homeier, J., F. Werner, S. Gradstein, S.-W. Breckle & M. Richter: (2008): Potential vegetation and floristic composition of andean forests in south ecuador, with a focus on the rbsf, in Beck, E., J. Bendix, I. Kottke, F. Makeschin & R. Mosandl (eds.) *Gradients in a Tropical Mountain Ecosystem of Ecuador*, *Ecological Studies*, vol. 198, 87–100, Springer, Berlin.

Jordan, E., L. Ungerechts, B. Cáceres, A. Penafiel & B. Francou: (2005): Estimation by photogrammetry of the glacier recession on the cotopaxi volcano (ecuador) between 1956 and 1997, *Hydrological Sciences-Journal-des Sciences Hydrologiques*, *50*, 949–961.

Lu, D. & Q. Weng: (2007): A survey of image classification methods and techniques for improving classification performance, *International Journal of Remote Sensing*, *28*, 823–870.

Malpica, J., M. Alonso & M. Sanz: (2007): Dempster-shafer theory in geographic information systems: A survey, *Expert Systems with Applications*, *32*, 47–55.

Mertikas, P. & M. Zervakis: (2001): Exemplifying the theory of evidence in remote sensing image classification, *International Journal of Remote Sensing*, *22*, 1081–1095.

NASA: (2002): Landsat 7 science datausers handbook, Tech. rep., National Aeronautics and Space Administration.

Parolly, G. & H. Kürschner: (2004): Ecosociological studies in ecuadorian bryophyte communities. ii. syntaxonomy of the submontane and montane epiphytic vegetation of s ecuador, *Nova Hedwigia*, *79*, 377–424.

PAULSCH, A.: (2002): *Development and Application of a Classification System for Undisturbed and Disturbed Tropical Montane Forests on Vegetation Structure*, Dissertation thesis, Fakultät für Biologie, Chemie und Geowissenschaften der Universität Bayreuth.

PEDDLE, D. & A. SMITH: (2005): Spectral mixture analysis of agricultural crops: endmember validation and biophysical estimation in potato plots, *International Journal of Remote Sensing*, *26*, 4959–4979.

RIAÑO, D., E. CHUVIECO, J. SALAS & I. AGUADO: (2003): Assessment of different topographic corrections in landsat-tm data for mapping vegetation types, *IEEE Transactions on Geoscience and Remote Sensing*, *41*, 1056–1061.

RICHTER, M.: (2003): Using plant functional types and soil temperatures for ecoclimatic interpretation in southern ecuador, *Erdkunde*, *57*, 161–181.

SALOVAARA, K., S. THESSLER, R. MALIK & H. TUOMISTO: (2005): Classification of amazonian primary rain forest vegetation using landsat ETM+ satellite imagery, *Remote Sensing of Environment*, *97*, 39–51.

SCHWEITZER, C., G. RÜCKER, C. CONRAD, G. STRUNZ & J. BENDIX: (2005): Knowledge-based land use classification combining expert knowledge, GIS, multitemporal landsat 7 ETM+ and MODIS time series data in khorezem, uzbekistan, *Göttinger Geographische Abhandlungen*, *113*, 116–123.

SHEPHERD, J. & J. DYMOND: (2003): Correcting satellite imagery for the variance of reflectance and illumination with topography, *International Journal of Remote Sensing*, *24*, 3503–3514.

SOHN, Y. & R. MCCOY: (1997): Mapping desert shrub rangeland using spectral unmixing and modeling spectral mixtures with tm data, *Photogrammetric Engineering and Remote Sensing*, *63*, 707–716.

SONG, C.: (2005): Spectral mixture analysis for subpixel vegetation fractions in the urban environment: How to incorporate endmember variability?, *Remote Sensing of Environment*, *95*, 248–263.

STORY, M. & R. CONGALTON: (1986): Accuracy assessment: A user's perspective, *Photogrammetric Engineering and Remote Sensing*, *52*, 397–399.

TOTTRUP, C.: (2004): Improving tropical forest mapping using multi-data landsat TM data and pre-classification image smoothing, *International Journal of Remote Sensing*, *25 No.4*, 717–730.

Valencia, R., C. Cerón, W. Palacios & R. Sierra: (1999): *Propuesta preliminar de un sistema de clasificación de vegetación para el Ecuador continental*, chap. Las formaciones naturales de la sierra del Ecuador, 79–108, Proyecto INEFAN/GEF-BIRF y EcoCiencia, Quito, Ecuador.

Werner, F., J. Homeier & S. Gradstein: (2005): Diversity of vascular epiphytes on isolated remnant trees in the montane forest belt of southern ecuador, *Ecotropica*, *11*, 21–40.

Zhu, H.: (2005): Linear spectral unmixing assisted by probability guided and minimum residual exhaustive search for subpixel classification, *International Journal of Remote Sensing*, *26*, 5585–5601.

4 Sensitivity of PFT Parameter

This chapter was submitted 29 May 2010 to *Computers & Geosciences*.

Sensitivity of the Community Land Model to plant and soil parameters for the prediction of commonly required parameters for applied ecologic and socio-economic studies

Dietrich Göttlicher*‡, Thomas Nauss§ and Jörg Bendix‡

‡Faculty of Geography, Philipps-Universität Marburg, Deutschhausstr. 10, 35037 Marburg, Germany
§Faculty of Geography, University of Bayreuth, 95440 Bayreuth, Germany

A multi disciplinary research unit is investigating the landcover changes and ecological processes in the tropical mountain rainforest and pastures in southern Ecuador. To evaluate which parameters used in the Community Land Model are more dominant to various output results a sensitivity study is conducted. All implemented plant functional type parameters and also the soil parameters are altered in fixed rates one by one keeping the others constant. Five output parameters (surface air temperature, surface humidity, sensible heat flux, transpiration and evaporation) are chosen to determine the absolute and relative deviations. The results are used to decide which parameters must be gathered with priority in the field to properly parametrize the model for socio-economic applications. With respect to temperature and humidity simulations needed by the socio-economic projects, the variation of most investigated parameters of $\pm 30\,\%$ appeared to cause only negligible variations ($< 1\,\%$). Other output variables like transpiration and evaporation from the vegetation show much higher deviations ($> 30\,\%$) especially by variations of the structural parameter (leaf area index). In summary, the operation of the SVAT model with default parameters provides data accurate enough for the socio-economic investigations.

Keywords: CLM, SVAT, sensitivity, Ecuador, plant functional type

4.1 Introduction

Soil-vegetation-atmosphere transfer (SVAT) models are widely used within eco-climatological studies. Moreover, robust landsurface models are necessary for multidecadal global climate simulations (Foley et al., 2000). Since SVAT models simulate the land-atmosphere exchanges in response to atmospheric forcing and actual

land-cover, such models are also valueable for studies in the field of ecology oriented social science and economics.

The research unit *Biodiversity and Sustainable Management of a Megadiverse Mountain Ecosystem in South Ecuador* funded by the German research foundation (Deutsche Forschungsgemeinschaft, DFG) aims in the design of sustainable strategies and effective measures for the protection of the natural forests and for the regeneration of abandoned pasture areas in the mountain catchment of the Rio San Francisco within the Podocarpus-El Condor United Nations Biosphere Reserve (see http://www.tropicalmountainforest.org).

The research area is located in the Andes of Ecuador which are considered as one of the 'hottest' hotspots of vascular plant biodiversity worldwide (Brummitt & Lughadha, 2003; Barthlott et al., 2005; Jørgensen & Ulloa Ulloa, 1994) while at the same time the country suffers the highest rate ($-1.7\,\%$) of deforestation in the period 2000–2005 within South America (Mosandl et al., 2008). Forest clearing for conversion to agricultural land is the main threat to Ecuador's biodiversity but mainly due to the use of fire as an agricultural tool, the gained pasture areas cannot be used sustainably as they are overgrown by persistent weeds like the bracken fern (*Pteridium arachnoideum*) (Hartig & Beck, 2003).

Reforestation and repastorization of the abandoned agricultural areas must therefore become central elements of a sustainable development strategy for the country. Because of a lack of knowledge (and indigenous material), reforestation efforts supported by international organizations mainly rely on monocultures of exotic tree species and have shown only temporary and, at best, moderate success. In this situation, the livelihood of settlers is endangered while the (illegal) destruction of natural forests continues. Sustainable land use strategies however require a profound knowledge of the relevant ecosystem and of its human users.

Therefore the 25 interdisciplinary project teams of the research unit endeavour to generate this knowledge by investigating the mechanisms and processes of the natural ecosystem i. e. a tropical mountain rain forest and its anthropogenic replacement system within the catchment. In this context, several socio-economic project teams evaluate the interactions between human actors and the alteration of the landuse/landcover system and the resulting insights are forming the basis for the implementation of agent-based models. Preliminary surveys of local residents reveal that the knowledge about changes in local climate conditions due to changes in the landcover will influence the decision-making process. Therefore, the Community Land Model version 3.5 (CLM) (Oleson et al., 2004, 2008) should be used to simulate the alteration of local climate parameters by changes in the landcover.

One prerequisite for successfully applying the CLM in this context is the provision of area-wide datasets with a spatial resolution of about 30 m covering the distribution of the morphological properties of the relevant vegetation communities (i. e. plant functional types) and basic soil parameters. In addition, the physiological and optical properties of the vegetation communities have to be quantified using a set of

48 plant functional type parameters. These datasets are prepared by several project teams of the research unit but with respect to the complexity of the investigation area and the diversity of the landcover and vegetation types, uncertainties within these datasets are considerable.

Therefore, the sensitivity of the relevant CLM output parameters to plant and soil properties is investigated in a preparatory study. In the present context, the 2 m air temperature and humidity is of special importance for the socio-economic projects. Since insights into heat and humidity fluxes are also important background information with respect to the interpretation of the simulation results, the sensitivity of the sensible heat flux and the evaporation and transpiration from vegetation surfaces is also considered in this study. Depending on the results of this study, the botany, soil science and forestry project teams of the research unit will relay a special focus on the measurement and area-wide acquisition of those input parameters that have been identified as crucial for the simulation of these output parameters.

4.2 Sensitivity study setup

The input parameters of the CLM considered within this study can be divided into (i) time and space dependent vegetation structure (ii) space dependent soil parameters and (iii) time independent fixed plant functional types parameters. The former cover the top and bottom height of the canopy, the leaf and stem area index. The soil is characterized by the fraction of sand and clay and its albedo. The latter describe the morphological, physiological and optical properties of each plant functional type i. e. each vegetation community. Since the research area presented in the previous chapter is mainly composed by tropical tree, shrub, and grassland communities, the four already implemented plant functional types *evergreen tropical trees*, *shrubs*, *C3 grass*, and *C4 grass* are used within in this study.

To investigate the sensitivity of the simulated 2 m air temperature and humidity, the sensible heat flux, and the evaporation and transpiration from vegetation, on changes of the input parameters, the latter are changed by certain factors from a predefined mean value while all other parameters have been held constant. The mean values of the plant functional type parameters are taken from the CLM 3.5 standard configuration as described by Bonan et al. (2002) and Zeng (2001). The mean values of the vegetation structure and soil parameters which have been held constant over time for each model run are taken with respect to the results of different field surveys by botany, soil science, and forestry project teams of the research unit.

For the atmospheric forcing, a subset covering the Andean Ecuadorian region of the observation-based analyses combined with intramonthly variations from the NCEP/NCAR by (Qian et al., 2006) are used. For each modification of an input parameter, a three year model run has been started covering the time period between January 2003 and December 2005. The analysis of the deviations of the output

parameters is based on the monthly mean values of January 2005 and September 2005. These two month mark the end of a humid (January) and dry (September) period for which the influence of some of the input parameters differs considerably in magnitude.

4.3 Influence of vegetation structure and soil parameters

In order to investigate the influence of vegetation structure and soil parameters, the upper and lower height of the canopy layer, the leaf and stem area index, the sand and clay fraction of the soil layer as well as the soil colour have been modified one by one while all the respective other parameters have been held constant. Table 4.1 shows the deviation of the parameters for the three land cover types (grass, shrubs, trees) as well as for the soil parameters. The bold numbers represent the standard values of the parameters that have been used while one other parameter has been modified. The fraction of sand and clay is set to a standard value of 33 % each during the various model runs but is not used as an input value while the soil texture itself is changed. As one can see from the percentage deviation, the initial parameter values have generally been decreased or increased by factor 2 in three steps. One exception is the canopy top height for trees which has been increased only up to 140 % (i. e. from 25 m to 35 m) since a further increase would have caused problems with respect to the meteorological initialization in the planetary boundary layer.

The influence of these modifications on the resulting values of the 2 m air temperature and humidity, the sensible heat flux and the evaporation and transpiration from vegetation surfaces is discussed in the next sections. A graphical overview of this influence can be seen for each output parameter in figures 4.1 to 4.5 while tables 4.3 to 4.7 give a comprehensive overview of the absolute results and percentage deviations relative to the average value also shown in the tables.

4.3.1 Monthly vegetation height

Generally, the vegetation height affects the aerodynamic resistance to matter and energy fluxes by changing the roughness length z_0 and displacement height d which are plant specific but constant fractions of the vegetation top height. An increase in vegetation height implies an increase in z_0 and therefore a decrease in the aerodynamic resistance which results in a closer coupling between the surface (i. e. the canopy layer) and the atmosphere.

The 2 m air temperature is based on the conservation of canopy energy and results from the computation of heat fluxes between the soil and canopy layer and the canopy layer and the atmosphere above respectively under the assumption that the air inside the canopy has a negligible heat storage capacity. Since the temperature

Table 4.1: Modification of morphological and soil related input parameters and percentage difference relative to the standard mean value (bold) used for this study. The standard mean value of the fraction of sand and clay is set to 33 % each. The numbers in brackets indicate the modification ID of the figures 4.1, 4.2, 4.4, 4.5 and 4.3.

Grass Parameters							
Height Top	0.25	0.34	0.42	**0.50**	0.67	0.83	1.00
(0 – 6)	50.00 %	67.00 %	83.00 %	100.00 %	133.00 %	166.00 %	200.00 %
Height Bottom	0.01	0.01	0.01	**0.01**	0.01	0.02	0.02
(7 – 13)	50.00 %	67.00 %	83.00 %	100.00 %	133.00 %	166.00 %	200.00 %
LAI	1.00	1.34	1.66	**2.00**	2.66	3.32	4.00
(14 – 20)	50.00 %	67.00 %	83.00 %	100.00 %	133.00 %	166.00 %	200.00 %
SAI	0.13	0.17	0.21	**0.25**	0.33	0.42	0.50
(21 – 27)	50.00 %	67.20 %	83.20 %	100.00 %	132.00 %	166.00 %	200.00 %
Shrub Parameters							
Height Top	0.25	0.34	0.42	**0.50**	0.67	0.83	1.00
(0 – 6)	50.00 %	67.00 %	83.00 %	100.00 %	133.00 %	166.00 %	200.00 %
Height Bottom	0.05	0.07	0.08	**0.10**	0.13	0.17	0.20
(7 – 13)	50.00 %	67.00 %	83.00 %	100.00 %	133.00 %	166.00 %	200.00 %
LAI	1.50	2.01	2.49	**3.00**	3.99	4.98	6.00
(14 – 20)	50.00 %	67.00 %	83.00 %	100.00 %	133.00 %	166.00 %	200.00 %
SAI	0.13	0.17	0.21	**0.25**	0.33	0.42	0.50
(21 – 27)	50.00 %	67.20 %	83.20 %	100.00 %	132.00 %	166.00 %	200.00 %
Tree Parameters							
Height Top	12.50	16.75	20.75	**25.00**	29.25	33.30	35.00
(0 – 6)	50.00 %	67.00 %	83.00 %	100.00 %	117.00 %	133.20 %	140.00 %
Height Bottom	2.00	2.68	3.32	**4.00**	5.32	6.64	8.00
(7 – 13)	50.00 %	67.00 %	83.00 %	100.00 %	133.00 %	166.00 %	200.00 %
LAI	2.00	2.68	3.32	**4.00**	5.32	6.64	8.00
(14 – 20)	50.00 %	67.00 %	83.00 %	100.00 %	133.00 %	166.00 %	200.00 %
SAI	0.38	0.50	0.62	**0.75**	1.00	1.25	1.50
(21 – 27)	50.00 %	67.07 %	83.07 %	100.00 %	133.07 %	166.00 %	200.00 %
Soil parameters							
Sand / Clay	0/0	100/0	0/100	20/20	46/20	46/46	20/46
(28 – 34)							
Soil Color	11.00	13.00	15.00	**17.00**	19.00	20.00	20.00
(35 – 41)	64.71 %	76.47 %	88.24 %	100.00 %	111.76 %	117.65 %	117.65 %

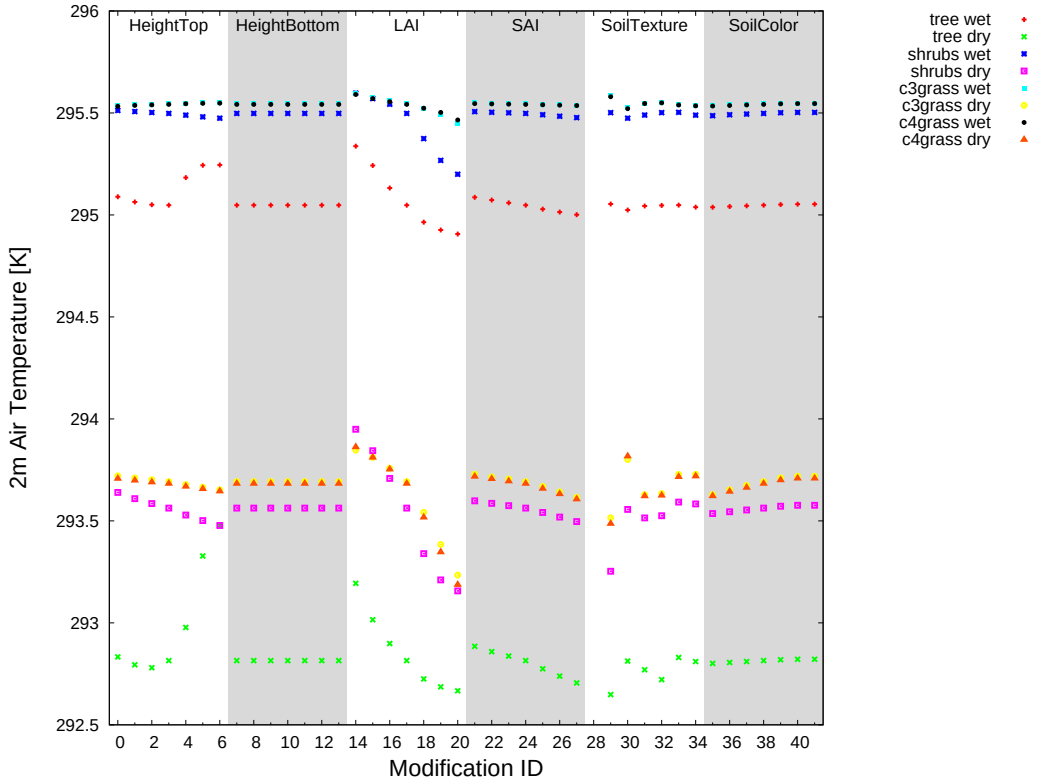

Figure 4.1: Air temperature (K) at 2 m above ground as a function of different values for the plant morphological and soil parameters stated in table 4.1.

T_s of the canopy layer is considered to equal the air temperature at height $z_0 + d$, differences in the sensible heat flux at this height level have to be balanced by sensible heat from the vegetation and the ground. This results in small positive correlations of the 2 m air temperature and the top-height of vegetation for grass during the wet season while negative correlations exist for the dry period (see figure 4.1). Shrubs show a negative correlation for wet and especially for dry conditions and evergreen tropical trees show a small negative correlation for canopy top heights below 25 m and a strong positive correlation for canopy top heights above 25 m. The latter can be explained by competing influences of an increased roughness leading to a stronger coupling to the (colder) atmosphere and increasing energy storage capacities for thicker canopy layers.

The negative correlation of air temperature for shrubs under dry conditions can be explained by the enhanced entrainment of slightly colder air due to a more pronounced atmospheric coupling for larger vegetation heights. With respect to transpiration, associated changes in the vapour pressure deficit due to enhanced turbulences are generally not (dry period) or negatively (wet period) correlated to the canopy top height except for trees during dry periods, where a positive correlation exists up

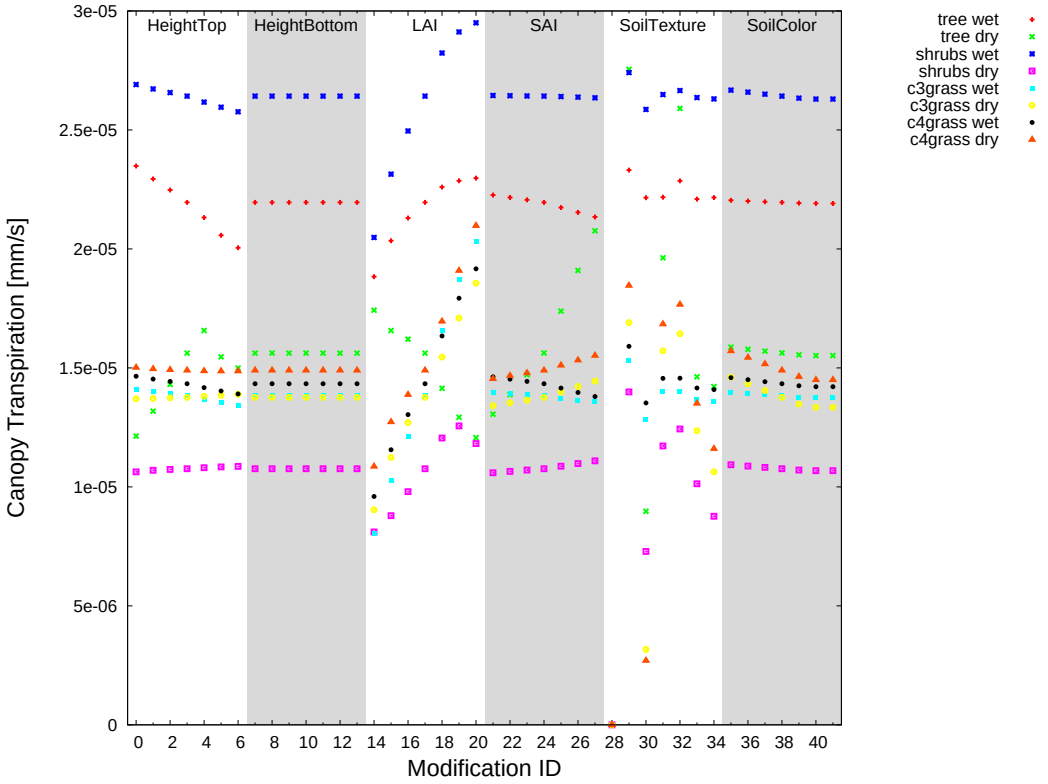

Figure 4.2: Transpiration (mm/s) from vegetation as a function of different values for the plant morphological and soil parameters stated in table 4.1.

to heights of about 30 m (see figure 4.2).

The influences of the canopy height on the evaporation from vegetation has negligible influences except for tree heights above 25 m which lead to a positive correlation (see figure 4.3). Even though the partly increasing transpiration and evaporation leads to an increase in the latent heat fluxes, these energy losses can be counterbalanced by sensible heat fluxes from the ground surface layer except for trees under dry conditions.

For all other conditions, a positive correlation between the sensible heat flux and the vegetation height due to the stronger coupling between the surface layer and the atmosphere exists (see figure 4.4). As a consequence of the transpiration and evaporation fluxes, the specific humidity shows a slight increase with canopy height for trees while for shrubs and grass, no or a small negative trend can be identified. The canopy bottom height shows no influence on the resulting parameters.

The dependencies stated above lead to negligible percentage differences ($\ll 1\,\%$) in the resulting 2 m air temperatures and specific humidities but absolute temperature differences can exceed 0.5 K for trees during dry conditions (see table 4.3 and 4.4). For the sensible heat flux, deviations of about 8 % from the mean value have

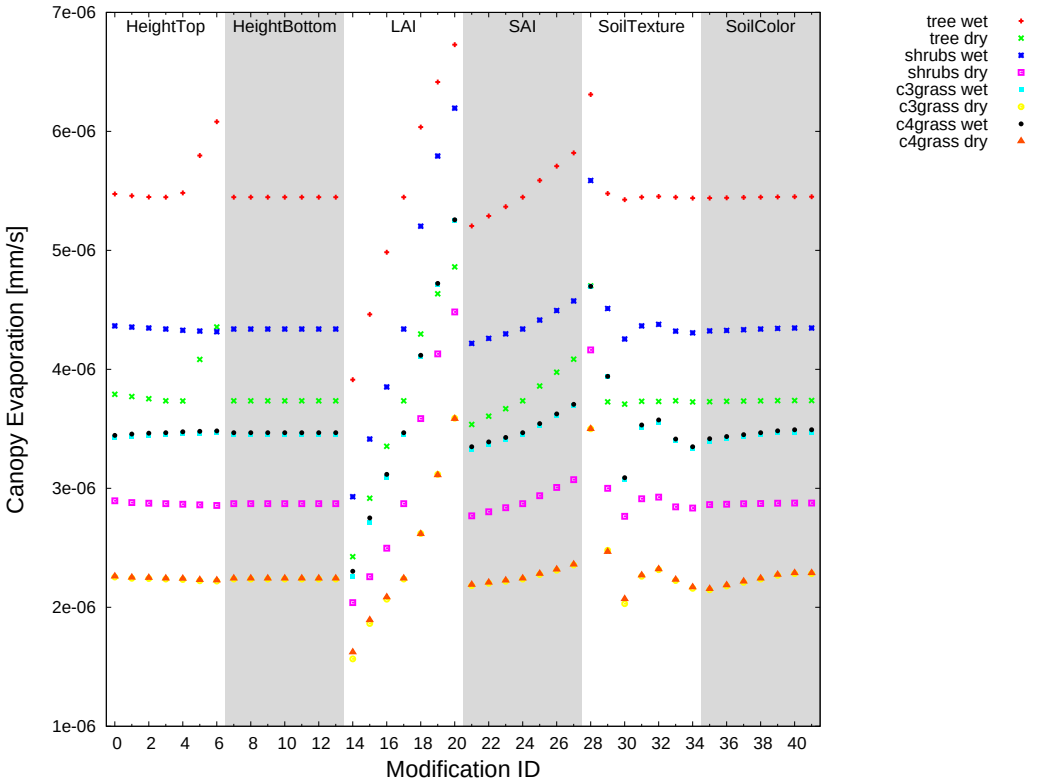

Figure 4.3: Evaporation (mm/s) from vegetation as a function of different values for the plant morphological and soil parameters stated in table 4.1.

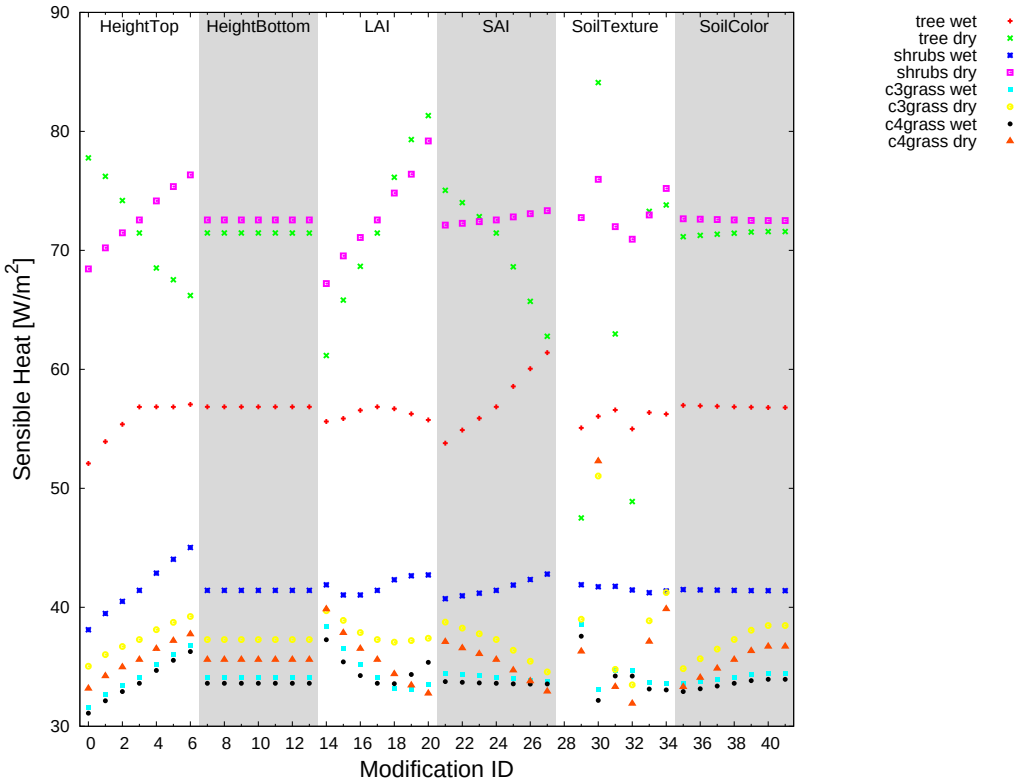

Figure 4.4: Sensible heat flux (W/m^2) as a function of different values for the plant morphological and soil parameters stated in table 4.1.

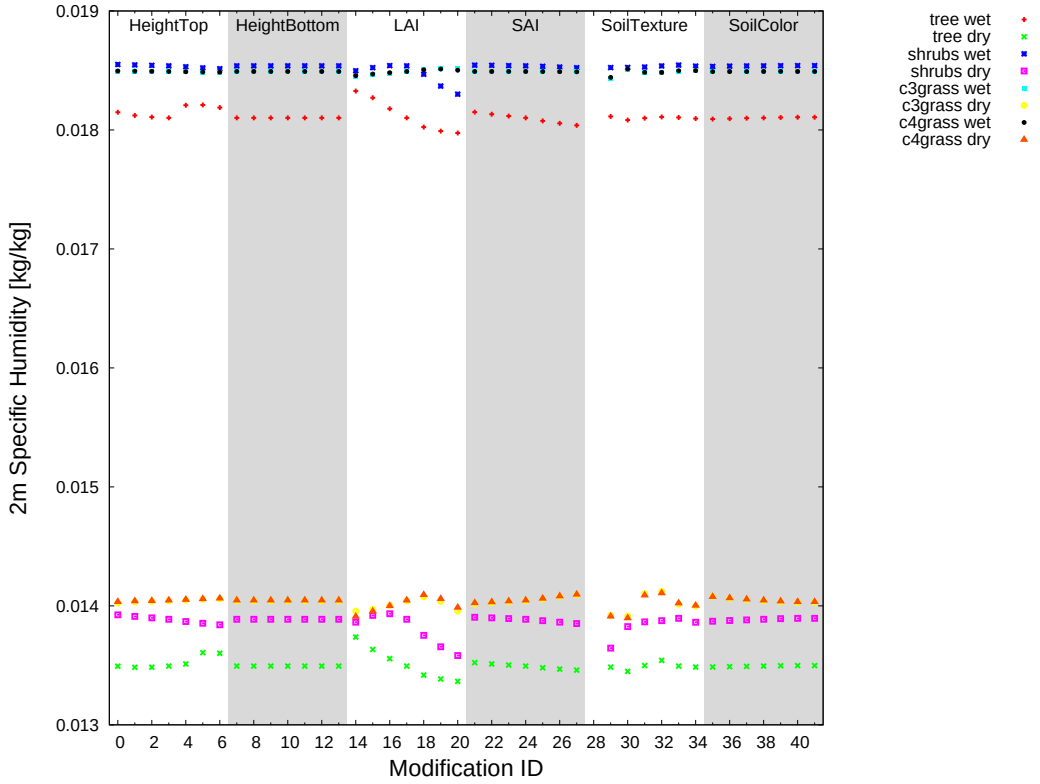

Figure 4.5: Air humidity (kg/kg) at 2 m above ground a function of different values for the plant morphological and soil parameters stated in table 4.1.

to be expected (see table 4.5), if the vegetation top height changes by the factors of table 4.1 (i. e. by a factor of ± 2 except for trees where the increase of vegetation top height is limited to a factor of $+1.4$). Larger percentage differences can be seen only for transpiration and evaporation from trees during dry conditions with values of 16.63 % and -22.33 % respectively which equals absolute deviations of 62 mm/month and -349 mm/month. For grass and shrubs, the deviation in evaporation and transpiration is below 3 % for changes in the vegetation height by factor ± 2 (see table 4.6 and 4.7). The bottom height of the canopy layer has no influence on any of the output parameters considered.

As a consequence of the already mentioned humidity fluxes, the specific air humidity shows negative correlations with vegetation height except for shrubs and grass during dry conditions (see figure 4.5). For the evaporation (see figure 4.3) no significant influence of the vegetation top height exists. The same is true for the bottom height of the vegetation canopy for all parameters.

4.3.2 Leaf and stem area index

The leaf area index (LAI) and its sunlit and shaded fractions have a dominant influence on the radiative transfer inside the canopy and in turn on the energy available for photosynthesis, heat and water vapour fluxes. Consequently, the 2 m air temperature shows a negative correlation with increasing LAI values (see figure 4.1) because of increasing shading effects and a positive correlated increase in transpiration and evaporation with leaf area exists (see figure 4.2, 4.3) resulting in an evaporative heat loss of the canopy air. Except for grass during dry conditions and for large trees (>25 m), the sensible heat flux shows a positive correlation with the leaf area index (see figure 4.4). The energy reduction at the ground surface due to an increased shading with increasing leaf area index significantly reduces the evaporation from the surface layer except for grass areas (during dry conditions) which explains the predominately negative correlations between the LAI and the specific air humidity at 2 m height (see figure 4.5).

The stem area index (SAI) is also positively correlated with the canopy energy budget and generally shows the same tendencies as the LAI. One exception is the transpiration which shows a positive correlation with SAI for trees during dry conditions resulting in deviations of the sensible heat flux accordingly. The reason for that is unclear but might be related to effects of the closure of the canopy energy budget by numerical iteration leading to a decrease of evaporation and an increase in the soil water available for transpiration.

As for changes in the canopy height, changes in the LAI and SAI have a negligible percentage influence on the 2 m air temperature and humidity but this time, the air temperature deviation over grass and shrubs can exceed 0.5 K and the air humidity exceeds 1 % for trees and shrubs under dry conditions. For the sensible heat fluxes and especially for the evapotranspiration, the differences resulting from changing leaf and stem areas are larger than the ones from the canopy height alteration. In general, the largest deviations are related to dry conditions and do not exceed about 14% for the sensible heat flux but reach up to 60 % for the evaporation if the grass leaf area index is increased by factor 2. Since transpiration is at least partly controlled by the plants, an increase in the leaf area does generally result in smaller alterations that do not exceed 25 % for trees and shrubs and 47 % for grass. The SAI has only a minor influence except for trees during dry conditions where it can induce an increase of the transpiration by 33 % (see tables 4.3 to 4.7).

4.3.3 Soil properties

Soil water availability is - among others - a function of the sand/clay fraction with feedbacks on field capacity, wilting point and water availability. For transpiration, the latter factors lead to a negative correlation with increasing clay fraction of the underlying soil. The same tendency can be found for evaporation. Under dry condi-

Table 4.2: Tendency of the correlation between the computed values of the 2 m air temperature (TSA), the 2 m air humidity ($Q2M$), the sensible heat flux (FSH), the evaporation ($QVEGE$) as well as the transpiration ($QVEGT$) from vegetation surfaces and the morphological and soil related input parameters described in table 4.1.

Surface Parameter		TSA	$Q2M$	FSH	$QVEGE$	$QVEGT$
Height Top						
Trees	Wet Period	- +	- +	+	- +	-
	Dry Period	- +	0 +	-	- +	+ -
Shrubs	Wet Period	-	0	+	0	-
	Dry Period	-	-	+	0	0
Grass	Wet Period	0	0	+	0	-
	Dry Period	-	0	+	0	0
Height Bottom						
Trees	Wet Period	0	0	0	0	0
	Dry Period	0	0	0	0	0
Shrubs	Wet Period	0	0	0	0	0
	Dry Period	0	0	0	0	0
Grass	Wet Period	0	0	0	0	0
	Dry Period	0	0	0	0	0
LAI						
Trees	Wet Period	-	-	+ -	+	+
	Dry Period	-	-	+	+	-
Shrubs	Wet Period	-	-	+	+	+
	Dry Period	-	-	+	+	+ -
Grass	Wet Period	-	0	- +	+	+
	Dry Period	-	+	-	+	+
SAI						
Trees	Wet Period	-	-	+	+	-
	Dry Period	-	-	-	+	+
Shrubs	Wet Period	-	0	+	+	0
	Dry Period	-	-	+	+	+
Grass	Wet Period	0	0	-	+	-
	Dry Period	-	+	-	+	+
Clay						
Trees	Wet Period	-	+	+	-	-
	Dry Period	+	-	+	0	-
Shrubs	Wet Period	-	0	-	-	-
	Dry Period	+	0	+	-	-
Grass	Wet Period	-	+	-	-	-
	Dry Period	+	-	+	-	-
Color						
Trees	Wet Period	0	0	0	0	-
	Dry Period	0	0	0	0	-
Shrubs	Wet Period	0	0	0	0	-
	Dry Period	+	0	0	0	-
Grass	Wet Period	0	0	+	+	-
	Dry Period	+	0	+	+	-

Table 4.3: Absolute values (K) and relative deviation from the mean value (%) for the air temperature in 2 m height with respect to the modification of morphological and soil related input parameters described in table 4.1.

Trees	Height Top	Height Bot	LAI	SAI	Sand Clay	Soil Color
Wet Period						
Minimum	295.05	295.05	294.91	295.00	295.02	295.04
	0.00 %	0.00 %	-0.05 %	-0.02 %	-0.01 %	-0.00 %
Maximum	295.25	295.05	295.34	295.09	295.05	295.05
	0.07 %	0.00 %	0.10 %	0.01 %	0.00 %	0.00 %
Difference	0.20	0.00	0.43	0.09	0.03	0.01
Average	295.05	295.05	295.05	295.05	295.04	295.05
Dry Period						
Minimum	292.78	292.81	292.67	292.71	292.65	292.80
	-0.01 %	0.00 %	-0.05 %	-0.04 %	-0.04 %	-0.00 %
Maximum	293.48	292.82	293.19	292.89	292.83	292.82
	0.23 %	0.00 %	0.13 %	0.02 %	0.02 %	0.00 %
Difference	0.70	0.00	0.53	0.18	0.18	0.02
Average	292.81	292.81	292.81	292.81	292.77	292.81
Shrubs	**Height Top**	**Height Bot**	**LAI**	**SAI**	**Sand Clay**	**Soil Color**
Wet Period						
Minimum	295.47	295.50	295.20	295.48	295.47	295.49
	-0.01 %	0.00 %	-0.10 %	-0.01 %	-0.01 %	-0.00 %
Maximum	295.51	295.50	295.60	295.51	295.50	295.50
	0.01 %	0.00 %	0.03 %	0.00 %	0.00 %	0.00 %
Difference	0.04	0.00	0.40	0.03	0.03	0.02
Average	295.50	295.50	295.50	295.50	295.49	295.50
Dry Period						
Minimum	293.48	293.56	293.16	293.50	293.25	293.54
	-0.03 %	0.00 %	-0.14 %	-0.02 %	-0.09 %	-0.01 %
Maximum	293.64	293.56	293.95	293.60	293.59	293.58
	0.03 %	0.00 %	0.13 %	0.01 %	0.03 %	0.00 %
Difference	0.16	0.00	0.79	0.10	0.34	0.04
Average	293.56	293.56	293.56	293.56	293.51	293.56
C3 Grass	**Height Top**	**Height Bot**	**LAI**	**SAI**	**Sand Clay**	**Soil Color**
Wet Period						
Minimum	295.54	295.54	295.45	295.54	295.53	295.54
	-0.00 %	0.00 %	-0.03 %	-0.00 %	-0.01 %	-0.00 %
Maximum	295.55	295.54	295.60	295.55	295.59	295.55
	0.00 %	0.00 %	0.02 %	0.00 %	0.01 %	0.00 %
Difference	0.01	0.00	0.15	0.01	0.06	0.01
Average	295.54	295.54	295.54	295.54	295.55	295.54
Dry Period						
Minimum	293.65	293.69	293.23	293.62	293.52	293.63
	-0.01 %	0.00 %	-0.16 %	-0.03 %	-0.04 %	-0.02 %
Maximum	293.72	293.69	293.85	293.73	293.80	293.72
	0.01 %	0.00 %	0.05 %	0.01 %	0.06 %	0.01 %
Difference	0.07	0.00	0.61	0.11	0.29	0.09
Average	293.69	293.69	293.69	293.69	293.63	293.69
C4 Grass	**Height Top**	**Height Bot**	**LAI**	**SAI**	**Sand Clay**	**Soil Color**
Wet Period						
Minimum	295.53	295.54	295.47	295.54	295.52	295.53
	-0.00 %	0.00 %	-0.03 %	-0.00 %	-0.01 %	-0.00 %
Maximum	295.55	295.54	295.59	295.55	295.58	295.55
	0.00 %	0.00 %	0.02 %	0.00 %	0.01 %	0.00 %
Difference	0.02	0.00	0.13	0.01	0.06	0.01
Average	295.54	295.54	295.54	295.54	295.55	295.54
Dry Period						
Minimum	293.65	293.68	293.19	293.61	293.49	293.62
	-0.01 %	0.00 %	-0.17 %	-0.03 %	-0.05 %	-0.02 %
Maximum	293.71	293.68	293.86	293.72	293.82	293.71
	0.01 %	0.00 %	0.06 %	0.01 %	0.07 %	0.01 %
Difference	0.06	0.00	0.67	0.11	0.33	0.09
Average	293.68	293.68	293.68	293.68	293.62	293.68

Table 4.4: Absolute values (g/kg) and relative deviation from the mean value (%) for the specific air humidity in 2 m height with respect to the modification of morphological and soil related input parameters described in table 4.1.

Trees	Height Top	Height Bot	LAI	SAI	Sand Clay	Soil Color
Wet Period						
Minimum	181.02	181.02	179.75	180.38	180.83	180.91
	0.00 %	-0.00 %	-0.70 %	-0.35 %	-0.09 %	-0.06 %
Maximum	182.10	181.02	183.27	181.50	181.13	181.07
	0.60 %	0.00 %	1.25 %	0.27 %	0.08 %	0.03 %
Difference	1.09	0.00	3.52	1.11	0.30	0.15
Average	181.02	181.02	181.02	181.02	180.99	181.02
Dry Period						
Minimum	134.84	134.94	133.66	134.60	134.49	134.86
	-0.08 %	-0.00 %	-0.95 %	-0.25 %	-0.37 %	-0.06 %
Maximum	136.07	134.94	137.38	135.23	135.42	134.98
	0.83 %	0.00 %	1.80 %	0.22 %	0.32 %	0.03 %
Difference	1.23	0.00	3.72	0.63	0.93	0.12
Average	134.94	134.94	134.94	134.94	134.99	134.94
Shrubs	**Height Top**	**Height Bot**	**LAI**	**SAI**	**Sand Clay**	**Soil Color**
Wet Period						
Minimum	185.15	185.39	183.01	185.23	185.24	185.34
	-0.13 %	0.00 %	-1.28 %	-0.08 %	-0.02 %	-0.02 %
Maximum	185.50	185.39	185.40	185.45	185.45	185.41
	0.06 %	0.00 %	0.01 %	0.03 %	0.09 %	0.01 %
Difference	0.36	0.00	2.40	0.22	0.21	0.07
Average	185.39	185.39	185.39	185.39	185.29	185.39
Dry Period						
Minimum	138.41	138.87	135.82	138.51	136.45	138.71
	-0.34 %	-0.00 %	-2.20 %	-0.26 %	-1.59 %	-0.12 %
Maximum	139.25	138.87	139.34	139.05	138.95	138.95
	0.27 %	0.00 %	0.33 %	0.12 %	0.22 %	0.06 %
Difference	0.84	0.00	3.51	0.54	2.50	0.24
Average	138.87	138.87	138.87	138.87	138.65	138.87
C3 Grass	**Height Top**	**Height Bot**	**LAI**	**SAI**	**Sand Clay**	**Soil Color**
Wet Period						
Minimum	184.85	184.90	184.51	184.89	184.36	184.88
	-0.02 %	0.00 %	-0.21 %	-0.00 %	-0.25 %	-0.01 %
Maximum	184.93	184.90	185.20	184.90	185.07	184.91
	0.02 %	0.00 %	0.17 %	0.00 %	0.13 %	0.00 %
Difference	0.08	0.00	0.69	0.01	0.71	0.03
Average	184.90	184.90	184.90	184.90	184.83	184.90
Dry Period						
Minimum	140.24	140.42	139.56	140.16	139.13	140.29
	-0.13 %	-0.00 %	-0.61 %	-0.18 %	-1.34 %	-0.09 %
Maximum	140.60	140.42	140.76	140.93	141.21	140.78
	0.13 %	0.00 %	0.24 %	0.36 %	0.14 %	0.26 %
Difference	0.36	0.00	1.19	0.77	2.08	0.49
Average	140.42	140.42	140.42	140.42	141.02	140.42
C4 Grass	**Height Top**	**Height Bot**	**LAI**	**SAI**	**Sand Clay**	**Soil Color**
Wet Period						
Minimum	184.87	184.91	184.57	184.89	184.41	184.90
	-0.03 %	0.00 %	-0.19 %	-0.01 %	-0.23 %	-0.01 %
Maximum	184.96	184.91	185.12	184.92	185.13	184.92
	0.02 %	0.00 %	0.11 %	0.00 %	0.15 %	0.00 %
Difference	0.09	0.00	0.55	0.03	0.71	0.01
Average	184.91	184.91	184.91	184.91	184.84	184.91
Dry Period						
Minimum	140.35	140.47	139.10	140.25	138.97	140.34
	-0.09 %	-0.00 %	-0.97 %	-0.16 %	-1.37 %	-0.09 %
Maximum	140.64	140.47	140.93	140.96	141.08	140.76
	0.12 %	0.00 %	0.33 %	0.35 %	0.13 %	0.21 %
Difference	0.29	0.00	1.83	0.71	2.11	0.42
Average	140.47	140.47	140.47	140.47	140.89	140.47

Table 4.5: Absolute values (W/m^2) and relative deviation from the mean value (%) for the sensible heat flux with respect to the modification of morphological and soil related input parameters described in table 4.1.

Trees	Height Top	Height Bot	LAI	SAI	Sand Clay	Soil Color
Wet Period						
Minimum	52.09	56.84	55.62	53.79	54.99	56.79
	-8.36 %	-0.00 %	-2.16 %	-5.38 %	-2.81 %	-0.11 %
Maximum	57.05	56.85	56.85	61.40	56.58	56.97
	0.36 %	0.00 %	0.00 %	8.02 %	0.00 %	0.22 %
Difference	4.96	0.00	1.23	7.61	1.59	0.19
Average	56.84	56.85	56.85	56.85	56.58	56.85
Dry Period						
Minimum	66.21	71.46	61.16	62.78	47.51	71.15
	-7.35 %	-0.00 %	-14.41 %	-12.14 %	-24.55 %	-0.42 %
Maximum	77.77	71.46	81.33	75.04	84.10	71.58
	8.83 %	0.00 %	13.81 %	5.03 %	33.54 %	0.19 %
Difference	11.56	0.00	20.17	12.26	36.59	0.43
Average	71.46	71.46	71.46	71.45	62.98	71.44
Shrubs	**Height Top**	**Height Bot**	**LAI**	**SAI**	**Sand Clay**	**Soil Color**
Wet Period						
Minimum	38.11	41.42	41.03	40.72	41.22	41.39
	-7.98 %	-0.00 %	-0.94 %	-1.70 %	-1.29 %	-0.07 %
Maximum	45.02	41.42	42.72	42.79	41.90	41.49
	8.70 %	0.00 %	3.14 %	3.31 %	0.32 %	0.15 %
Difference	6.91	0.00	1.69	2.07	0.67	0.09
Average	41.42	41.42	41.42	41.42	41.76	41.42
Dry Period						
Minimum	68.44	72.55	67.21	72.13	70.94	72.50
	-5.67 %	-0.00 %	-7.37 %	-0.59 %	-1.47 %	-0.07 %
Maximum	76.34	72.55	79.20	73.33	75.97	72.66
	5.22 %	0.00 %	9.16 %	1.08 %	5.53 %	0.14 %
Difference	7.90	0.00	11.99	1.21	5.03	0.15
Average	72.55	72.55	72.55	72.55	71.99	72.55
C3 Grass	**Height Top**	**Height Bot**	**LAI**	**SAI**	**Sand Clay**	**Soil Color**
Wet Period						
Minimum	31.62	34.14	33.11	33.75	33.06	33.57
	-7.37 %	-0.00 %	-2.99 %	-1.13 %	-4.79 %	-1.64 %
Maximum	36.80	34.14	38.39	34.44	38.54	34.41
	7.81 %	0.00 %	12.46 %	0.90 %	10.97 %	0.80 %
Difference	5.18	0.00	5.27	0.69	5.47	0.83
Average	34.14	34.14	34.14	34.14	34.73	34.14
Dry Period						
Minimum	35.05	37.29	37.07	34.57	33.48	34.85
	-6.01 %	-0.00 %	-0.59 %	-7.30 %	-3.75 %	-6.56 %
Maximum	39.23	37.29	39.71	38.75	51.03	38.47
	5.19 %	0.00 %	6.50 %	3.92 %	46.73 %	3.15 %
Difference	4.18	0.00	2.65	4.18	17.55	3.62
Average	37.29	37.29	37.29	37.29	34.78	37.29
C4 Grass	**Height Top**	**Height Bot**	**LAI**	**SAI**	**Sand Clay**	**Soil Color**
Wet Period						
Minimum	31.10	33.61	33.58	33.55	32.17	32.92
	-7.46 %	-0.00 %	-0.09 %	-0.18 %	-6.00 %	-2.06 %
Maximum	36.28	33.61	37.27	33.76	37.57	33.94
	7.95 %	0.00 %	10.91 %	0.44 %	9.77 %	1.00 %
Difference	5.18	0.00	3.70	0.21	5.40	1.03
Average	33.61	33.61	33.61	33.61	34.23	33.61
Dry Period						
Minimum	33.18	35.60	32.76	32.94	31.91	33.32
	-6.80 %	-0.00 %	-7.97 %	-7.49 %	-4.24 %	-6.42 %
Maximum	37.74	35.60	39.85	37.10	52.29	36.71
	6.02 %	0.00 %	11.94 %	4.21 %	56.90 %	3.10 %
Difference	4.56	0.00	7.09	4.16	20.37	3.39
Average	35.60	35.60	35.60	35.60	33.32	35.60

Table 4.6: Absolute values (mm/month) and relative deviation from the mean value (%) for the evaporation from vegetation with respect to the modification of morphological and soil related input parameters described in table 4.1.

Trees	Height Top	Height Bot	LAI	SAI	Sand Clay	Soil Color
Wet Period						
Minimum	544.70	544.70	391.30	520.50	542.60	544.00
	0.00 %	0.00 %	-28.16 %	-4.44 %	-0.39 %	-0.13 %
Maximum	608.10	544.70	672.90	581.90	631.00	545.10
	11.64 %	0.00 %	23.54 %	6.83 %	15.84 %	0.07 %
Difference	63.40	0.00	281.60	61.40	88.40	1.10
Average	544.70	544.70	544.70	544.70	544.70	544.70
Dry Period						
Minimum	373.40	373.50	242.50	353.70	370.80	372.80
	-0.03 %	0.00 %	-35.07 %	-5.30 %	-0.62 %	-0.19 %
Maximum	435.60	373.50	486.10	408.50	470.10	373.80
	16.63 %	0.00 %	30.15 %	9.37 %	26.00 %	0.08 %
Difference	62.20	0.00	243.60	54.80	99.30	1.00
Average	373.50	373.50	373.50	373.50	373.10	373.50
Shrubs	**Height Top**	**Height Bot**	**LAI**	**SAI**	**Sand Clay**	**Soil Color**
Wet Period						
Minimum	431.60	433.90	292.90	421.80	425.50	432.30
	-0.53 %	0.00 %	-32.50 %	-2.79 %	-2.52 %	-0.37 %
Maximum	436.50	433.90	619.50	457.50	558.70	434.70
	0.60 %	0.00 %	42.77 %	5.44 %	28.00 %	0.18 %
Difference	4.90	0.00	326.60	35.70	133.20	2.40
Average	433.90	433.90	433.90	433.90	436.50	433.90
Dry Period						
Minimum	285.60	287.10	203.90	276.90	276.50	286.30
	-0.52 %	0.00 %	-28.98 %	-3.55 %	-5.05 %	-0.31 %
Maximum	289.50	287.10	448.20	307.30	416.30	287.60
	0.84 %	0.00 %	56.11 %	7.04 %	42.96 %	0.14 %
Difference	3.90	0.00	244.30	30.40	139.80	1.30
Average	287.10	287.10	287.10	287.10	291.20	287.20
C3 Grass	**Height Top**	**Height Bot**	**LAI**	**SAI**	**Sand Clay**	**Soil Color**
Wet Period						
Minimum	342.60	344.90	226.00	332.90	307.70	339.40
	-0.67 %	0.00 %	-34.47 %	-3.48 %	-12.31 %	-1.59 %
Maximum	346.50	344.90	525.00	369.20	469.80	347.30
	0.46 %	0.00 %	52.22 %	7.05 %	33.88 %	0.70 %
Difference	3.90	0.00	299.00	36.30	162.10	7.90
Average	344.90	344.90	344.90	344.90	350.90	344.90
Dry Period						
Minimum	222.00	223.70	156.60	218.20	203.00	214.70
	-0.76 %	0.00 %	-30.00 %	-2.46 %	-10.22 %	-4.02 %
Maximum	225.40	223.70	358.90	235.50	350.00	228.30
	0.76 %	0.00 %	60.44 %	5.27 %	54.80 %	2.06 %
Difference	3.40	0.00	202.30	17.30	147.00	13.60
Average	223.70	223.70	223.70	223.70	226.10	223.70
C4 Grass	**Height Top**	**Height Bot**	**LAI**	**SAI**	**Sand Clay**	**Soil Color**
Wet Period						
Minimum	344.50	346.70	230.30	334.90	308.90	341.70
	-0.63 %	0.00 %	-33.57 %	-3.40 %	-12.54 %	-1.44 %
Maximum	348.20	346.70	525.70	370.60	469.80	349.20
	0.43 %	0.00 %	51.63 %	6.89 %	33.01 %	0.72 %
Difference	3.70	0.00	295.40	35.70	160.90	7.50
Average	346.70	346.70	346.70	346.70	353.20	346.70
Dry Period						
Minimum	222.80	224.40	162.30	219.10	207.10	215.60
	-0.71 %	0.00 %	-27.67 %	-2.36 %	-8.77 %	-3.92 %
Maximum	226.10	224.40	358.50	236.10	350.00	228.90
	0.76 %	0.00 %	59.76 %	5.21 %	54.19 %	2.01 %
Difference	3.30	0.00	196.20	17.00	142.90	13.30
Average	224.40	224.40	224.40	224.40	227.00	224.40

Table 4.7: Absolute values (mm/month) and relative deviation from the mean value (%) for the transpiration from vegetation with respect to the modification of morphological and soil related input parameters described in table 4.1.

Trees	Height Top	Height Bot	LAI	SAI	Sand Clay	Soil Color
Wet Period						
Minimum	2005.00	2195.60	1883.50	2134.30	0.00	2191.10
	-8.69 %	-0.00 %	-14.21 %	-2.79 %	-100.00 %	-0.20 %
Maximum	2348.50	2195.70	2297.40	2226.50	2331.20	2204.30
	6.96 %	0.00 %	4.64 %	1.41 %	5.14 %	0.40 %
Difference	343.50	0.10	413.90	92.20	2331.20	13.20
Average	2195.70	2195.70	2195.60	2195.60	2217.20	2195.50
Dry Period						
Minimum	1213.30	1562.20	1207.00	1305.30	0.00	1551.70
	-22.33 %	0.00 %	-22.75 %	-16.47 %	-100.00 %	-0.72 %
Maximum	1657.00	1562.30	1742.60	2076.50	2755.00	1587.00
	6.08 %	0.01 %	11.53 %	32.89 %	40.37 %	1.54 %
Difference	443.70	0.10	535.60	771.20	2755.00	35.30
Average	1562.10	1562.20	1562.40	1562.60	1962.70	1562.90
Shrubs	**Height Top**	**Height Bot**	**LAI**	**SAI**	**Sand Clay**	**Soil Color**
Wet Period						
Minimum	2576.20	2642.20	2048.10	2635.10	0.00	2629.60
	-2.50 %	0.00 %	-22.49 %	-0.26 %	-100.00 %	-0.47 %
Maximum	2690.60	2642.20	2950.10	2644.80	2741.10	2667.50
	1.83 %	0.00 %	11.65 %	0.10 %	3.48 %	0.96 %
Difference	114.40	0.00	902.00	9.70	2741.10	37.90
Average	2642.30	2642.20	2642.20	2642.10	2648.90	2642.10
Dry Period						
Minimum	1063.40	1076.40	810.70	1059.30	0.00	1068.10
	-1.21 %	0.00 %	-24.68 %	-1.59 %	-100.00 %	-0.77 %
Maximum	1086.20	1076.40	1256.20	1109.30	1399.00	1093.10
	0.91 %	0.00 %	16.70 %	3.06 %	19.36 %	1.55 %
Difference	22.80	0.00	445.50	50.00	1399.00	25.00
Average	1076.40	1076.40	1076.40	1076.40	1172.10	1076.40
C3 Grass	**Height Top**	**Height Bot**	**LAI**	**SAI**	**Sand Clay**	**Soil Color**
Wet Period						
Minimum	1342.10	1382.20	804.40	1357.20	0.00	1373.90
	-2.90 %	0.00 %	-41.80 %	-1.81 %	-100.00 %	-0.60 %
Maximum	1411.30	1382.20	2030.10	1397.10	1531.60	1398.90
	2.11 %	0.00 %	46.87 %	1.08 %	9.24 %	1.21 %
Difference	69.20	0.00	1225.70	39.90	1531.60	25.00
Average	1382.20	1382.20	1382.20	1382.20	1402.00	1382.20
Dry Period						
Minimum	1370.00	1376.20	904.10	1341.10	0.00	1334.20
	-0.46 %	0.00 %	-34.30 %	-2.55 %	-100.00 %	-3.04 %
Maximum	1389.10	1376.20	1856.10	1444.50	1690.30	1461.00
	0.93 %	0.00 %	34.87 %	4.96 %	7.55 %	6.17 %
Difference	19.10	0.00	952.00	103.40	1690.30	126.80
Average	1376.30	1376.20	1376.20	1376.20	1571.60	1376.10
C4 Grass	**Height Top**	**Height Bot**	**LAI**	**SAI**	**Sand Clay**	**Soil Color**
Wet Period						
Minimum	1390.40	1433.50	959.70	1379.80	0.00	1420.90
	-3.01 %	0.00 %	-33.05 %	-3.75 %	-100.00 %	-0.87 %
Maximum	1465.10	1433.50	1916.30	1462.80	1590.90	1459.20
	2.20 %	0.00 %	33.68 %	2.04 %	9.25 %	1.80 %
Difference	74.70	0.00	956.60	83.00	1590.90	38.30
Average	1433.60	1433.50	1433.50	1433.50	1456.20	1433.40
Dry Period						
Minimum	1486.70	1490.00	1085.70	1454.40	0.00	1449.90
	-0.22 %	0.00 %	-27.13 %	-2.38 %	-100.00 %	-2.68 %
Maximum	1501.50	1490.00	2097.70	1551.80	1846.10	1571.00
	0.77 %	0.00 %	40.79 %	4.15 %	9.63 %	5.44 %
Difference	14.80	0.00	1012.00	97.40	1846.10	121.10
Average	1490.00	1490.00	1490.00	1489.90	1684.00	1489.90

tions, the decrease in evapotranspiration also dominates the air humidity leading to a negative correlation with the clay fraction while for wet conditions, no or positive correlations can be found. The sensible heat flux trend shows the opposite behaviour as the air humidity with positive (negative) correlations for trees and dry shrubs and grass land areas (wet shrubs and grass land areas) and the air temperature generally follows the same trends as the sensible heat flux.

The soil colour is a proxy for the soil albedo with larger values represent darker soils and therefore a lower albedo and increasing absorption coefficients for electromagnetic radiation. It shows no influence on trees and shrubs except for the transpiration which has a negative correlation (i. e. positive correlation with soil albedo). For grasslands, the soil surface has a stronger influence on the resulting parameters and generally shows a positive correlation between the soil colour and the respective energy and flux parameters.

Since soil water also has a major influence on the heat exchange, the deviations in the sensible heat flux that result from rather extreme soil modifications (see table 4.1) are larger than for changes in any of the morphological parameters discussed so far. For trees the deviations exceed 30 % for pure sand or clay soils and for grasslands, a deviation larger 50 % can be identified. Yet one should to keep in mind, that such extreme soil conditions can rather be found under vegetation in real case scenarios. The same is true for the evaporation results which also exceed 50 % for the case of an ideal silt soil (0 % sand and clay fraction) but show only negligible influence of the soil substrate for all other input modifications. The maximum influence of the soil composition on the transpiration is smaller than for the evaporation but still shows an increase of 40 % under dry conditions and soils with a 46 % sand and 20 % clay fraction. Air temperature and humidity are again barely effected by the soil composition and the soil colour also has only a minor influence (generally way below 5 %) on all discussed output parameters (see tables 4.3 to 4.7).

4.4 Influence of the parametrization of the plant functional types

Beside vegetation structure and soil parameters, the influence of the plant physiological behaviour on the computed parameters is investigated. To simulate the vegetation communities already used in the previous chapter (i. e. evergreen tropical trees, shrubs, C3 and C4 grass), each of these plant functional types (PFT) is described by 48 parameters. Similar to the study setup in section 4.3, each of the plant specific parameters has been modified by ±30 % from the standard values used within the CLM. The resulting changes in the air temperature and humidity, the sensible heat flux and the evaporation and transpiration from vegetation exceed ±1 % only for 19 of the 48 parameters mainly related to plant morphology, plant

Table 4.8: PFT parameters leading to a change of more than 1 % in at least one of the output values discussed in this study.

PFT parameter	Symbol
roughness length/canopy top height	R_{z0m}
slope of conductance-to-photosynthesis relationship	m
quantum efficiency at 25℃	qe
leaf reflectance (VIS)	α_{vis}^{leaf}
leaf reflectance (NIR)	α_{nir}^{leaf}
stem reflectance (NIR)	α_{nir}^{stem}
leaf transmittance (VIS)	τ_{vis}^{leaf}
leaf transmittance (NIR)	τ_{nir}^{leaf}
stem transmittance (NIR)	τ_{nir}^{stem}
leaf/stem orientation index	χ_l
CLM rooting distribution parameter a	r_a
CLM rooting distribution parameter b	r_b
specific leaf area at the top of the canopy	SLA_{sun}
dSLA/dLAI	$dSLA/dLAI$
leaf C/N	C_{leaf}/N_{leaf}
fraction of leaf N in Rubisco enzyme	$N_{Rubisco}$
soil water potential at full stomatal opening	β_{so}
soil water potential at full stomatal closure	β_{sc}
nitrogen limitation factor for non-CN mode	N_{limit}

optical properties, photosynthesis and plant physiology. Table 4.8 gives an overview of these 19 parameters and their formula symbols used within the following tables.

As can be seen from table 4.9, the 2 m air temperature is not affected by changes of any of the PFT parameters mentioned in table 4.8 and the corresponding air humidity is only modified over grassland areas during dry conditions by changes of the conductance-to-photosynthesis relationship (m). The sensible heat flux and the transpiration is affected by many of the PFT parameters while influences on the evaporation from vegetation are again restricted to grassland (except for changes in the conductance-to-photosynthesis relationship of shrubs under dry conditions). In most of the cases where an output value is affected by changes in a PFT parameter, this is for both wet and dry conditions. If the influence is restricted to only one condition, this is generally during the dry period for evaporation and transpiration but during the wet period for the sensible heat flux. In addition, deviations exceeding 10 % (indicated by * in table 4.9) can only be found for the sensible heat flux and the transpiration.

Tables 4.10 through 4.13 give an overview of the resulting relative deviations from the average value of each output parameter for a negative (D_{Neg}) or positive

Table 4.9: Dependency of the computed values of the 2 m air humidity ($Q2M$), the sensible heat flux (FSH), the evaporation ($QVEGE$) as well as the transpiration ($QVEGT$) from vegetation from the parametrizations of the tree (T), shrub (S) and grassland ($C3$ and $C4$) plant functional types for wet (W) and dry (D) conditions. Indices marked with * indicate deviations exceeding 10 %. The meaning of abbreviations of the PFT parameters is given in table 4.8.

$Q2M$			FSH								$QVEGE$						$QVEGT$							
R_{z0m}			T_W	T_D	S_W	S_D	$C3_W$	$C3_D$	$C4_W$	$C4_D$						T_W	T_D^*	S_W		$C3_W$		$C4_W$	
m	$C3_D$	$C4_D$	T_W^*	T_D^*	S_W^*	S_D^*	$C3_W^*$		$C4_W^*$	$C4_D$	S_D	$C3_W$	$C3_D$	$C4_W$	$C4_D$	T_W^*	T_D^*	S_W^*	S_D^*	$C3_W^*$	$C3_D^*$	$C4_W^*$	$C4_D^*$
qe			T_W	T_D^*	S_W		$C3_W$	$C3_D$	$C4_W$	$C4_D$					$C4_D$	T_W	T_D^*	S_W	S_D	$C3_W$	$C3_D$	$C4_W^*$	$C4_D$
α_{leaf}^{vis}			T_W				$C3_W$	$C3_D$		$C4_D$							T_D			$C3_W$		$C4_W$	
α_{leaf}^{nir}			T_W	T_D^*	S_W	S_D	$C3_W^*$	$C3_D^*$	$C4_W^*$	$C4_D^*$						T_W	T_D^*	S_W		$C3_W^*$	$C3_D$	$C4_W^*$	$C4_D$
α_{nir}^{stem}			T_W	T_D			$C3_W$	$C3_D$	$C4_W$	$C4_D$							T_D			$C3_W$		$C4_W$	
τ_{leaf}^{vis}								$C3_D$		$C4_D$							T_D						
τ_{nir}^{leaf}			T_W	T_D	S_W	S_D	$C3_W$	$C3_D^*$	$C4_W$	$C4_D^*$						T_W	T_D			$C3_W$	$C3_D$	$C4_W$	
τ_{nir}^{stem}							$C3_W$	$C3_D$	$C4_W$	$C4_D$										$C3_W$		$C4_W$	
χ_l								$C3_D$					$C3_D$		$C4_D$		T_D				$C3_D$	$C4_W$	$C4_D$
r_a				T_D				$C3_D$		$C4_D$							T_D		S_D		$C3_D$		
r_b			T_W	T_D	S_W	S_D		$C3_D$		$C4_D$						T_W	T_D	S_W	S_D^*		$C3_D$		$C4_D$
SLA_{sun}			T_W	T_D^*	S_W		$C3_W$	$C3_D$	$C4_W$	$C4_D$			$C3_D$			T_W	T_D^*	S_W	S_D	$C3_W^*$		$C4_W$	$C4_D$
$dSLA/dLAI$				T_D												T_W	T_D						
C_{leaf}/N_{leaf}			T_W	T_D^*	S_W		$C3_W$	$C3_D$	$C4_W$	$C4_D$			$C3_D$			T_W	T_D^*	S_W	S_D	$C3_W^*$		$C4_W$	$C4_D$
$N_{Rubisco}$			T_W	T_D^*	S_W		$C3_W$		$C4_W$	$C4_D$		$C3_W$	$C3_D$			T_W	T_D^*	S_W	S_D	$C3_W^*$	$C3_D$	$C4_W$	$C4_D$
β_{so}				T_D													T_D				$C3_D$		$C4_D$
β_{sc}				T_D				$C3_D$		$C4_D$							T_D		S_D		$C3_D$		$C4_D$
N_{limit}			T_W	T_D^*	S_W		$C3_W$		$C4_W$	$C4_D$		$C3_W$	$C3_D$			T_W	T_D^*	S_W	S_D	$C3_W^*$	$C3_D$	$C4_W$	$C4_D$

(D_{Pos}) modification of the respective PFT parameter by 30 % and for each plant functional type. Since the changes of the parametrization has no influence on the 2 m air temperature, it is not considered in these tables. The same applies for the 2 m air humidity even though changes in the conductance-to-photosynthesis relationship (m) over grassland areas lead to a maximum deviation of 1.03 % during dry conditions.

Out of the remaining output parameters, the sensible heat flux is influenced from most of the PFT parameters followed by the transpiration and finally the evaporation. The latter shows (almost) no dependency from the PFT parameters for trees and shrubs and the sensitivity of grassland is mainly restricted to nutrition and photosynthesis related parameters also controlling the transpiration and therefore the water vapour pressure deficit in the vicinity of the plants. With deviations of the evaporation generally not exceeding 2 % except for modifications of the conductance-to-photosynthesis relationship (m) for C4 grass, the sensitivity is insignificant (see tables 4.12 and 4.13).

In contrast to the evaporation, deviations of the transpiration values are more significant and considerably exceed 10 % or even 20 % especially for trees (see tables 4.10 and 4.11). At this, the largest deviations can be found during dry periods and depend on modifications of the slope of conductance-to-photosynthesis relationship (m), the quantum efficiency at 25°C(qe) , the leaf C/N ratio (C_{leaf}/N_{leaf}), the fraction of leaf N in the Rubisco enzyme ($N_{Rubisco}$), and the nitrogen limitation factor (N_{limit}). These PFT parameters have a major influence on the simulated metabolism which is linked to water uptake and stomata resistance. For wet conditions or grassland areas, the deviations are generally smaller but the conductance relationship and the quantum efficiency still lead to maximum deviations between 15 % and 25 % (see tables 4.12 and 4.13).

Because changes in the transpiration have a negative feedback on the sensible heat flux, the latter decreases (increases) if the transpiration increases (decreases) caused by changes in the parametrization of the metabolism of the vegetation types. Although the resulting deviations of the sensible heat flux are generally less than 10 % to 15 %, the feedback can clearly be identified for all vegetation types (see tables 4.10 to 4.13). In addition, changes in the absorption properties of the plants expressed by the reflection and transmission of leafs and stems ($\alpha^{\cdots}_{\cdots}$ and $\tau^{\cdots}_{\cdots}$) lead to changes in the sensible heat flux which are most significant for grassland areas where they could exceed 30 % although the majority of deviations is below 15 % to 10 % (see tables 4.12 and 4.13). For trees under dry conditions, they could reach up to 15 % to 20 % (see tables 4.10).

Table 4.10: Mean values and relative deviations from the mean values (%) for the sensible heat flux (FSH, W/m^2), the evaporation and transpiration from vegetation ($QVEGE$ and $QVEGT$, mm/month) with respect to the negative (D_{Neg}) and positive (D_{Pos}) modifications of the PFT parameters for trees. If no values are given in the table, the respective deviations are less than 1 %.

	FSH			$QVEGE$			$QVEGT$		
Trees	Mean	D_{Neg}	D_{Pos}	Mean	D_{Neg}	D_{Pos}	Mean	D_{Neg}	D_{Pos}
Wet Period									
R_{z0m}	56.84	96.66	102.13				2195.71	102.84	97.83
m	56.84	115.81	86.49				2195.71	81.25	115.86
qe	56.84	107.01	94.21				2195.71	91.61	106.80
α_{vis}^{leaf}	56.84	101.28	98.72						
α_{nir}^{leaf}	56.84	108.03	89.03				2195.71	103.03	95.83
α_{nir}^{stem}	56.84	101.45	98.47						
τ_{vis}^{leaf}									
τ_{nir}^{leaf}	56.84	104.49	94.59				2195.71	101.73	97.90
τ_{nir}^{stem}									
χ_l									
r_a									
r_b	56.84	102.27	98.15				2195.71	97.38	102.13
SLA_{sun}	56.84	93.03	104.46				2195.71	108.16	94.70
$dSLA/dLAI$							2195.71	101.00	99.06
C_{leaf}/N_{leaf}	56.84	92.01	104.87				2195.71	109.36	94.20
$N_{Rubisco}$	56.84	106.27	93.97				2195.71	92.53	107.07
β_{so}									
β_{sc}									
N_{limit}	56.84	106.27	93.97				2195.71	92.53	107.07
Dry Period									
R_{z0m}	71.46	105.04	95.48				1562.09	88.38	109.05
m	71.46	72.23	115.51				1562.09	152.48	69.92
qe	71.46	72.27	113.35				1562.09	154.92	73.77
α_{vis}^{leaf}							1562.09	101.85	98.44
α_{nir}^{leaf}	71.46	114.75	79.35				1562.09	88.80	116.62
α_{nir}^{stem}	71.46	102.73	97.11				1562.09	97.86	102.31
τ_{vis}^{leaf}							1562.09	101.26	98.83
τ_{nir}^{leaf}	71.46	108.12	90.20				1562.09	93.94	107.43
τ_{nir}^{stem}									
χ_l							1562.09	98.20	101.82
r_a	71.46	102.29	98.52				1562.09	95.14	103.11
r_b	71.46	95.09	98.39				1562.09	109.70	103.30
SLA_{sun}	71.46	114.58	80.37				1562.09	71.54	138.84
$dSLA/dLAI$	71.46	103.10	96.91				1562.09	93.89	106.10
C_{leaf}/N_{leaf}	71.46	115.10	78.55				1562.09	70.52	142.45
$N_{Rubisco}$	71.46	73.56	113.83				1562.09	152.27	72.98
β_{so}	71.46	98.43	101.38				1562.09	103.09	97.28
β_{sc}	71.46	102.77	97.89				1562.09	93.62	104.74
N_{limit}	71.46	73.56	113.83				1562.09	152.27	72.98

Table 4.11: Same as table 4.10 but for shrubs.

Shrubs	FSH Mean	D_{Neg}	D_{Pos}	$QVEGE$ Mean	D_{Neg}	D_{Pos}	$QVEGT$ Mean	D_{Neg}	D_{Pos}
Wet Period									
R_{z0m}	41.42	95.81	103.21				2642.27	101.02	99.13
m	41.42	117.72	90.32				2642.27	82.72	109.49
qe	41.42	106.09	95.35				2642.27	94.08	104.51
α_{vis}^{leaf}									
α_{nir}^{leaf}	41.42	103.88	95.49				2642.27	102.78	96.60
α_{nir}^{stem}									
τ_{vis}^{leaf}									
τ_{nir}^{leaf}	41.42	101.09	98.86						
τ_{nir}^{stem}									
χ_l									
r_a									
r_b	41.42	102.01	99.01				2642.27	98.12	100.99
SLA_{sun}	41.42	94.31	104.73				2642.27	105.57	95.37
$dSLA/dLAI$									
C_{leaf}/N_{leaf}	41.42	93.57	105.24				2642.27	106.30	94.86
$N_{Rubisco}$	41.42	107.13	95.16				2642.27	93.01	104.74
β_{so}									
β_{sc}									
N_{limit}	41.42	107.13	95.16				2642.27	93.01	104.74
Dry Period									
R_{z0m}	72.55	97.13	102.03						
m	72.55	88.91	100.25	287.15	98.83	100.37	1076.42	137.06	100.52
qe							1076.42	101.38	99.18
α_{vis}^{leaf}									
α_{nir}^{leaf}	72.55	104.40	94.83						
α_{nir}^{stem}									
τ_{vis}^{leaf}									
τ_{nir}^{leaf}	72.55	101.22	98.71						
τ_{nir}^{stem}									
χ_l									
r_a							1076.42	96.97	102.11
r_b	72.55	103.54	99.80				1076.42	86.99	100.97
SLA_{sun}							1076.42	101.46	97.50
$dSLA/dLAI$									
C_{leaf}/N_{leaf}							1076.42	101.56	97.00
$N_{Rubisco}$							1076.42	95.92	101.50
β_{so}									
β_{sc}							1076.42	96.65	102.04
N_{limit}							1076.42	95.92	101.50

Table 4.12: Same as table 4.10 but for C3 grass.

C3 Grass	FSH Mean	D_{Neg}	D_{Pos}	$QVEGE$ Mean	D_{Neg}	D_{Pos}	$QVEGT$ Mean	D_{Neg}	D_{Pos}
Wet Period									
R_{z0m}	34.14	96.14	102.89				1382.22	101.18	99.00
m	34.14	111.81	92.24	344.92	98.18	100.60	1382.22	75.61	115.16
qe	34.14	102.94	99.15				1382.22	94.41	101.62
α_{vis}^{leaf}	34.14	101.21	98.77				1382.22	101.03	98.90
α_{nir}^{leaf}	34.14	115.38	78.42				1382.22	115.00	76.16
α_{nir}^{stem}	34.14	102.18	97.73				1382.22	102.25	97.60
τ_{vis}^{leaf}									
τ_{nir}^{leaf}	34.14	107.09	91.81				1382.22	107.21	91.18
τ_{nir}^{stem}	34.14	101.42	98.54				1382.22	101.49	98.45
χ_l									
r_a									
r_b									
SLA_{sun}	34.14	93.60	106.02				1382.22	112.68	87.83
$dSLA/dLAI$									
C_{leaf}/N_{leaf}	34.14	93.60	106.02				1382.22	112.68	87.83
$N_{Rubisco}$	34.14	108.32	95.09	344.92	98.86	100.48	1382.22	83.09	109.73
β_{so}									
β_{sc}									
N_{limit}	34.14	108.32	95.09	344.92	98.86	100.48	1382.22	83.09	109.73
Dry Period									
R_{z0m}	37.29	96.99	102.04						
m				223.72	93.17	101.61	1376.25	78.78	98.08
qe	37.29	97.98	100.62				1376.25	101.70	99.27
α_{vis}^{leaf}	37.29	102.02	97.89						
α_{nir}^{leaf}	37.29	127.43	62.69				1376.25	96.17	96.54
α_{nir}^{stem}	37.29	103.90	95.94						
τ_{vis}^{leaf}	37.29	101.21	98.76						
τ_{nir}^{leaf}	37.29	112.55	85.64				1376.25	98.69	100.34
τ_{nir}^{stem}	37.29	102.51	97.42						
χ_l	37.29	98.91	100.96	223.72	98.83	101.31	1376.25	101.89	98.23
r_a	37.29	98.66	100.66				1376.25	101.21	99.41
r_b	37.29	95.94	102.72				1376.25	105.43	96.24
SLA_{sun}	37.29	101.43	99.63	223.72	101.41	98.14			
$dSLA/dLAI$									
C_{leaf}/N_{leaf}	37.29	101.43	99.63	223.72	101.41	98.14			
$N_{Rubisco}$				223.72	96.89	101.07	1376.25	90.39	100.82
β_{so}							1376.25	98.16	101.43
β_{sc}	37.29	101.11	99.21				1376.25	96.94	102.13
N_{limit}				223.72	96.89	101.07	1376.25	90.39	100.82

Table 4.13: Same as table 4.10 but for C4 grass.

C4 Grass	FSH Mean	D_{Neg}	D_{Pos}	$QVEGE$ Mean	D_{Neg}	D_{Pos}	$QVEGT$ Mean	D_{Neg}	D_{Pos}
Wet Period									
R_{z0m}	33.61	96.12	102.94				1433.55	101.23	98.95
m	33.61	112.00	93.18	346.72	97.82	100.54	1433.55	75.58	112.74
qe	33.61	107.47	95.66				1433.55	86.16	107.78
α_{vis}^{leaf}							1433.55	101.53	98.36
α_{nir}^{leaf}	33.61	114.87	78.94				1433.55	115.73	75.48
α_{nir}^{stem}	33.61	102.11	97.81				1433.55	102.35	97.50
τ_{vis}^{leaf}									
τ_{nir}^{leaf}	33.61	106.83	92.08				1433.55	107.56	90.84
τ_{nir}^{stem}	33.61	101.37	98.60				1433.55	101.55	98.38
χ_l							1433.55	101.54	98.52
r_a									
r_b									
SLA_{sun}	33.61	98.27	102.24				1433.55	103.52	95.50
$dSLA/dLAI$									
C_{leaf}/N_{leaf}	33.61	98.27	102.24				1433.55	103.52	95.50
$N_{Rubisco}$	33.61	103.38	98.63				1433.55	93.25	102.78
β_{so}									
β_{sc}									
N_{limit}	33.61	103.38	98.63				1433.55	93.25	102.78
Dry Period									
R_{z0m}	35.60	96.58	102.38						
m	35.60	102.48	102.26	224.38	92.80	101.93	1490.01	73.03	99.08
qe	35.60	98.53	102.53	224.38	98.81	100.62	1490.01	98.02	97.62
α_{vis}^{leaf}	35.60	102.26	97.67						
α_{nir}^{leaf}	35.60	128.88	63.01				1490.01	96.06	95.25
α_{nir}^{stem}	35.60	103.95	95.93						
τ_{vis}^{leaf}	35.60	101.36	98.62						
τ_{nir}^{leaf}	35.60	112.87	85.62						
τ_{nir}^{stem}	35.60	102.55	97.40						
χ_l				224.38	98.93	101.25	1490.01	101.44	98.65
r_a	35.60	98.94	100.43						
r_b	35.60	94.88	103.68				1490.01	106.15	95.40
SLA_{sun}	35.60	96.78	101.63				1490.01	105.74	95.84
$dSLA/dLAI$									
C_{leaf}/N_{leaf}	35.60	96.78	101.63				1490.01	105.74	95.84
$N_{Rubisco}$	35.60	102.14	97.72				1490.01	94.02	104.18
β_{so}							1490.01	98.77	101.00
β_{sc}	35.60	101.54	98.97				1490.01	96.57	102.25
N_{limit}	35.60	102.14	97.72				1490.01	94.02	104.18

4.5 Summary and conclusion

In this study, the influence of changes in the vegetation structure, soil and plant functional type parameters on certain output variables from the CLM model have been examined. Therefore, mean vegetation structure and soil parameters have been modified mainly by a factor of 2 (see table 4.1) and the parameters describing evergreen tropical tree, shrub, C3 and C4 grass plant functional types have been modified by ±30 % from the standard values used within the CLM (see section 4.4). Since the deviation of the output parameters also depends on the general atmospheric conditions, the simulations encompassed one wet and one dry period.

In general, the influence of these parameters on the simulated monthly mean values of the 2 m air temperature and humidity are negligible for most applications. The deviations resulting from modifications of the input parameters for the vegetation structure and soil parameters are well below 1 % except for the stem area index which leads to a deviation of −2.20 % for shrubs under dry conditions. However one has to keep in mind that for the 2 m air temperature, such deviations correspond to absolute deviations of up to 0.5 K. This could lead to problems if the absolute output values are of importance and not the differences between several scenario runs. Variations in the plant functional type parametrizations have no consequence on the computed air temperatures and humidities.

In contrast to the air humidity, hydrological parameters like the evaporation and transpiration from vegetation are stronger affected by changes in the structural and PFT specific parameters. In this context one has to mention the influence of changes in the leaf area index on the evaporation which could lead to deviations of around 30 % with peaks of around 60 % for shrubs, C3 and C4 grass under dry conditions. At the same time, the evaporation is rather independent from changes of the PFT parametrization which lead to deviations in the respective output values of generally less than 2 %.

As for the evaporation the transpiration from vegetation shows a strong dependency on the leaf area index with similar deviations of the output values although the maximum deviations are a little smaller. In addition, changes of the stem area index lead to a variance of the transpiration by −16 % to 33 % for trees under dry conditions while for all other vegetation types and conditions the deviations are (well) below 5 %. Another difference lays in the stronger influence especially of the plant functional type parametrizations directly relevant for photosynthesis and plant metabolism which could induce deviations of more than 50 % for trees under dry conditions. Yet, the influence of the majority of PFT parameters that induce a change in the transpiration at all is restricted to much less than 10 %.

Since water vapour fluxes have feedbacks on the sensible heat flux, the latter is also affected by changes of the photosynthesis and metabolism controlling parameters. The resulting deviations however are generally smaller and do not exceed −30 % to 15 %. A stronger influence emanates from leaf and stem optical properties that

could lead to changes in the sensible heat flux between −40 % to 30 %. Compared to these figures, the influence of the leaf area index with maximum deviations of about 14% is rather small.

All other morphological and plant functional type parameters that have not been explicitly mentioned in the paragraphs above have only minor influences on the resulting values of the evaporation, transpiration and sensible heat flux. Magnitudes of deviations due to changes in the soil composition are comparable to or even exceed the maximum deviations presented above. However, the applied modifications to the composition parameters are much larger than the modifications of all other input parameters and rather extreme (encompassing 100 % sand, silt, and clay soils). Therefore the actual error of area wide soil datasets e. g. generated by geostatistical techniques and as a consequence the resulting deviations of the output parameters can be assumed to be significantly smaller than the modifications of the soil parameters in this sensitivity study.

Considering these sensitivities one can conclude that the general lack of highly accurate morphological and plant physiological datasets in the framework of social (economic) studies has no significant influence on the output values of interest (i. e. mainly the air temperature and humidity).

Acknowledgements

This work was funded by the German Research Foundation (DFG) in the scope of the Research Unit FOR816 'Biodiversity and Sustainable Management of a Megadiverse Mountain Ecosystem in South Ecuador', subproject Z1.1 (NA 783/1-1).

References

Barthlott, W., J. Mutke, M. D. Rafiqpoor, G. Kier & H. Kreft: (2005): Global centres of vascular plant diversity, *Nova Acta Leopoldina, NF 92*, 61–83.

Bonan, G., K. Oleson, M. Vertenstein, S. Levis, X. Zeng, Y. Dai, R. Dickinson & Z.-L. Yang: (2002): The land surface climatology of the community land model coupled to the NCAR community climate model, *Journal of Climate*, *15*, 3123–3149.

Brummitt, N. & E. N. Lughadha: (2003): Biodiversity: Where's hot and where's not, *Conservation Biology*, *17*, 1442–1448.

Foley, J. A., S. Levis, M. H. Costa, W. Cramer & D. Pollard: (2000): Incorporating dynamic vegetation cover within global climate models, *Ecological Applications*, *10*, 1620–1632.

Hartig, K. & E. Beck: (2003): The bracken fern (Pteridium arachnoideum (Kaulf.) Maxon) dilemma in the andes of southern ecuador, *Ecotropica*, *9*, 3–13.

Jørgensen, P. M. & C. Ulloa Ulloa: (1994): Seed plants of the high andes of ecuador – a checklist, Tech. rep., Aarhus University Reports 34.

Mosandl, R., S. Günter, B. Stimm & M. Weber: (2008): Ecuador suffers the highest deforestation rate in south america, in Beck, E., J. Bendix, I. Kottke, F. Makeschin & R. Mosandl (eds.) *Gradients in a Tropical Mountain Ecosystem of Ecuador*, *Ecological Studies*, vol. 198, chap. 4, Springer, Berlin.

Oleson, K. W., Y. Dai, G. Bonan, M. Bosilovich, R. Dickinson, P. Dirmeyer, F. Hoffman, P. Houser, S. Levis, G. Y. Niu, P. Thornton, M. Vertenstein, Z. L. Yang & X. Zeng: (2004): Technical description of the community land model (clm), Tech. Rep. NCAR/TN-461+STR, NCAR Technical Note.

Oleson, K. W., G.-Y. Niu, Z.-L. Yang, D. M. Lawrence, P. E. Thornton, P. J. Lawrence, R. Stöckli, R. E. Dickinson, G. B. Bonan, S. Levis, A. Dai & T. Qian: (2008): Improvements to the community land model and their impact on the hydrological cycle, *Journal of Geophysical Research*, *113*, G01021.

Qian, T., A. Dai, K. E. Trenberth & K. W. Oleson: (2006): Simulation of global land surface conditions from 1948 to 2004. part i: Forcing data and evaluations, *Journal of Hydrometeorology*, *7*, 953–975.

Zeng, X.: (2001): Global vegetation root distribution for land modeling, *Journal of Hydrometeorology*, *2*, 525–530.

5 Quantification of Optical Properties

This chapter was printed in *Ecological Modelling*, Vol. 222, Issue 3, 10 February 2011, pp. 493–502 . The manuscript was submitted 3 June 2010, in final form 13 September 2010.

Optical Properties of Selected Plants from a Tropical Mountain Ecosystem – Traits for Plant Functional Types to Parametrize a Land Surface Model

Dietrich Göttlicher*‡, Janina Albert‡, Thomas Nauss§ and Jörg Bendix‡

‡Faculty of Geography, Philipps-Universität Marburg, Deutschhausstr. 10, 35037 Marburg, Germany
§Faculty of Geography, University of Bayreuth, 95440 Bayreuth, Germany

The optical properties (reflectance and transmittance) of selected leaves from a tropical mountain rainforest in southern Ecuador are determined to parametrize optical traits of plant functional types (PFT) of a state of the art land model (Community Land Model, CLM). 46 spatially dominating species are selected from 4 different forest types, the subpáramo and a succession stage of pasture areas representing ecologically predefined functional types within the study area. Measurements are conducted under a standardized experimental setup with a field spectrometer covering the radiation between 305–1305 nm. The results of the optical properties of all species are checked for similarity by cluster analysis and are compared to the composition of species of the predefined PFTs. Furthermore the results are compared to other studies, the default values for the globally defined PFT of tropical evergreen trees in the CLM and another forest growth model operated in the same study area. The results show that the clusters aggregated by the reflectance, transmittance or combined properties do not represent the predefined PFTs. The values of the other studies suggests a reassessment of the experimental setup for the transmittance measurements. Nevertheless, new reflectance values for the regionalized PFTs can be determined. The optical values differ from the CLM-PFT of tropical evergreen trees, and new values for the reflectance are recommended.

Keywords: CLM, SVAT, reflectance, transmittance, Ecuador

5.1 Introduction

Biodiversity is threatened by human impacts in various ways. Global climate change (Sala et al., 2000) and pressure on existing natural ecosystems by a growing human community lead to a loss or shift of habitats (Colwell et al., 2008). A major task

in order to secure biodiversity for future generations will be to protect areas, reinstall destroyed ecosystems and develop sustainable management systems.

The high mountains of southern Ecuador represent not only a major hotspot of plant biodiversity (Barthlott et al., 2007), but also an area in which the natural ecosystems are under extreme pressure, resulting in a major loss of natural forests (Mosandl et al., 2008). The German research unit 'Biodiversity and Sustainable Management of a Megadiverse Mountain Ecosystem in South Ecuador' (www.tropicalmountainforest.org) investigates the processes and interactions in this area from a biological, climatological and a socio-economical point of view (Beck et al., 2008).

To support the outcome of different landuse scenarios and to document the changes in eco-climatological parameters, a soil-vegetation-atmosphere-transfer (SVAT) scheme is implemented. The *Community Land Model* (CLM, Bonan et al., 2002b; Dickinson et al., 2006; Oleson et al., 2008) is used to model energy and water fluxes under different landuse developments. This model is highly adapted to the study area and a major task is to provide suitable regionalized parameters, especially for the characterization of the vegetation. CLM describes the vegetation through plant functional types (PFT) rather than biomes (Bonan et al., 2002a).

All PFTs are represented by their spatial delineation, their time and space variant value of leaf and stem area indices (LAI, SAI), their top and bottom canopy height, and 48 invariant functional parameters concerning optical, morphological and physiological specifications. A sensitivity study of these PFT-parameters (Göttlicher et al., 2010) concludes that the optical properties of the PFT, in addition to the LAI, have a major influence on the modelling results and deserve a more sophisticated assignment than other parameters.

Spatial delineation in this rugged and difficult to access terrain is done with by classifying satellite data (Göttlicher et al., 2009). The endmembers and allocated training sites used for this classification are determined by botanical distinction (Homeier et al., 2008). The results of the satellite classification are proven to be good, according to the accuracy assessment calculating a contingency matrix using independent ground truth sites. The overall accuracy is 87.3 % and the Kappa value is 0.86 (Göttlicher et al., 2009). The vegetation units could be determined even in a subpixel proportion using a modified linear spectral unmixing technique (Zhu, 2005). The question remains if these botanically derived vegetation units used in the satellite classification are actually functional groups in the sense of the PFT concept (Lavorel et al., 2007; Smith et al., 1997). This paper examines the following questions:

1. Are the vegetation units from the satellite classification analog to the clusters of similar behaviour in reflectance and transmittance, and can they be interpreted as PFTs, at least in regard to spectral properties?

2. What are the mean reflectance and transmittance values of each PFT, and do they vary significantly that it is worthwhile to distinguish between them?

3. What are the mean reflectance and transmittance values for all measured tropical trees, and how significantly do they differ from the initial values of the global dataset provided by the CLM?

The paper gives a short introduction to the study site (section 5.2.1), followed by a description of the measurement setup, the collected plants and the statistical analysis (see sections 5.2.2, 5.2.3 and 5.2.4). The results of the field observations and the cluster analysis are presented in section 5.3. In section 5.4 the results are highlighted in comparison to the predefined values. Section 5.5 summarizes the potential use of the study.

5.2 Methods and Material

5.2.1 Study site

The study site is located in the Andes of South Ecuador. The mentioned research unit operates the Estación Científica San Francisco (ECSF) between the two provincial capitals Loja and Zamora in cooperation with the foundation 'Nature and Culture International'. The catchment of the Rio San Francisco comprises the central investigation area (see fig. 5.1). The valley reaches from 1800 m up to 3200 m above sea level (asl). The southern slopes are predominantly covered with indigenous mountain forest types in their typical altitudinal belts. The northern slopes show the anthropogenic replacement systems of pastures (dominated by *Setaria sphacelata*), abandoned pasture areas overgrown by bracken fern (*Pteridium arachnoideum*) and reforested areas (mainly with the exotic pine *Pinus patula*). A detailed land cover classification (Göttlicher et al., 2009) based on satellite data was conducted to determine the spatial distribution of the dominant vegetation units. A general overview of the ecological environment can be found in Beck et al. (2008).

5.2.2 Measurements

All measurements of the leaf reflectance and transmittance are performed with a portable spectrometer from tec5 AG (Oberursel, Germany, www.tec5.com). The custom made 'HandySpec® Field' consists of two separate sensors to cover a cumulative spectral range from 305–1705 nm. The sun is used as the original light source, so that the device has two channels, one measuring the incoming solar radiation from the hemisphere above (reference channel) and one detecting the reflectance from underneath (sample channel). To calibrate the two different sensors, as well as the reference and the sample channels, a measurement with a classified white

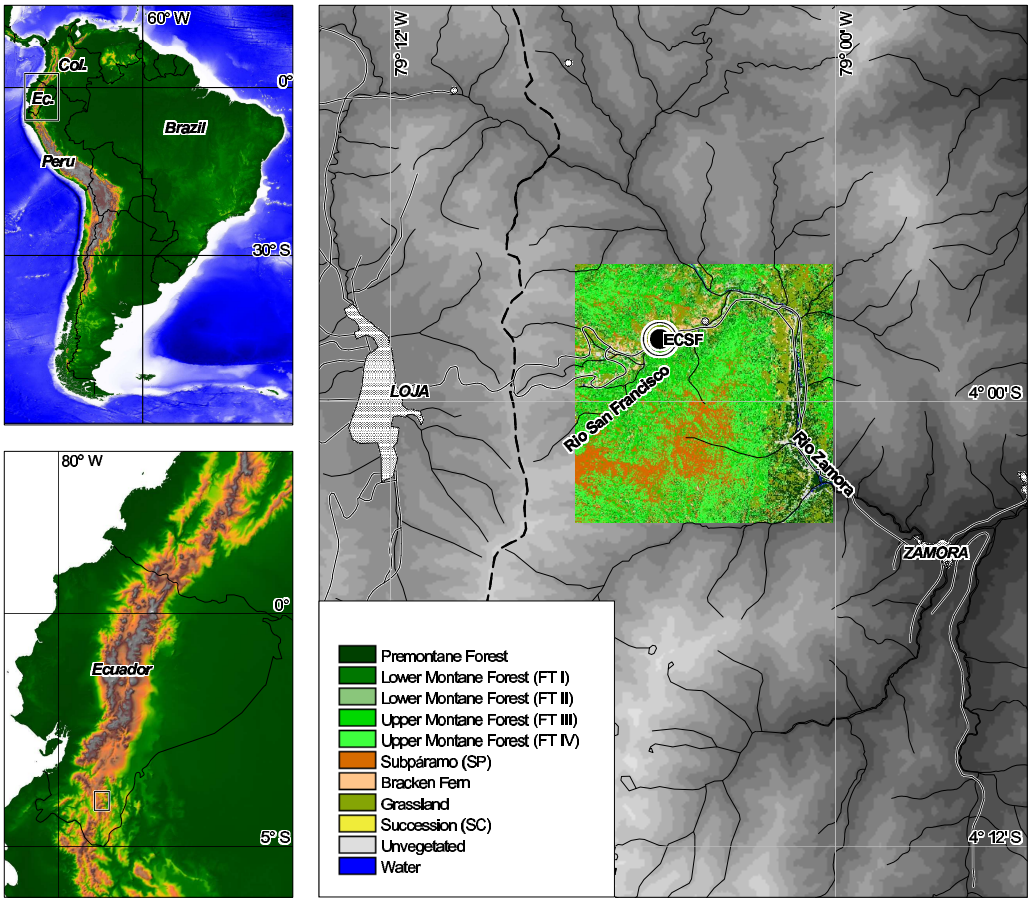

Figure 5.1: Location of the study site and vegetation units from satellite classification.

Table 5.1: Technical specifications of the two sensors from the used spectrometer.

	Sensor 1 VIS	Sensor 2 NIR
spectral range [nm]	305–1100	960–1705
pixel dispersion [nm]	3.3	1.5
type	MMS 1 NIR enh.	PGS NIR 1.7
vendor	Carl Zeiss	Carl Zeiss
integration time [ms]	1.5–6000	1.5–6000
radiometric resolution [bit]	15	15

standard (Spectralon) is taken at fixed intervals. The technical specifications of the spectrometer are shown in table 5.1. All final measurements for the statistical analysis consist of the mean of three consecutively executed exposures. The raw data from the reference and sample channel is processed on the fly on a connected laptop using the vendor software MultiSpec®Pro and is saved in separate ASCII textfiles. The spectral raw data is interpolated to steps of 1 nm. The reflectance α as well as the transmittance τ are calculated in % with the formula (TEC5, 2005) as follows:

$$\frac{\alpha}{100} = \frac{S/R_s}{(C/W)/R_c} \tag{5.1}$$

where S is the raw counts of the sample channel, R_s is the raw counts of the reference channel, C is the raw counts of the sample channel from the last white standard calibration, R_c is the corresponding raw counts of the reference channel and W is the sensor specific correction coefficient for the white standard provided by the vendor. Thus, the second half of the term $(C/W)/R_c$ represents a calibration factor.

The post processing includes the storage of all spectrums in a relational database with sufficient metadata on the sampling and measuring circumstances (photo of sample, timestamp of sampling and measurement, short notices to the weather, species or probe name and geographic coordinates of the sampling site).

Reflectance

The reflectance measurements are conducted in a defined setup rather than in the field to guarantee consistent conditions. The sensor head is fixed to a stand to provide an invariant distance to the sample of 33 cm. The leaves are cut at the edge if necessary to prevent overlapping layers (i. e. a constant leaf area index of 1 is guaranteed). A special foil is used underneath the probe to minimize the reflectance from the base caused by unavoidable, minuscule gaps between the individual leaves and by the radiation transmitted by the leaves (see fig. 5.2)

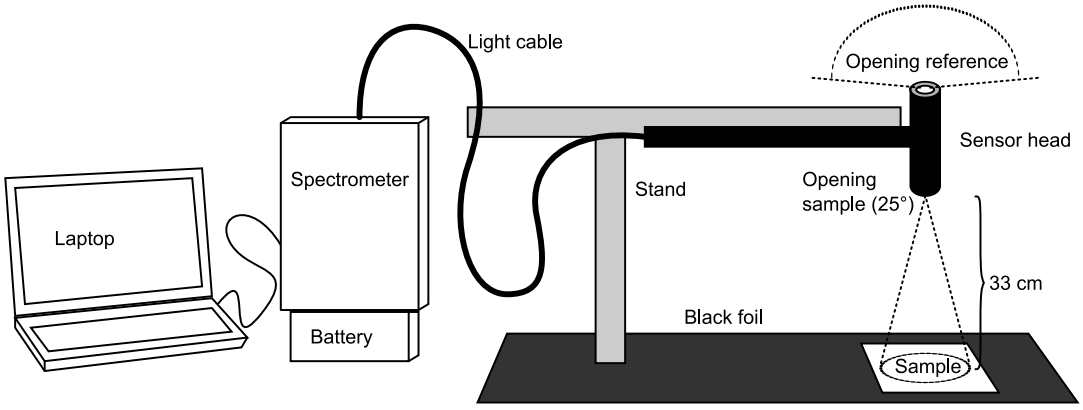

Figure 5.2: Experimental setup for measuring reflectance.

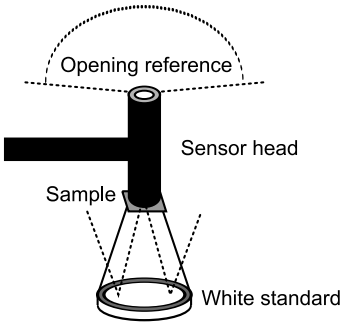

Figure 5.3: Experimental setup for measuring transmittance.

Transmittance

The transmission is also measured in a defined setup. The leaf is clipped with a special device directly beneath the opening of the reflection channel at the sensor head. The white standard is mounted underneath the opening, providing the light to be transmitted through the leaf (see fig. 5.3). This procedure does not work if the leaves are very small, because the sample does not completely cover the opening.

5.2.3 Collected Plants and Vegetation Units

All 46 measured plants used in this study are collected in the immediate vicinity of the ECSF research station, where the measurements are performed. A selection of only some plant species was necessary due to the high biodiversity of the study area (more than 280 tree species Homeier & Werner, 2007). The first criteria is to select all dominant species according to spatial crown coverage in different vegetation units. Secondly, all species relevant for other working groups (especially the forestry groups) are selected. All selected plants are kept in plastic bags and

are watered until measuring. Under normal conditions, the measuring takes place immediately, but at the latest 24 hours after the selection, to guarantee no change in the optical behaviour (FOLEY et al., 2006).

The vegetation units (HOMEIER et al., 2008) distinguish between 4 forest types, the Subpáramo and a succession stage from abandoned pastures. Forest type I (FT_I) dominates the valley bottom and major ravines from 1800 m up to 2200 m asl. Forest type II (FT_{II}) is described as forest along ridges and upper slopes from approximately 1900 m to 2100 m asl. Forest Type III (FT_{III}) continues on the ridges and upper slopes from 2100 m to 2250 m asl. Forest type IV (FT_{IV}) is monodominated by *Purdiaea nutans* and stretches from 2250 m up to the timberline at around 2700 m asl. The Subpáramo (SP) is dominated by shrubs, also called evergreen elfin forest, and rises from the timberline up to approx. 3150 m asl. Initially, the successional stages (SC) are typically covered entirely by the bracken fern and at a later stage replaced by shrubs. This paper deals exclusively with the appearance of shrubs, because the bracken fern could be classified as a PFT of its own. *Eukalyptus spec.* and *Pinus patula* are characterized as exotic since they were introduced as forestry plants. Table 5.2 gives an overview of all measured plant species and the vegetation units the most closely belong to.

5.2.4 Statistics

All statistical analyses are calculated using the free software package *R* (R DEVELOPMENT CORE TEAM, 2009). Initially, the stability and reliability of the used spectrometer is checked. Three measured spectra of the same plant are compared with the spectra of all other plants. The spectra of the same plant are meant to show significant correlation with each other and significant contrast to all other plants.

For all further calculations, the mean of the three initial measurements for each taxa is used. Three different sections are analysed: first the reflectance, second the transmittance and third the combination of both. A hierarchical agglomerative cluster method is used to group the species together. The dissimilarity between the variables is calculated by the Euclidian distance (KAUFMAN & ROUSSEEUW, 2005). The clustering algorithm is based on the Ward method (WARD, 1963). The clustering is performed with the *agnes* command of the *R*-package *cluster* (MAECHLER et al., 2005).

The resulting composition of the clusters is compared with the classification of species into the botanically derived vegetation units. It is examined whether these units mirror the optical traits and can be interpreted as functional types. The statistical mean for the visible (305–699 nm) and the near infrared (700–1305 nm) part of the spectrum is determined in order to compare the results of the single species with the standard values of the predefined PFTs of the CLM (OLESON et al., 2004, p. 23). Mean spectra are calculated for all species belonging to the single clusters as well as the vegetation units. Aggregated values are calculated for

Table 5.2: List of species, referring codes and dominate vegetation units.

Species	Code	Vegetation unit
Alnus acuminata	alna	FT_I
Cecropia andina	cecd	FT_I
Cecropia angustifolia	cecg	FT_I
Cedrela montana	cedm	FT_I
Ficus citrifolia	fici	FT_I
Ficus cuatrecasana	ficu	FT_I
Ficus spec.	fic	FT_I
Heliocarpus americanus	hela	FT_I
Inga spec.	ing	FT_I
Isertia laevis	isel	FT_I
Piptocoma discolor	pipd	FT_I
Tabebuia chrysantha	tabc	FT_I
Tibouchina lepidota	tibe	FT_I
Alzatea verticillata	alzv	FT_{II}
Hyeronima moritziana	hyem	FT_{II}
Miconia punctata	micp	FT_{II}
Vismia tomentosa	vist	FT_{II}
Abarema killipii	abak	FT_{II} and FT_{III}
Alchornea grandiflora	alcg	FT_{II} and FT_{III}
Clethra revoluta	cler	FT_{II} and FT_{III}
Graffenrieda emarginata	grae	FT_{II} and FT_{III}
Miconia spec. 3	mic3	FT_{II} and FT_{III}
Podocarpus oleifolius	podo	FT_{II} and FT_{III}
Aniba spec.	ani	FT_{III}
Clusia spec. 1	clu1	FT_{III}
Dictyocarium lamarckianum	dicl	FT_{III}
Hedyosmum spec.	hed	FT_{III}
Licaria subsessils	lics	FT_{III}
Myrcia spec.	myc	FT_{III}
Ocothea benthamiana	ocob	FT_{III}
Purdiaea nutans	purn	FT_{III} and FT_{IV}
Clusia spec. 2	clu2	SP
Miconia spec. 1	mic1	SP
Miconia spec. 2	mic2	SP
Myrica pubescens	myip	SP
Schefflera spec.	sch	SP
Ageratina dendroides	aged	SC
Baccharis genistelloides	bacg	SC
Baccharis latifolia	bacl	SC
Brachytotum spec.	bra	SC
Monochaetum lineatum	monl	SC
Rubus spec.	rub	SC
Sticherus spec.	sti	SC
Tibouchina laxa	tiba	SC
Eukalyptus spec.	euk	exotic
Pinus patula	pinp	exotic

the visible and near infrared section for the means of the clusters, the vegetation units and all tree species to use with the SVAT model.

5.3 Results

5.3.1 Plant Spectra

The initial three measurements of each of the same species, which are averaged for further calculations, always are more similar to each other than they are different from other species. This verifies the importance of further statistical analysis.

All spectra show the typical shape of reflectance and transmittance curves based on green vegetation. Figure 5.4 shows exemplarily the curves for spectral reflectance and transmittance for three selected species. The reflectance curve starts with relative low values between 5–7 % in the visible sector (blue light), followed by a small peak up to 10–15 % around the green light range (490–560 nm). A significant steep increase up to 40–60 % occurs at the change-over from red light to the near infrared range (*red edge* around 700 nm). The values for the near infrared section stay at this high level but exhibit greater inter-species variability than visible light.

The curves for transmittance also show a typical shape, starting with even smaller values (1–5 %) in the visible section and abruptly rising up to 15–25 % at the red edge. The magnitude and shape of the curves also differ more significantly in the infrared section than in the visible section.

5.3.2 Cluster Analysis

All three agglomorative cluster analyses using all single values in the spectral range from 305–1305 nm (of the reflectance (fig. 5.5), of the transmittance (fig. 5.6) and of the combined data (fig. 5.7) show similar results. All dendrograms are grouped into five clusters. This number represents the amount of predefined vegetation units without considering forest type IV, because it is mono-dominated by only one species. Within the transmittance data, only one species (*Tabebuia chrysantha*) is kept outside a cluster due to the exceptionally high transmittance values in the near infrared section. Because there is no evidence that this measurement is faulty, the value and the species is not considered to be an outlier or rejected from the combined data.

The agglomerative coefficient AC, which is a dimensionless indicator of the grouping structure ranging between 0 and 1 (Kaufman & Rousseeuw, 2005), is 0.96 for the reflectance data, 0.97 for the transmittance and 0.92 for the combined data. High AC-values indicate a clear structure where low values tends to represent only one large cluster. These values do not show the quality of the clustering results because they are dependent on the numbers of objects to be clustered (which are equal

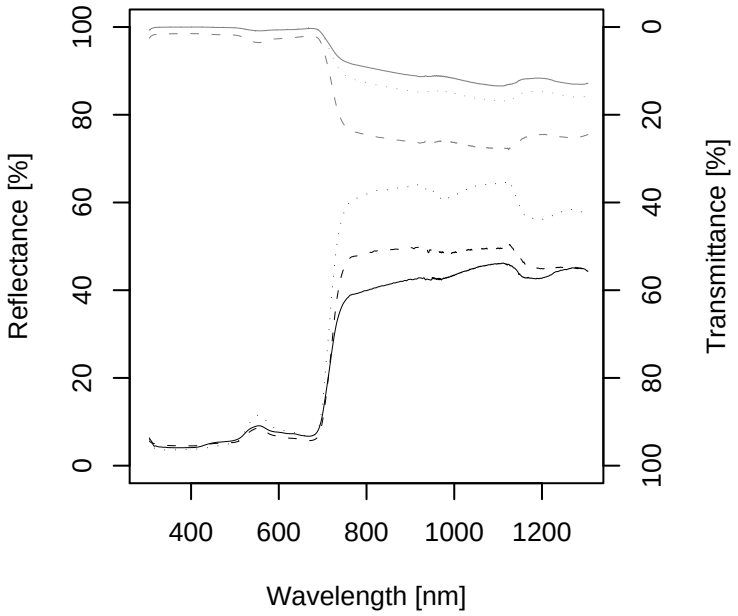

Figure 5.4: Example of three single reflectance (black) and transmittance (grey) spectra. Solid *Purdiaea nutans* (FT_{IV}, woody tree, maximum height 5–20 m, very slow growing), dashed *Tabebuia chrysantha* (FT_I, woody tree), dotted *Graffenrieda emarginata* (FT_{II} and FT_{III}, woody tree, maximum height 4–15 m, slow growing).

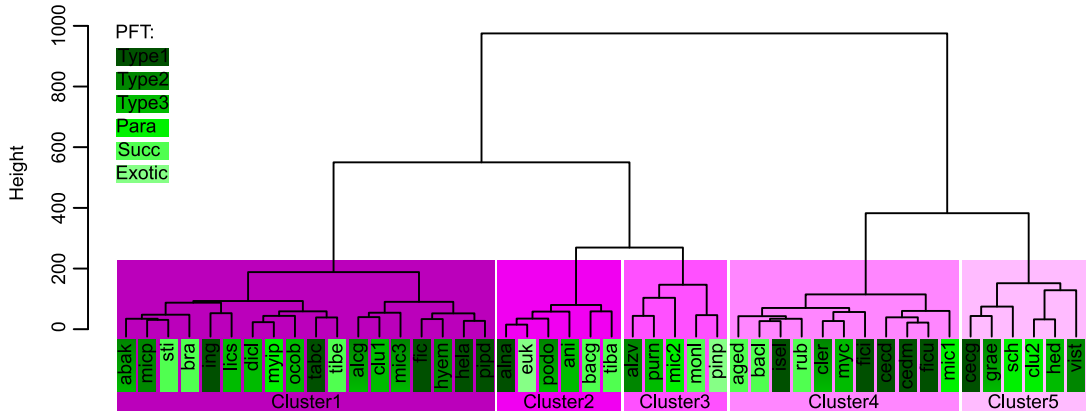

Figure 5.5: Dendrogram of the cluster analysis of the reflectance data. The dimensionless height indicates the distance of the links between the species

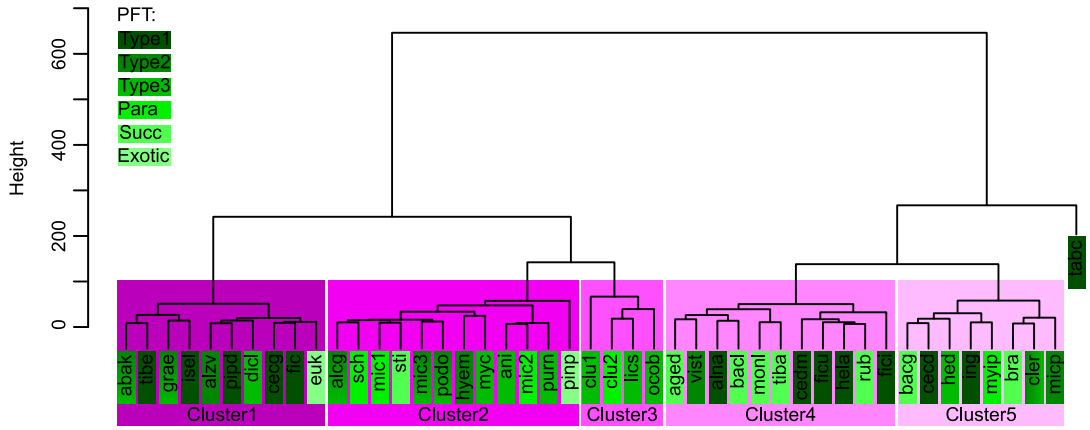

Figure 5.6: Dendrogram of the cluster analysis of the transmittance data. The dimensionless height indicates the distance of the of the links between the species

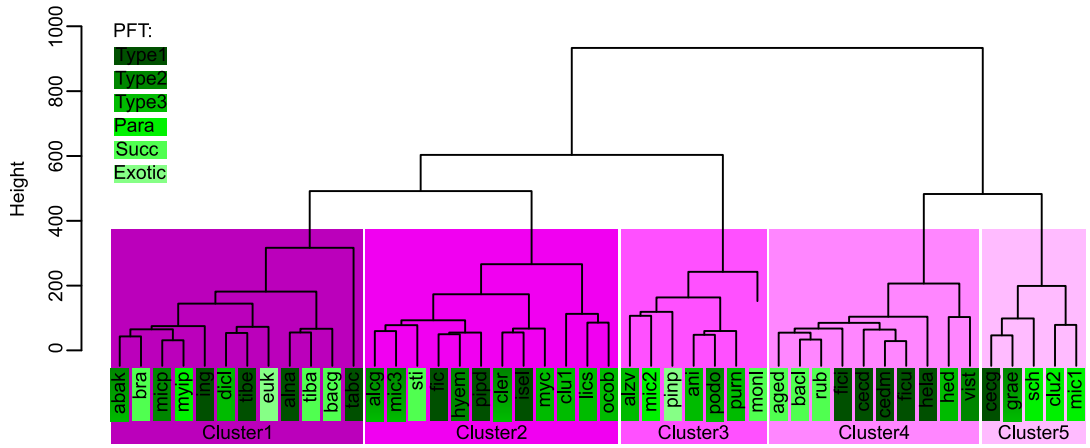

Figure 5.7: Dendrogram of the cluster analysis of the combined reflectance and transmittance data. The dimensionless height indicates the distance of the links between the species

in this case). The colours underlying the species' names in the figures 5.5–5.7 show their dominant related vegetation unit. Each cluster has a minimum of 4 species (cluster 3 transmittance), whereas the maximum is 18 (cluster 1 reflectance). The majority of the clusters are comprised of around 10 species.

5.3.3 Cluster versus Vegetation Unit

A comparison of the results of the cluster analysis with the composition of the vegetation units reveals that the clusters do not clearly represent one of the vegetation units. Table 5.3 summarizes the distribution of the single species on the clusters.

An examination of the reflectance data reveals that FT_I is mostly represented in cluster C1 (46.2 %) but this makes only 28.6 % of the cluster composition. For C1 FT_{II} (40.0 %), FT_{III} (50.0 %) and SP (40.0 %) show also a maximum of the relative frequency. The overall maximum value of a cluster frequency is found in C2 (41.7 %) but only represents 38.5 % of the PFT FT_I. In the remaining clusters, the frequencies show lower values, with local maximums spread over 2 to 4 PFTs.

The transmittance data have a similar appearance, with no distinct correlation between clusters and PFTs. The highest frequency values can be observed in FT_{SC} (62.5 %), representing 45.5 % of C2. The same representation ratio of C2 is shown by FT_I. C5 is composed of 75.0 % FT_{III}, but this is only 21.4 % of this PFT. The maximum representation ratios of C4 are equally spread over 4 PFTs. The maximum ratio of C3 is 42.9 % (FT_{III}) and of C1 is 41.7 % (FT_I).

The highest PFT value in the combined data can be found from SP (60.0 %) representing half of cluster 5. C2 is also described as 50 % of one PFT (38.5 % of FT_I). C1, C3 and C4 are all dominated by one PFT (33.3 % of FT_I, 46.7 % of FT_{III} and 42.9 % of FT_{III} respectively). A clear mapping of the PFTs to the clusters is not possible.

5.4 Discussion

5.4.1 Reflectance and Transmittance Values

Comparison of the measured reflectance and transmittance values of single species to other examinations produces divergent results. On the one hand, the reflectance values are very similar to the results of various studies (trees mostly in tropical dry forest, Castro-Esau et al. (2006); trees from tropical rain forest in Costa Rica, Clark et al. (2005) and Poorter et al. (1995); tropical trees from various sites Lee & Graham (1986)). The study of Poorter et al. (2000) conducted on trees in the cloud forest of Venezuela allows a direct comparison of the combined value for photosynthetically active radiation (PAR, 400–700 nm). Some of the trees even belong to the same genus. The mean percentage in the range between 400–700 nm

Table 5.3: Number of species of each botanically derived PFT against the calculated clusters and their relative frequency in the clusters (rows) and the PFT (columns). PFT FT_{IV} is not considered because of the domination of only 1 species. Higher total numbers of species depend on the assignment of some species to more than one vegetation unit. One species in the transmittance section is not assigned to a cluster. Maximum values of the frequencies of each cluster and PFT are marked in **bold**.

		FT_I	%	FT_{II}	%	FT_{III}	%	SP	%	SC	%	Σ
Reflec-	C1	6	**46.2**	4	**40.0**	7	**50.0**	2	**40.0**	2	25.0	21
tance	%	28.6		19.0		**33.3**		9.5		9.5		
	C2	5	38.5	2	20.0	2	14.3	0	0.0	3	**37.5**	12
	%	**41.7**		16.7		16.7		0.0		25.0		
	C3	1	7.7	1	10.0	2	14.3	0	0.0	2	25.0	6
	%	16.7		16.7		**33.3**		0.0		**33.3**		
	C4	0	0.0	1	10.0	1	7.1	1	20.0	1	12.5	4
	%	0.0		**25.0**		**25.0**		**25.0**		**25.0**		
	C5	1	7.7	2	20.0	2	14.3	2	**40.0**	0	0.0	7
	%	14.3		**28.6**		**28.6**		**28.6**		0.0		
	Σ	13		10		14		5		8		50
Trans-	C1	5	**41.7**	3	30.0	3	21.4	0	0.0	0	0.0	11
mit-	%	**45.5**		27.3		27.3		0.0		0.0		
tance	C2	5	**41.7**	1	10.0	0	0.0	0	0.0	5	**62.5**	11
	%	**45.5**		9.1		0.0		0.0		**45.5**		
	C3	0	0.0	4	**40.0**	6	**42.9**	3	**60.0**	1	12.5	14
	%	0.0		28.6		**42.9**		21.4		7.1		
	C4	2	16.7	2	20.0	2	14.3	1	20.0	2	25.0	9
	%	**22.2**		**22.2**		**22.2**		11.1		**22.2**		
	C5	0	0.0	0	0.0	3	21.4	1	20.0	0	0.0	4
	%	0.0		0.0		**75.0**		25.0		0.0		
	Σ	12		10		14		5		8		49
Com-	C1	4	30.8	2	20.0	2	14.3	1	20.0	3	**37.5**	12
bined	%	**33.3**		16.7		16.7		8.3		25.0		
	C2	5	**38.5**	1	10.0	1	7.1	0	0.0	3	**37.5**	10
	%	**50.0**		10.0		10.0		0.0		30.0		
	C3	3	23.1	4	**40.0**	7	**50.0**	0	0.0	1	12.5	15
	%	20.0		26.7		**46.7**		0.0		6.7		
	C4	0	0.0	2	20.0	3	21.4	1	20.0	1	12.5	7
	%	0.0		28.6		**42.9**		14.3		14.3		
	C5	1	7.7	1	10.0	1	7.1	3	**60.0**	0	0.0	6
	%	16.7		16.7		16.7		**50.0**		0.0		
	Σ	13		10		14		5		8		50

is reported as 7.1 for shade leaves and 7.2 for sunlit leaves and is identical with the mean of 7.1 % in PAR for all measured trees of this study.

On the other hand, the transmittance values in the near infrared area are much too low compared to the studies of Poorter et al. (1995) and Lee & Graham (1986). The study of Poorter et al. (2000) again allows a direct comparison of the mean value for the transmittance in the PAR. Shaded and sunlit leaves are reported with 3.0 % and 1.9 % respectively, in contrast to 0.5 % from our study. The low transmittance values in the near infrared section will produce much too high absorption rates and a resulting heating of the leaves. One reason for the low transmittance values is most likely the experimental setup. Consequently, the presented experimental setup for the transmittance measurements has to be reassessed, and the values are considered only to be practicable for relative intercomparison within the samples of this study.

5.4.2 Optical Properties of the Clusters

The determination of the amount of groups in an agglomerative cluster analysis is a subjective task. In this study, the number of PFTs which are composed of more than 1 species are considered as the number of clusters to allow comparisons between them. The results of the comparison of the predefined PFTs and the clusters do not match very well. This is may due to the fact that the vegetation units consist of multiple tree species with all different physiological approaches. This leads to the consideration of whether the PFTs for the regional setup of the CLM in the study area have to be newly defined on behalf of the clustering results. On the other hand, it has to be kept in mind that the spatial delineation of the PFTs is an unavoidable task to run the model. The spatial distribution of the PFTs is only achieveable using remote sensing data and will not work for the composition of the clusters.

Preexaminations (Albert, 2009) on the relationship of the reflectance in the near infrared and morphological traits (thickness of leaves, relative thickness of spongy mesophyll, trichomes, thickness of cuticule) of the plant leaves show no significant correlation, in contrast with other investigations, which find a relationship between optical and physiological/morphological properties (Billings & Morris, 1951; Knapp & Carter, 1998; Slaton et al., 2001; Poorter et al., 2000). Bicoloured leaves, however, tend to have higher reflectance values. Other attempted explanations for the variation in optical behaviour are stress (i.e. competition, infection with fungi, lack of nitrogen or water, increase in carbon dioxide or ozone) and the accompanying loss of chlorophyll (Carter & Knapp, 2001). But these are not examined in this study and cannot be taken into consideration when explaining the composition of the clusters. Consequently, the true reason for optical variance and, consequently, the composition of the clusters are not detected and make a new definition of regionalized PFTs impracticable.

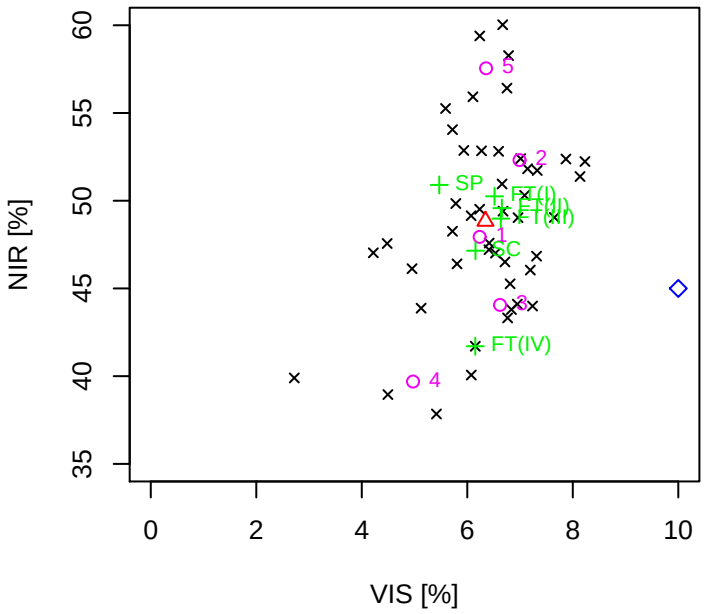

Figure 5.8: Values of reflectance in the visible (VIS) and near infrared (NIR) section for all single measurements (black symbols corresponding to the cluster number), the mean for the clusters (magenta symbols), the mean for the vegetation units (green crosses), the mean of all tree data (red triangle) and the standard value of evergreen broadleaf tropical trees from the CLM (blue rhombus).

5.4.3 Optical Properties of the CLM

The actual values which are needed for the CLM are aggregated values of reflectance and transmittance over the wavelengths between 305–699 nm (visible) and 700–1305 nm (near infrared). Figure 5.8 and fig. 5.9 illustrate the reflectance and transmittance values for the visible and near infrared section for all calculated clusters, the mean of the PFTs, the mean of all measured tree data and the relevant value supplied with the CLM.

Figure 5.8 shows that the standard reflectance value of the CLM for evergreen tropical trees lies well within the range of the near infrared section but exceeds the values in the visible section. Figure 5.9 also documents the low values of transmittance in both the near infrared and the visible section. Table 5.4 gives the relative and absolute differences between the standard CLM-value for broadleaf evergreen trees (BET) and the measured tree data of this study. A weighted mean in relation to the abundance of the species within this vegetation type is not considered because

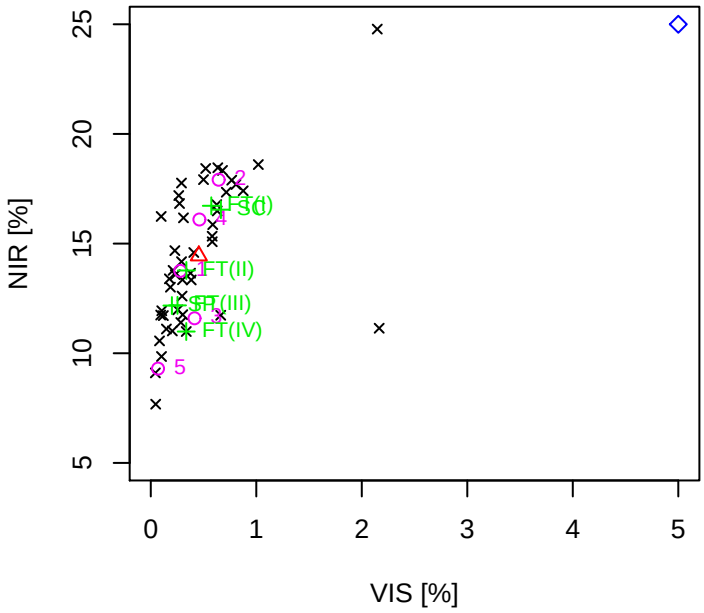

Figure 5.9: Values of transmittance in the visible (VIS) and near infrared (NIR) section for all single measurements (black symbols corresponding to the cluster number), the mean for the clusters (magenta symbols), the mean for the vegetation units (green crosses), the mean of all tree data (red triangle) and the standard value of evergreen broadleaf tropical trees from the CLM (blue rhombus).

Table 5.4: Calculated values (%) of reflectance (α) and transmittance (τ) in the visible (vis) and near infrared (nir) sector for all trees ($BET_{tropical}$) compared to the CLM standard input value ($CLM_{BET_{trop}}$) of broadleaf evergreen tropical trees with absolute (Δ_{abs}) and relative (Δ_{rel}) difference.

PFT	α_{vis}	α_{nir}	τ_{vis}	τ_{nir}
$CLM_{BET_{trop}}$	10.0	45.0	5.0	25.0
$BET_{tropical}$	6.6	49.4	0.4	14.4
Δ_{abs}	3.4	−4.4	4.6	10.6
Δ_{rel}	34.0	9.8	92.0	42.4

most of the spatially dominating species are considered.

The highest discrepancy, both in relative and absolute values, are allocated in the transmittance data due to the afore mentioned questionable experimental setup for measuring. The minimum relative difference can be found at the reflectance of the NIR section but still shows a value of approx. 10 %. Variations of the optical parameters within all standard CLM-PFTs (e.g. needleleaf trees, deciduous trees, grasses and crops in the range of 7–11 % for α_{vis}, 35–58 % for α_{nir}, 5–7 % for τ_{vis} and 10–25 % for τ_{nir} Oleson et al., 2004, table 3.1, p. 28) differ roughly in the same amount as the data of the tropical trees and shrubs presented in this paper.

The original CLM data is taken from the work of Dorman & Sellers (1989) and was compiled from various sources. Another reason for the higher discrepancy in the NIR section, independent of the experimental setup, could be that the interval of the wavelength is not clearly defined. The technical description of the CLM (Oleson et al., 2004) states only the split point of 700 nm between visible and near infrared light. Dorman & Sellers (1989) defines the NIR section with 700–4000 nm and Sellers (1985) with 700–3000 nm in contrast to 700–1305 nm used in this study.

The sampling method of these data values could be another cause for this discrepancy. Sellers et al. (1989) which is stated as one of the various sources mentioned above, refer to the initial dataset provided by Willmott & Klink (1986). Unfortunately, in these conference proceedings, neither actual values for the optical properties nor any methods or species are stated and it is assumed that all information was provided by personal communication. Furthermore, Sellers et al. (1989, p. 731) adjusted the original values (α_{nir} from 0.40 to 0.45 and τ_{nir} from 0.55 to 0.25) after an unexplained literature review and some field observations. Finally, the authors of this article assume that in Sellers et al. (1989, table 2) the values for transmittance and reflectance in the visible sector are switched by accident and are correctly cited in Dorman & Sellers (1989, table 2) as they are used in the CLM.

In general the procedure to determine not only the optical properties but most of

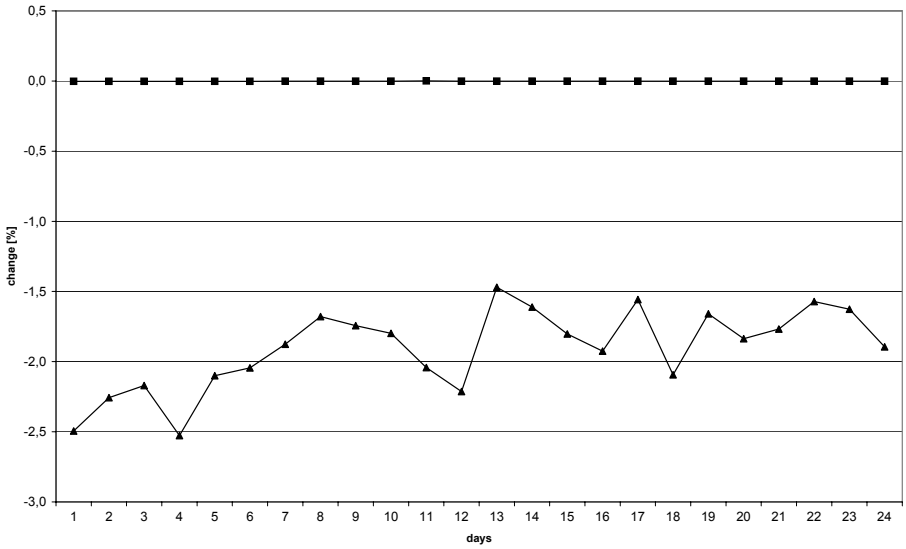

Figure 5.10: Changes in % for the air temperature in 2 m height (squares) and the sensible heat from vegetation (triangles) using the original CLM reflectance data for broadleaf evergreen tropical trees and the measured values presented in this study for 24 days.

the needed parameters of the PFT by averaging values from single species is questionable. Alternatively, parameters which can be measured for the whole vegetation can be used by inverse modelling to detect the composition of PFTs.

A simplified setup to run the CLM is accomplished to investigate the influence of the modified reflectance values for broadleaf evergreen tropical trees (7 % in the VIS and 49 % in the NIR instead of 10 % and 45 % respectively from the original data). Two modelruns are initialized using a spin-up time of one year under offline atmospheric forcing. Figure 5.10 shows the relative changes for the air temperature in 2 m height (TSA) and the sensible heat from the vegetation (FSH_V) for 24 days after the spin-up time.

The new reflectance values show no or negligible influence in the TSA output. Absolute values differ only in the maximum range of 0.07 K. Output variables which are more connected to the influence of the vegetation parametrization like the FSH_V show a small influence in the range of 1.5–2.5 % with a maximum absolute difference of approx. 20 W/m^2.

5.4.4 Optical Properties of FORMIND

Another working group within the research unit compiles plant functional types for a different purpose, but is scientifically comparable because it worked at the same study site. DISLICH et al. (2009) need PFTs to run the forest growth model FORMIND (KÖHLER, 2000). In their work, the grouping of 71 species into 7 PFTs are based on both the maximum diameter at breast height and the growth rate of the trees. Due to the experimental setup, these PFTs are all located in the lower forest type along the ridges and upper slopes (FT_{II}). The irradiance on a single leaf at a specific height within the crown is calculated using a light extinction coefficient (k) and a leaf transmission coefficient (m). The transmission coefficient is not divided into visible and near infrared components, but corresponds to the presented transmittance values in the PAR. DISLICH et al. (2009, table 2) use $m = 0.1$ (which is 10 %) for all PFTs referring to LARCHER (2001). A combined transmittance value from the collected data of PAR for all trees of FT_{II} produces 0.4 % and for all conjointly listed trees (19 species assembled of all trees from FT_{II} and a few from FT_I and FT_{III}) a value of 0.3 %. This also corresponds to the low transmittance values of this study.

5.5 Conclusions

The measurements of reflectance and transmittance of leaves of selected plants from a tropical mountain rain forest reveal that the predefined values for the globally aligned plant functional type of tropical evergreen trees of the CLM vary between approx. 10 and 90 %. Due to the high deviance of the transmittance values to data of earlier studies, only the reflected radiation is considered for further use.

Nevertheless, this study suggests that the standard input values of leaf reflectance within the CLM should be modified. The PFT of broadleaf evergreen tropical trees ($BET_{tropical}$) might be set to a reflectance percentage of 7 % in the visible and 49 % in the near-infrared section (see table 5.4). The transmittance should be examined using a reassessed experimental setup. A verification of the optical values for all other globally implemented PFTs of the CLM should be performed in further studies.

The clustering of the optical properties of the single species does not match with the composition of PFTs using botanically derived vegetation groups. Future investigations on other plant traits (physiology) could perhaps support the selected functional types. As long as remote sensing remains the only possibility to delineate the spatial distribution of the regionalized PFTs, it is impractical to define other functional groups based on the cluster analysis. Consequent, new values for the reflectance properties of the adapted PFTs are applied as stated in table 5.5 for use in a regional setup of the CLM in prospective examinations. As long as the transmittance measurements are not verified, the standard values of the CLM are

Table 5.5: Calculated values (%) of reflectance (α) in the visible (vis) and near infrared (nir) sector for the botanically derived PFTs.

PFT	α_{vis}	α_{nir}
FT_I	6.5	50.3
FT_{II}	6.7	49.6
FT_{III}	6.6	49.0
FT_{IV}	6.2	41.7
SP	5.5	50.9
SC	6.2	47.2

used.

A recent publication by USTIN & GAMON (2010) describes the use of remote sensing to distinguish plant functional types. It states that a modern interpretation of PFTs (a continuous flow rather than discrete classes of vegetation) and the development of new remote sensing techniques and instruments (hyperspectral sensors, light detection and ranging (LiDAR) methods to receive data about the vertical structure of the vegetation) are technically feasible. The proposed new concept of 'optical types' verifies in several experiments the link between observations of backscattering of radiation and physiological, morphological and optical plant traits, as well as environmental conditions. The concept needs further investigation, but '...offers the potential to create a universal solution'(USTIN & GAMON, 2010, p. 811) to distinguish functional groups of vegetation viewed from space. This encourages the presented approach to retain the PFTs recovered by satellite data. Possibly, the use of higher resolution satellite data, in combination with data of the vertical structure of the vegetation - which will become available in the near future - may conclude in new or adapted plant functional types.

Acknowledgements

This work was funded by the German Research Foundation (DFG) in the scope of the Research Unit FOR816 'Biodiversity and Sustainable Management of a Megadiverse Mountain Ecosystem in South Ecuador', subproject Z1.1 (NA 783/1-1). The authors extend their thanks to Jürgen Homeier and Florian Werner for help with the selection and determination of the measured plants and to two anonymous reviewers for constructive comments and suggestions on the manuscript.

5.6 Appendix

Raw data

Table 5.6: Reflectance and transmittance values for all measured species in the visible (VIS) and near infrared (NIR) section in %. Additional the used code and the dominant vegetation unit is shown.

Species	Code	Vegetation unit	Reflectance VIS	Reflectance NIR	Transmittance VIS	Transmittance NIR
Abarema killipii	abak	Type 2 and 3	5.72	48.26	0.23	14.68
Ageratina dendroides	aged	succession	7.01	52.40	0.72	17.34
Alchornea grandiflora	alcg	Type 2 and 3	7.09	50.31	0.09	11.74
Alnus acuminata	alna	Type 1	7.24	44.00	0.50	17.92
Alzatea verticillata	alzv	Type 2	6.08	40.07	0.30	13.35
Aniba spec.	ani	Type 3	6.84	43.80	0.15	11.11
Baccharis genistelloides	bacg	succession	6.81	45.26	0.63	16.49
Baccharis latifolia	bacl	succession	7.33	51.72	0.77	17.89
Brachytotum spec.	bra	succession	4.48	47.56	0.58	15.34
Cecropia andina	cecd	Type 1	5.93	52.87	0.63	16.78
Cecropia angustifolia	cecg	Type 1	6.67	60.03	0.23	13.58
Cedrela montana	cedm	Type 1	6.27	52.84	1.02	18.60
Clethra revoluta	cler	Type 2 and 3	7.87	52.38	0.58	15.08
Clusia spec. 1	clu1	Type 3	6.23	49.52	0.05	7.68
Clusia spec. 2	clu2	Páramo	5.59	55.26	0.08	10.56
Dictyocarium lamarckianum	dicl	Type 3	7.31	46.84	0.19	13.01
Eukalyptus spec.	euk	exotic	6.95	44.11	0.21	13.78
Ficus spec.	fic	Type 1	8.14	51.38	0.29	17.76
Ficus citrifolia	fici	Type 1	6.59	52.82	0.52	18.42
Ficus cuatrecasana	ficu	Type 1	7.65	49.05	0.18	13.39
Graffenrieda emarginata	grae	Type 2 and 3	6.24	59.39	0.29	14.18
Hedyosmum spec.	hed	Type 3	6.11	55.92	0.27	16.83
Heliocarpus americanus	hela	Type 1	6.07	49.15	0.68	18.34
Hyeronima moritziana	hyem	Type 2	6.96	49.03	0.10	11.94
Inga spec.	ing	Type 1	4.22	47.03	0.10	16.24
Isertia laevis	isel	Type 1	7.14	51.82	0.38	13.65
Licaria subsessils	lics	Type 3	4.95	46.13	0.10	9.85
Miconia spec. 1	mic1	Páramo	5.72	54.05	0.28	11.40
Miconia spec. 2	mic2	Páramo	2.72	39.90	0.20	11.02
Miconia spec. 3	mic3	Type 2 and 3	6.68	49.40	0.26	11.98
Miconia punctata	micp	Type 2	6.41	47.21	0.59	15.87
Monochaetum lineatum	monl	succession	5.41	37.84	0.81	17.69
Myrcia spec.	myc	Type 3	8.23	52.24	0.30	12.61
Myrica pubescens	myip	Páramo	6.53	47.02	0.31	16.17
Ocothea benthamiana	ocob	Type 3	6.71	46.51	0.04	9.10
Pinus patula	pinp	exotic	4.49	38.95	2.16	11.14
Piptocoma discolor	pipd	Type 1	5.78	49.84	0.38	13.34
Podocarpus oleifolius	podo	Type 2 and 3	6.76	43.32	0.66	11.73
Purdiaea nutans	purn	Type 3	6.15	41.71	0.34	10.99
Rubus spec.	rub	succession	6.66	50.95	0.64	18.46
Schefflera spec.	sch	Páramo	6.78	58.27	0.12	11.72
Sticherus spec.	sti	succession	6.41	47.59	0.30	11.76
Tabebuia chrysantha	tabc	Type 1	5.81	46.40	2.15	24.78
Tibouchina laxa	tiba	succession	5.12	43.87	0.88	17.41
Tibouchina lepidota	tibe	Type 1	7.19	46.05	0.41	14.59
Vismia tomentosa	vist	Type 2	6.75	56.41	0.27	17.19

References

Albert, J.: (2009): Classification of vegetation of a tropical mountain rainforest in south ecudor using spectral traits (klassifikation der vegetation eines tropischen bergregenwaldes in südecuador anhand spektraler eigenschaften), thesis at the University of Cologne, Department of Ecology. In German.

Barthlott, W., A. Hostert, G. Kier, W. Küper, H. Kreft, J. Mutke, M. Rafiqpoor & J. H. Sommer: (2007): Geographic patterns of vascular plant diversity at continental to global scale, *Erdkunde*, *61*, 305–315.

Beck, E., J. Bendix, I. Kottke, F. Makeschin & R. Mosandl (eds.): (2008): *Gradients in a Tropical Mountain Ecosystem of Ecuador*, *Ecological Studies*, vol. 198, Springer, Berlin, Heidelberg.

Billings, W. D. & R. J. Morris: (1951): Reflection of visible and infrared radiation from leaves of different ecological groups, *American Journal of Botany*, *38*, 327–331.

Bonan, G., S. Levis, L. Kergoat & K. Oleson: (2002a): Landscapes as patches of plant functional types: An integrating concept for climate and ecosystem models, *Global Biochemical Cycles*, *16 No.2*, 5–1–5–30.

Bonan, G., K. Oleson, M. Vertenstein, S. Levis, X. Zeng, Y. Dai, R. Dickinson & Z.-L. Yang: (2002b): The land surface climatology of the community land model coupled to the NCAR community climate model, *Journal of Climate*, *15*, 3123–3149.

Carter, G. A. & A. K. Knapp: (2001): Leaf optical properties in higher plants: linking spectral characteristics to stress and chlorophyll concentration, *Am. J. Bot.*, *88*, 677–684.

Castro-Esau, K. L., G. A. Sánchez-Azofeifa, B. Rivard, S. J. Wright & M. Quesada: (2006): Variability in leaf optical properties of mesoamerican trees and the potential for species classification, *American Journal of Botany*, *93*, 517–530.

Clark, M. L., D. A. Roberts & D. B. Clark: (2005): Hyperspectral discrimination of tropical rain forest tree species at leaf to crown scales, *Remote Sensing of Environment*, *96*, 375–398.

Colwell, R. K., G. Brehm, C. L. Cardelus, A. C. Gilman & J. T. Longino: (2008): Global warming, elevational range shifts, and lowland biotic attrition in the wet tropics, *Science*, *322*, 258–261.

Dickinson, R., K. Oleson, G. Bonan, F. Hoffman, P. Thornton, M. Vertenstein, Z. Yang & X. Zeng: (2006): The community land model and its climate statistics as a component of the community climate system model, *Journal of Climate*, *19*, 2302–2324.

Dislich, C., S. Günter, J. Homeier, B. Schröder & A. Huth: (2009): Simulating forest dynamics of a tropical montane forest in south ecuador, *Erdkunde*, *63*, 347–364.

Dorman, J. & P. Sellers: (1989): A global climatology of albedo, roughness length and stomatal resistance for atmospheric general circulation models as represented by the simple biosphere model (sib), *J. Appl. Meteor.*, *28*, 833–855.

Foley, S., B. Rivard, G. A. Sanchez-Azofeifa & J. Calvo: (2006): Foliar spectral properties following leaf clipping and implications for handling techniques, *Remote Sensing of Environment*, *103*, 265–275.

Göttlicher, D., T. Nauss & J. Bendix: (2010): Sensitivity of the community land model to plant and soil parameters for the prediction of commonly required parameters for applied ecologic and socio-economic studies, *Computers & Geosciences*, *submitted*.

Göttlicher, D., A. Obregón, J. Homeier, R. Rollenbeck, T. Nauss & J. Bendix: (2009): Land cover classification in the Andes of southern Ecuador using Landsat ETM+ data as a basis for SVAT modeling, *International Journal of Remote Sensing*, *30*, 1867–1886.

Homeier, J. & F. Werner: (2007): Spermatophyta – checklist of the reserva biológica san francisco (prov. zamora-chinchipe, s-ecuador), *Ecotropical Monographs*, *4*, 15–58.

Homeier, J., F. Werner, S. Gradstein, S.-W. Breckle & M. Richter: (2008): Potential vegetation and floristic composition of andean forests in south ecuador, with a focus on the rbsf, in Beck, E., J. Bendix, I. Kottke, F. Makeschin & R. Mosandl (eds.) *Gradients in a Tropical Mountain Ecosystem of Ecuador*, *Ecological Studies*, vol. 198, 87–100, Springer, Berlin.

Kaufman, L. & P. J. Rousseeuw: (2005): *Finding Groups in Data - An Introduction to Cluster Analysis*, Wiley Series in Probability and Statistics, Wiley-Interscience, New York.

Knapp, A. K. & G. A. Carter: (1998): Variability in leaf optical properties among 26 species from a broad range of habitats, *American Journal of Botany*, *85*, 940–946.

Köhler, P.: (2000): *Modelling anthropogenic impacts on the growth of tropical rain forests – using an individual-oriented forest growth model for the analyses of logging and fragmentation in three case studies*, Ph.D. thesis, Department of Physics and the Center for Environmental Systems Research, University of Kassel, Der Andere Verlag, Osnabrück, Germany.

Larcher, W.: (2001): *Ökophysiologie der Pflanzen*, *UTB für Wissenschaft*, vol. 8074, 6th edn., Ulmer, Stuttgart.

Lavorel, S., S. Díaz, J. H. C. Cornelissen, E. Garnier, S. P. Harrison, J. G. Pausas, N. Pérez-Harguindeguy, C. Roumet & C. Urcelay: (2007): Plant functional types: Are we getting any closer to the holy grail?, in Canadell, J. G., D. E. Pataki & L. F. Pitelka (eds.) *Terrestrial Ecosystems in a Changing World*, chap. 13, 149–164, Springer, Berlin, Heidelberg.

Lee, D. W. & R. Graham: (1986): Leaf optical properties of rainforest sun and extreme shade plants, *American Journal of Botany*, *73*, 1100–1108.

Maechler, M., P. Rousseeuw, A. Struyf & M. Hubert: (2005): Cluster analysis basics and extensions, URL `http://cran.r-project.org/web/packages/cluster/`, 2010-06-10.

Mosandl, R., S. Günter, B. Stimm & M. Weber: (2008): Ecuador suffers the highest deforestation rate in south america, in Beck, E., J. Bendix, I. Kottke, F. Makeschin & R. Mosandl (eds.) *Gradients in a Tropical Mountain Ecosystem of Ecuador*, *Ecological Studies*, vol. 198, chap. 4, Springer, Berlin.

Oleson, K. W., Y. Dai, G. Bonan, M. Bosilovich, R. Dickinson, P. Dirmeyer, F. Hoffman, P. Houser, S. Levis, G. Y. Niu, P. Thornton, M. Vertenstein, Z. L. Yang & X. Zeng: (2004): Technical description of the community land model (clm), Tech. Rep. NCAR/TN-461+STR, NCAR Technical Note.

Oleson, K. W., G.-Y. Niu, Z.-L. Yang, D. M. Lawrence, P. E. Thornton, P. J. Lawrence, R. Stöckli, R. E. Dickinson, G. B. Bonan, S. Levis, A. Dai & T. Qian: (2008): Improvements to the community land model and their impact on the hydrological cycle, *Journal of Geophysical Research*, *113*, G01021.

Poorter, L., R. Kwant, R. Hernández, E. Medina & M. J. A. Werger: (2000): Leaf optical properties in venezuelan cloud forest trees, *Tree Physiology*, *20*, 519–526.

Poorter, L., S. F. Oberbauer & D. B. Clark: (1995): Leaf optical properties along a vertical gradient in a tropical rain forest canopy in costa rica, *American Journal of Botany*, *82*, 1257–1263.

R Development Core Team: (2009): *R: A Language and Environment for Statistical Computing*, R Foundation for Statistical Computing, Vienna, Austria, URL `http://www.R-project.org`, ISBN 3-900051-07-0.

Sala, O. E., I. Chapin, F. Stuart, J. J. Armesto, E. Berlow, J. Bloomfield, R. Dirzo, E. Huber-Sanwald, L. F. Huenneke, R. B. Jackson, A. Kinzig, R. Leemans, D. M. Lodge, H. A. Mooney, M. Oesterheld,

N. L. Poff, M. T. Sykes, B. H. Walker, M. Walker & D. H. Wall: (2000): Global biodiversity scenarios for the year 2100, *Science*, *287*, 1770–1774.

Sellers, P.: (1985): Canopy reflectance, photosynthesis and transpiration, *International Journal of Remote Sensing*, *6*, 1335–1372.

Sellers, P. J., W. J. Shuttleworth, J. L. Dorman, A. Dalcher & J. M. Roberts: (1989): Calibrating the simple biosphere model for amazonian tropical forest using field and remote sensing data. part i: Average calibration with field data, *Journal of Applied Meteorology*, *28*, 727–759.

Slaton, M. R., J. Hunt, E. Raymond & W. K. Smith: (2001): Estimating near-infrared leaf reflectance from leaf structural characteristics, *American Journal of Botany*, *88*, 278–284.

Smith, T. M., H. H. Shugart & F. I. Woodward (eds.): (1997): *Plant functional types – their relevance to ecosystem properties and global change*, *International Geosphere-Biosphere Programme Book Series*, vol. 1, Cambridge University Press, New York.

tec5: (2005): *HandySpec Field - Systemdescription and Documentation*, tec5 AG, Oberursel, Germany, in german.

Ustin, S. L. & J. A. Gamon: (2010): Remote sensing of plant functional types, *New Phytologist*, *186*, 795–816.

Ward, J. H. J.: (1963): Hierarchical grouping to optimize an objective function, *Journal of the American Statistical Association*, *58*, 236–244.

Willmott, C. J. & K. M. Klink: (1986): A representation of the terrestrial biosphere for use in global climate studies, in *Proceedings of the ISLSCP Conference*, ESA SP-248, 109–112, Rome Italy.

Zhu, H.: (2005): Linear spectral unmixing assisted by probability guided and minimum residual exhaustive search for subpixel classification, *International Journal of Remote Sensing*, *26*, 5585–5601.

6 Summary and Outlook

6.1 Summary

Global biodiversity is threatened by climate and land cover change. The research unit 'Biodiversity and Sustainable Management of a Megadiverse Mountain Ecosystem in South Ecuador' (FOR 816) funded by the German research council (Deutsche Forschungsgemeinschaft, DFG) is working in one of the hottest hotspots of biodiversity of the world. In this region the pressure from the local population on the environment is severe resulting in a high deforestation rate. Sustainable management systems have to be developed on a regional scale to counteract the loss of livelihood of the local population.

Numerical models are capable to investigate the changes of the mentioned future land cover changes and its response to climatic and hydrologic variability. The chance to test numerously land use scenarios without interfering into the real environment offers the possibility to investigate and to evaluate the proposed management strategies.

The presented work targets at an analysis of the impact of the predicted land cover changes in respect of the ecosystem services of climate and water regulation. Therefore a state-of-the-art land surface model called *Community Land Model* (CLM) is setup in a regional scale. The parametrization of the vegetation is implemented using plant functional types (PFT). The PFTs are defined a priori with vegetation classes based on ecological field surveys. Three central hypotheses are formulated to support the parametrization of the model. Accordingly, three work packages (WP) are established to test the hypotheses. In detail the results of the WPs and the review of the hypotheses are as follows:

Hypothesis 1 – WP 1

H 1 A continuous spatial delineation of land use classes based on ecological-functional field studies can be mapped in a subpixel accuracy from medium space-resolved satellite data.

WP 1 The spatial delineation of the PFTs is achieved by the use of classified Landsat ETM+ satellite data. Besides a hard classification using a maximum-likelihood algorithm, a soft classification method is conducted. The modified linear spectral unmixing approach offers percentage coverage of the PFTs in a subpixel resolution. The results of both classification schemes are good and the probability guided spectral unmixing is chosen for the determination of plant functional types for the land model. A similar model run done with a spatial distribution of land cover from both the hard and the soft classification clearly points to more realistic model results by using the land surface based on the probability guided spectral unmixing technique (chapter 3).
The hypothesis can be verified.

Hypothesis 2 – WP 2

H 2 Gradual changes in the composition of vegetation, its morphological, optical and physiological behavior do not have influence on the energy and water fluxes estimated in a SVAT model.

WP 2 A sensitivity study on all PFT parameters of the CLM is conducted. The experimental setup is characterized by numerous model runs with changing one specific parameter while all others are kept constant. The results are used to decide which parameters must be gathered in the field with priority in order to parametrize properly the model with regionalized PFTs. With respect to temperature and humidity, the variation of most investigated parameters of $\pm 30\,\%$ appeared to cause only negligible variations ($< 1\,\%$). Other output variables like transpiration and evaporation from the vegetation show much higher deviations especially by variations of the structural parameter (leaf area index $> 30\,\%$). A stronger influence also emanates from leaf and stem optical properties that could lead to changes in the sensible heat flux between $-40\,\%$ to $30\,\%$ (chapter 4).
This hypothesis is true for most of the PFT parameters concerning the output variables of temperature and humidity. Only the input values of LAI have a significant influence in many output variables and the optical traits in some variables.

Hypothesis 3 – WP 3

H 3 Clusters of species with similar plant optical properties reflect ecologically derived vegetation types.

WP 3 Optical properties (reflectance and transmittance) of leaves from relevant species of the predefined PFTs are measured using a new field spectrometer. The gathered spectra are clustered by the means of similarity and compared to the composition of the predefined PFTs. The results show that the clusters aggregated by the reflectance, transmittance or combined properties do not represent the predefined PFTs. The values of the other studies suggest a reassessment of the experimental setup for the transmittance measurements. Nevertheless, new reflectance values for the regionalized PFTs can be determined. The optical values differ from the CLM-PFT of tropical evergreen trees, and new values for the reflectance in the visible and near-infrared are recommended (chapter 5). The hypothesis has to be falsified. However, the regional setup is run with the PFTs defined from the vegetation units because of their distinct spatial delineation. The new means of reflectance data are used for the single PFTs accordingly.

The completed work offers a regionalized model setup to analyze different land cover developments in reference to energy and water fluxes between the soil, the vegetation and the atmosphere under changing climatic conditions. Besides the appraisal of the stated hypotheses other innovative contributions are made. The new values for the pre-installed CLM-PFT of tropical evergreen trees add to the current improvements made to the CLM as mentioned in Lawrence et al. (2010) for the new optical values of grass and crop.

6.2 Outlook

6.2.1 Preliminary Model Runs

Preliminary model runs are presented to demonstrate the potential of the regionalized land model. The first model runs in a preliminary setup are already presented in chapter 3. They include only coarse atmospheric forcing, no regionalized soil properties and no regionalized PFT parameters except their spatial distribution (especially no spatially differentiated LAI values). Therein, the differences between the two classification schemes are analyzed. Now the model runs represent the different output values due to change in land cover and change in atmospheric forcing. Therefore the following hypothetical alterations are taken place:

- **Scenario 1**: The areas with bracken fern and shrubs are converted to forests (reforestation of abandoned pastures)

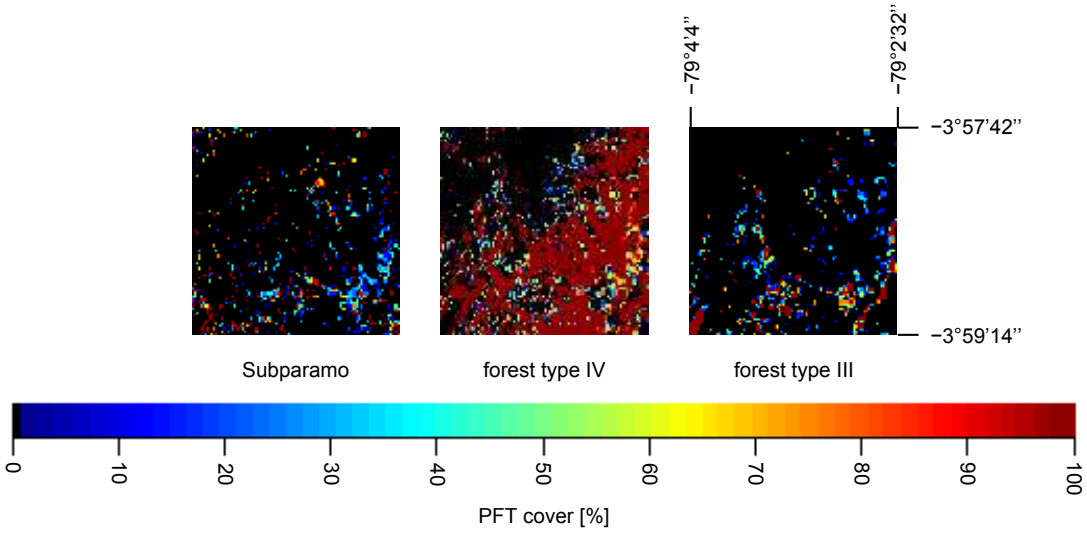

Figure 6.1: Distribution of PFT cover which are stable in the preliminary model runs.

- **Scenario 2**: The lower forest areas are converted to pastures (intensification of pasture farming)
- **Scenario 3**: The air temperature of the atmospheric forcing is increased by 3 K (climate change scenario)

Additionally, a control run with the estimated distribution of PFTs from the satellite data is conducted. The distribution of the PFTs which are stable throughout the model runs are presented in figure 6.1. The distribution of the changing PFTs are visualized in figure 6.2.

Atmospheric forcing is implemented from NCAR/NCEP reanalysis data (Qian et al., 2006; Kalnay et al., 1996). The increase in temperature in the latter model run is based on the highest values from the most likely (A1B) scenario of the Intergovernmental Panel on Climate Change (IPCC) / Special report on Emissions Scenarios (SRES[2]) simulations by the year 2100 (Christensen et al., 2007; Nakicenovic & Swart, 2000). The model is run with a spin-up time of one year. The output results are the daily mean of the last day of the first month after spin-up time. The soil is not regionalized and taken from the global data set supplied with the CLM. The results of a soft classification is used to determine the percentage and spatial distribution of the PFTs. For scenarios 1 and 2 to the new distribution of PFTs are simple calculated from the values of the control run.

Exemplarily, the results for the canopy transpiration are shown in figure 6.3. It is obviously that the higher temperatures in the atmospheric forcing (scenario 3) causes higher transpiration rates especially in the forest areas. The shift in land cover from forest to grasses (scenario 2) show a significant decrease in the transpiration rate in the affected areas. In the contrary to this, the transpiration rate rises in the areas

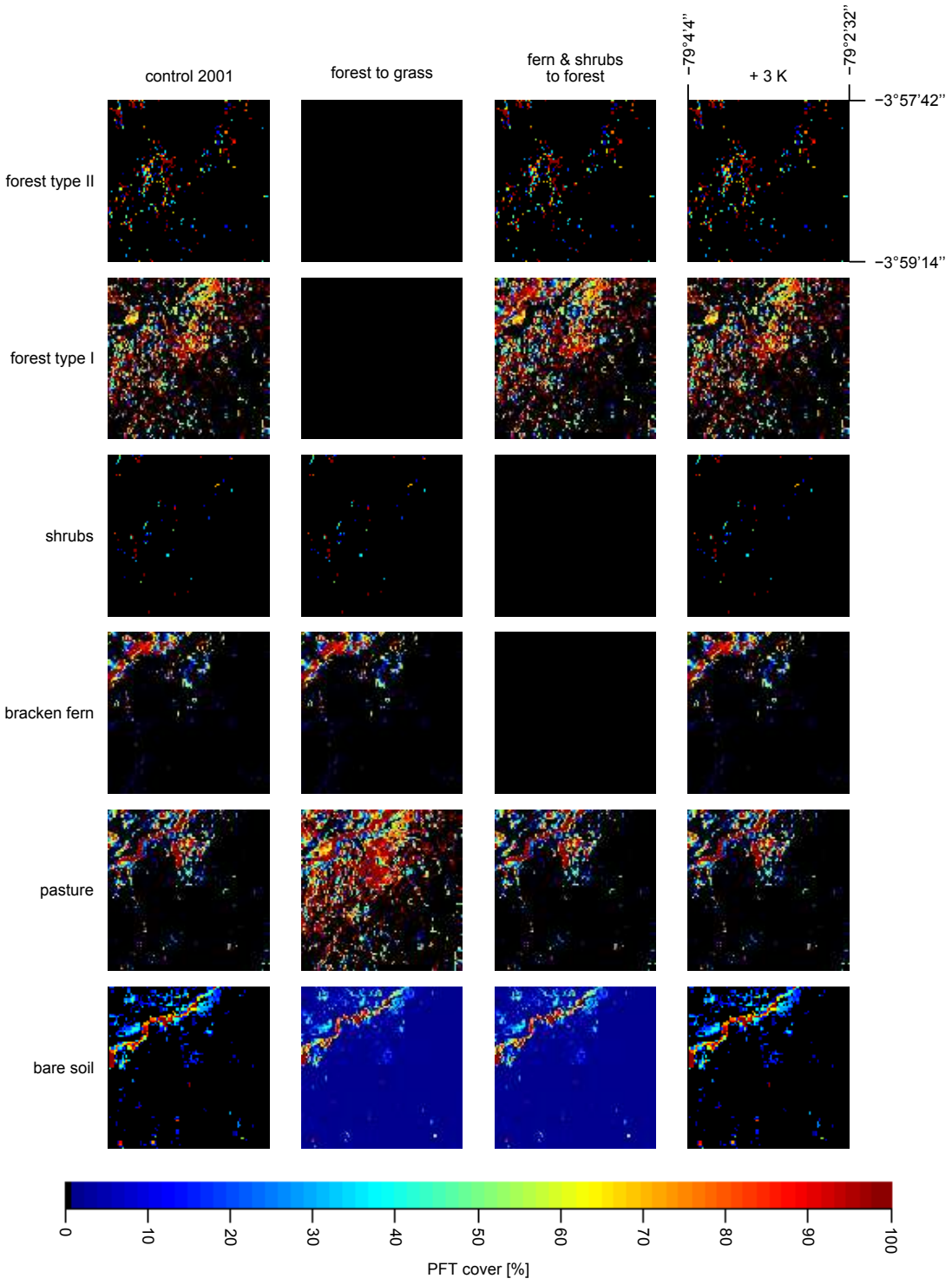

Figure 6.2: Distribution of PFT cover in the preliminary model runs.

which are subject to the change from successional stadiums to forest again (scenario 1).

The model demonstrate in these very simplified conditions its possibilities for the future work.

6.2.2 Future Work

Additional work has to be conducted to finish the spatial parametrization of the model in the future. Following steps are suggested by the author:

- Liess et al. (2009) are presenting a regionalization of soil types. For these soil types adequate values for the percentage of sand and clay have to be determined. This can be done directly over the soil type if appropriate or with the use of transfer functions including additional topographic features like the slope or altitude. Furthermore a soil color class has to be identified.

- The values of the LAI have to be determined for each PFT in spatial and temporal dependency. Therefore transfer functions from in situ LAI measurements and spatial corresponding values of vegetation indices from satellite data could be used.

- The experimental setup for the transmittance measurements of the leaves has to be redesigned and new values should be calculated.

- A major task is the preparation of a weather regionalization tool or at least the interpolation of static datasets from the station data within the study area to regionalize the atmospheric forcing to real conditions. First steps towards this achievement are presented by Fries et al. (2009) regarding the thermal structure.

- The responsible subprograms of the research unit have to specify in which way real case scenarios look like and should be implemented in the model and analyzed under different climatic conditions.

- Finally, the land model should be coupled to a mesoscale atmospheric model like the *Weather Research and Forecasting Model* (WRF) to analyze the feedbacks between land cover change and climate change.

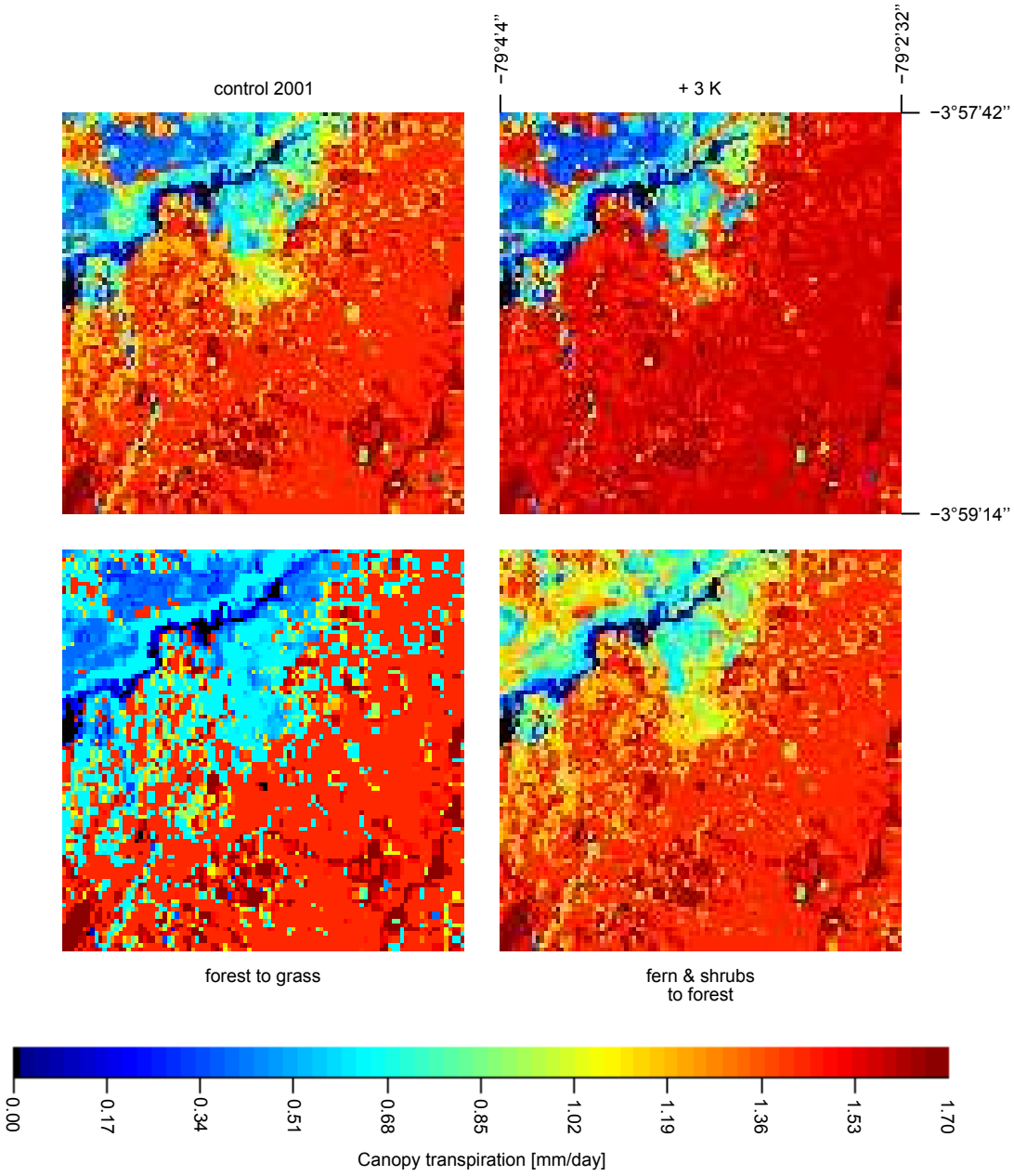

Figure 6.3: Results of the preliminary model runs for canopy transpiration.

References

Christensen, J., B. Hewitson, A. Busuioc, A. Chen, X. Gao, I. Held, R. Jones, R. Kolli, W.-T. Kwon, R. Laprise, V. M. na Rueda, L. Mearns, C. Menéndez, J. Räisänen, A. Rinke, A. Sarr & P. Whetton: (2007): Regional climate projections, in Solomon, S., D. Qin, M. Manning, Z. Chen, M. Marquis, K. Averyt, M. Tignor & H. Miller (eds.) *Climate Change 2007: The Physical Science Basis. Contribution of Working Group I to the Fourth Assessment Report of the Intergovernmental Panel on Climate Change*, chap. 11, 847–940, Cambridge University Press, Cambridge and New York, NY.

Fries, A., R. Rollenbeck, D. Göttlicher, T. Nauss, J. Homeier, T. Peters & J. Bendix: (2009): Thermal structure of a megadiverse andean mountain ecosystem in southern ecuador and its regionalization, *Erdkunde*, *63*, 321–335.

Kalnay, E., M. Kanamitsu, R. Kistler, W. Collins, D. Deaven, L. Gandin, M. Iredell, S. Saha, G. White, J. Woollen, Y. Zhu, A. Leetmaa, R. Reynolds, M. Chelliah, W. Ebisuzaki, W. Higgins, J. Janowiak, K. C. Mo, C. Ropelewski, J. Wang, R. Jenne & D. Joseph: (1996): The ncep/ncar 40-year reanalysis project, *Bulletin of the American Meteorological Society*, *77*, 437–471.

Lawrence, D., K. W. Oleson, M. G. Flanner, P. E. Thornton, S. C. Swenson, P. J. Lawrence, X. Zeng, Z.-L. Yang, S. Levis, K. Sakaguchi, G. B. Bonan & A. G. Slater: (2010): Parameterization improvements and functional and structural advances in version 4 of the community land model, *Journal of Advances in Modeling Earth Systems*, *Submitted*, on Discussion.

Liess, M., B. Glaser & B. Huwe: (2009): Digital soil mapping in southern ecuador, *Erdkunde*, *63*, 309–319.

Nakicenovic, N. & R. Swart (eds.): (2000): *Special Report on Emissions Scenarios: A Special Report of Working Group III of the Intergovernmental Panel on Climate Change*, Cambridge University Press, Cambridge.

Qian, T., A. Dai, K. E. Trenberth & K. W. Oleson: (2006): Simulation of global land surface conditions from 1948 to 2004. part i: Forcing data and evaluations, *Journal of Hydrometeorology*, *7*, 953–975.

7 Zusammenfassung

Klima- und Landnutzungsveränderungen bedrohen die globale Biodiversität. In einem der artenreichsten Gebiete der Welt arbeitet die von der Deutschen Forschungsgemeinschaft (DFG) finanzierte Forschergruppe 'Biodiversity and Sustainable Management of a Megadiverse Mountain Ecosystem in South Ecuador'(FOR 816). Von der lokalen Bevölkerung geht ein enormer Druck auf die Umwelt aus und resultiert in einer sehr hohen Entwaldungsrate. Um die Lebensgrundlage der örtlichen Bevölkerung zu wahren, müssen nachhaltige Bewirtschaftungssysteme entwickelt werden.

Zukünftige Landnutzungsveränderungen und ihre Auswirkungen auf klimatische und hydrologische Faktoren können mit numerischen Modellen untersucht werden. Entwickelte Managementstrategien können durch die Modellen untersucht und bewertet werden, ohne real in das Landschaftsgefüge einzugreifen.

Ziel der präsentierten Arbeit ist es, das Ausmaßder vorhergesagten Landnutzungsänderungen und ihre Auswirkungen auf die Ökosystemleistungen hinsichtlich der Regulation von Wasserflüssen und Klimaparameter zu analysieren. Um dieses zu erreichen, wird ein spezifisches, hochmodernes Austauschmodell der Energie- und Wasserflüsse (Community Land Model, CLM) zwischen Boden, Vegetation und der Atmosphäre in einer regionalen Auflösung aufgesetzt (auch SVAT-Modell genannt). Die Parametrisierung der Vegetation erfolgt über sogenannte Pflanzenfunktionstypen (PFT). Die PFT werden im vorhinein mit Hilfe von Vegetationseinheiten definiert, die auf ökologischen Felduntersuchungen beruhen. Die Parametrisierung des Models wird durch die Formulierung von 3 Hypothesen unterstützt. Um die Hypothesen zu testen, werden dementsprechend 3 Arbeitspakete (AP) etabliert. Die Ergebnisse der AP und die Bewertung der Hypothesen sind im Einzelnen:

Hypothese 1 – AP 1

H 1 Eine flächendeckende Abgrenzung von Landnutzungsklassen, basierend auf ökologisch-funktionalen Felduntersuchungen, aus mittel aufgelösten Satellitendaten ist mit einer Genauigkeit im Subpixelbereich möglich.

AP 1 Die räumliche Abgrenzung der PFT wird durch eine Klassifikation von Landsat ETM+ Satellitendaten erreicht. Neben einer harten Maximum-Likelihood Abschätzung wird eine weiche Klassifikation durchgeführt. Eine modifizierte lineare spektrale Entmischung errechnet prozentuale Anteile der PFT im Subpixelbereich. Die Ergebnisse beider Klassifikationsalgorithmen sind gut. Die Ergebnisse der weichen Klassifikation werden letztendlich zur Bestimmung der räumlichen Verteilung der PFT in dem Modell benutzt. Identische Simulationsläufe des Models mit beiden unterschiedlichen Klassifizierungsergebnissen zeigen, dass die Landnutzung der spektralen Entmischung ein klar realitätsnäheres Bild widerspiegeln (Kapitel 3).
Die Hypothese kann verifiziert werden.

Hypothese 2 – AP 2

H 2 Allmähliche Veränderungen in der Vegetationszusammensetzung und ihrem morphologischen, optischen und physiologischen Verhalten haben keinen Einfluss auf die berechneten Energie-und Wasserflüsse eines SVAT-Modells.

AP 2 Für alle PFT wurde eine Sensitivitätsstudie durchgeführt. Zahlreiche Modellläufe mit Veränderungen von einem Parameter, während alle anderen konstant gehalten werden, kennzeichnen den experimentellen Aufbau. Die Ergebnisse geben darüber Aufschluss, welche Parameter in Felduntersuchungen im besonderen Maße begutachtet werden müssen, um das Modell mit den regionalen PFT zu parametrisieren. Hinsichtlich der Temperatur und der Luftfeuchtigkeit haben Abweichungen von $\pm 30\,\%$ in den untersuchten Parametern eine nur geringfügige Auswirkung ($< 1\,\%$). Sehr viel höhere Abweichungen werden bei anderen Ausgabevariablen wie Transpiration und Evaporation der Vegetation festgestellt. Besonders strukturelle Parameter wie der Blattflächenindex zeigen große Veränderungen ($> 30\,\%$). Weiterhin zeigen die optischen Eigenschaften der Blätter und Stämme einen großen Einfluss und können Abweichungen im sensiblen Wärmestrom zwischen $-40\,\%$ und $30\,\%$ ausmachen (Kapitel 4).
Die Hypothese kann für die meisten PFT-Parameter im Hinblick auf die Ausgangsvariablen von Temperatur und Luftfeuchtigkeit angenommen werden. Auf viele Ausgabegrößen hat nur der Blattflächenindex einen signifikanten Einfluss, die optischen Eigenschaften beeinflussen noch wenige Variablen.

Hypothese 3 – AP 3

H 3 Ökologisch definierte Vegetationseinheiten spiegeln sich in Cluster wieder, die auf ähnlichen, optischen Eigenschaften der Pflanzen beruhen.

AP 3 Blätter relevanter Arten der definierten PFT werden mit einem Feldspektrometer hinsichtlich ihrer optischen Eigenschaften (Reflexion und Transmission) untersucht. Auf Grund der Ähnlichkeit der gemessenen Spektren werden Cluster gebildet und mit der Zusammensetzung der PFT verglichen. Die Ergebnisse zeigen, dass die Cluster der Reflexion, Transmission und auch der kombinierten Daten nicht den PFT entsprechen. Ein neues Design der Transmissionsmessungen wird durch einen Vergleich mit anderen Studien nahe gelegt. Dennoch können neue Reflexionswerte für die regionalisierten PFT bestimmt werden. Die gemessenen Werte weichen von den Werten für immergrüne tropische Bäume des CLM ab und es werden für die Reflexion im sichtbaren und nahen infraroten Bereich neue Werte vorgeschlagen (Kapitel 5).
Die Hypothese muss abgelehnt werden. Allerdings wird die regionalisierte Version des Models auf Grund der genauen räumlichen Differenzierung mit den auf den Vegetationseinheiten beruhenden PFT durchgeführt. Die neuen Mittelwerte für die Reflexion werden den entsprechenden PFT zugewiesen.

Die gesamte Arbeit bietet eine regionalisierte Modelumgebung, um verschiedene Landnutzungsänderungen im Hinblick auf ihre Auswirkungen auf die Energie- und Wasserströme zwischen Boden, Vegetation und Atmosphäre unter veränderlichen, klimatischen Verhältnissen zu analysieren. Neben der Bewertung der einzelnen Hypothesen hat die Arbeit andere innovative Beiträge geleistet. Die neuen Werte für den vorinstallierten CLM-PFT der immergrünen tropischen Bäume tragen zu den aktuellen Verbesserungen des CLM bei.

Erklärung

Ich versichere, dass ich meine Dissertation

Plant Functional Types for Land Surface Modelling in South Ecuador - Spatial Delineation, Sensitivity and Parameter Determination

selbständig, ohne unerlaubte Hilfe angefertigt und mich dabei keiner anderen als der von mir ausdrücklich bezeichneten Quellen und Hilfen bedient habe. Alle vollständigen oder sinngemäßen Zitate sind als solche gekennzeichnet.

Die Dissertation wurde in der jetzigen oder einer ähnlichen Form noch bei keiner anderen Hochschule eingereicht und hat noch keinen sonstigen Prüfungszweck gedient.

Eine frühere Promotion wurde von mir nicht versucht.

Ort / Datum	Unterschrift

Curriculum vitae

13.09.1971	geboren in Marl (Westfalen)
1978–1982	Gemeinschaftsgrundschule an der Emslandstraße, Marl
1982–1991	Albert-Schweitzer-Gymnasium, Marl
1988–1989	Gisborne Boys' High School, Gisborne, New Zealand
1991	Abitur
1991–1993	Zivildienst, Naturschutzgesellschaft Schutzstation Wattenmeer e.V., Wyk auf Föhr
1993–2001	Studium Geographie (Diplom), Schwerpunkt physische Geographie, Nebenfächer Geologie, Botanik und wiss. Naturschutz, Philipps-Universität Marburg
2001	Diplomabschluss Geographie
1998–2003	Gründer und Gesellschafter Apis@Orbi, Dippel Göttlicher Himmel Seul GbR für geographische Informationssysteme
2003–2007	Technischer Angestellter, DFG Forschergruppe 402, FB Geographie, Philipps-Universität Marburg
2007–2010	Wissenschaftlicher Angestellter, DFG Forschergruppe 816, FB Geographie, Philipps-Universität Marburg
seit 2010	Wissenschaftlicher Angestellter, Wissenschaftsverwaltung, FB Geographie, Philipps-Universität Marburg